General Disclaimer

One or more of the Following Statements may affect this Document

- This document has been reproduced from the best copy furnished by the organizational source. It is being released in the interest of making available as much information as possible.

- This document may contain data, which exceeds the sheet parameters. It was furnished in this condition by the organizational source and is the best copy available.

- This document may contain tone-on-tone or color graphs, charts and/or pictures, which have been reproduced in black and white.

- This document is paginated as submitted by the original source.

- Portions of this document are not fully legible due to the historical nature of some of the material. However, it is the best reproduction available from the original submission.

UARI Report No. 55

HYPERSONIC LAMINAR BOUNDARY LAYERS AROUND SLENDER BODIES

by

RAO V.S. YALAMANCHILI

and

D. R. JENG*

This research was supported partly by the National Aeronautics and Space Administration under grant NGL-01-002-001 (NsG-381/01-002-001) and North American Aviation, Inc. under contract No. M6NDDX-954065

University of Alabama Research Institute

Huntsville, Alabama

May 1968

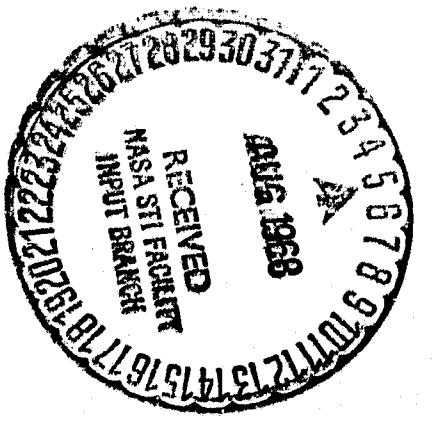

UARI Report No. 55

HYPERSONIC LAMINAR BOUNDARY LAYERS AROUND SLENDER BODIES

by

RAO V.S. YALAMANCHILI

and

D. R. JENG*

This research was supported partly by the National Aeronautics and Space Administration under grant NGL-01-002-001 (NsG-381/01-002-001) and North American Aviation, Inc. under contract No. M6NDDX-954065

University of Alabama Research Institute

Huntsville, Alabama

May 1968

ACKNOWLEDGEMENTS

The authors wish to express their sincere appreciation of the financial support of the North American Aviation under Contract No. M6NDDX-954065 and the NASA under research grant (NsG-381) NGL-01-002-001

We also express our gratitude to Drs. R. Hermann and J. J. Brainerd of the Research Institute, University of Alabama in Huntsville for their valuable suggestion in connection with this work, and Mrs. Ann White for typing this report.

* Present at the Department of Mechanical Engineering, University of Toledo, Toledo, Ohio.

ABSTRACT

The compressible laminar boundary layer equations are considered for hypersonic flow around a slender body. The most important interaction (i.e., the boundary layer-inviscid interaction), is taken into account. The tangent wedge formula for two dimensional bodies is used for the external pressure distribution. The boundary layer equations and the boundary conditions are transformed into a familiar form by using some features of the transformations of Howarth, Dorodnitsyn, Stewartson, and Mangler. A linear viscosity-temperature law and Newtonian fluid approximations are introduced.

The formulation of the problem is general and is applicable for both two dimensional and axisymmetric slender bodies. The assumption of a Prandtl number of unity and of an isothermal body are not mandatory but are invoked here to make the governing equations more tractable.

The solution of nonsimilar boundary layer equations is based on an integration by the method of steepest descent. Inversion of series is necessary to complete the integration. Because of the additional boundary condition at the separation point, as well as the characteristics of the flow field near and downstream of the separation point, the analysis is carried out separately for the flow ahead of separation and for the flow near and downstream of separation. Since the solution of nonsimilar boundary layer equations as well as tangent wedge formulation is coupled, an iteration scheme is developed.

The pressure distribution, skin friction, displacement thickness and heat transfer are computed for a flat plate in hypersonic flow. The calculations are

carried out for various wall conditions including heated plate and gas properties to demonstrate the physical aspects of the problem. The results are in reasonably good agreement with the available experimental observations and analytical solutions. It should be noted that the present results are computed without specifying any particular free stream Mach number.

One may expect to encounter rarefied gas effects in those regions of the flow possessing very sharp gradients (i.e., regions in which the velocity, pressure or temperature change appreciably in the space of a few mean free paths regardless of whether or not the absolute density of the gas flow is especially low). In addition to this rarefied gas effect in the vicinity of the leading edge, the merging of the shock wave and the boundary layer modifies the structure of the flow field at the leading edge. Therefore, the present results are applicable below the rarefaction parameter, $\bar{V}_\infty$ approximately equal to 0.15.

TABLE OF CONTENTS

LIST OF ILLUSTRATIONS

LIST OF ILLUSTRATIONS (cont.)

LIST OF SYMBOLS

A	=	coefficient in viscosity-temperature law, defined in Eq. (2.6), dimensionless
A_m	=	coefficients in the resulting inverted series, defined in Eq. (3.14), dimensionless
AS_m	=	coefficients in the resulting inverted series for separation point analyses, defined in Eq. (3.49), dimensionless
$a(\xi)$	=	$\frac{\partial^2 f}{\partial \eta^2}$ at $\eta = 0$ = unknown parameter in modified stream function, dimensionless
a_1, b_1	=	coefficients defined in Eq. (4.12) to obtain the initial estimate of pressure ratio
a_m	=	coefficients in series representation of modified stream function, defined in Eq. (3.6), dimensionless
B_m	=	coefficients defined in Eq. (3.18), dimensionless
$b(\xi)$	=	$\frac{\partial S}{\partial \eta}$ at $\eta = 0$ = unknown parameter in enthalpy function, dimensionless
b_m	=	coefficients in series representation of enthalpy function, defined in Eq. (3.7), dimensionless
C	=	common factor used in a series
C_f	=	skin friction coefficient, dimensionless
C_h	=	heat transfer coefficient, dimensionless
c	=	speed of sound, ft/sec (m/sec)
c_1	=	speed of sound at the edge of the boundary layer, ft/sec (m/sec)
c_m	=	coefficients defined in Eq. (3.13), dimensionless
c_p	=	specific heat at constant pressure, BTU/lbm $^\circ$R (cal/Kg $^\circ$K)

D_m = coefficients to represent the enthalpy at the edge of the boundary layer, defined in Eq. (3.31), dimensionless

$D1_m$ = coefficients to represent the integral I_1, defined in Eq. (3.34), dimensionless

$D2_m$ = coefficients to represent the integral I_2, defined in Eq. (3.38), dimensionless

$D3_m$ = coefficients to represent the integral I_3, defined in Eq. (3.42), dimensionless

DS_m = coefficients to represent the enthalpy at the edge of the boundary layer in separation point analysis, defined in Eq. (3.58), dimensionless

$DS1_m$ = coefficients to represent the integral I_1, in separation point analysis, defined in Eq. (3.61), dimensionless

$DS2_m$ = coefficients to represent the integral I_2, in separation point analysis, defined in Eq. (3.63), dimensionless

$DS3_m$ = coefficients to represent the integral I_3, in separation point analysis, defined in Eq. (3.65), dimensionless

dm = coefficients to represent the velocity at the edge of the boundary layer, defined in Eq. (3.23), dimensionless

dS_m = coefficients to represent the velocity at the edge of the boundary layer in separation point analysis, defined in Eq. (3.53), dimensionless

f = modified stream function, dimensionless

f (x) = general non-linear function, dimensionless

h = static enthalpy, BTU/lbm (cal/Kg)

h_s = $c_pT + \frac{u^2}{2}$ = local stagnation enthalpy, BTU/lbm (cal/Kg)

I_1, I_2, I_3 = integrals defined in Eq. (2.30 (a)), dimensionless

i = $\sqrt{-1}$ = complex constant, dimensionless

K	=	thermal conductivity, BTU/ft sec $^{\circ}R$ (cal/m sec $^{\circ}K$)
L	=	length of the body, ft (m)
M	=	Mach number, dimensionless
M_1	=	Mach number at the edge of the boundary layer, dimensionless
$P(\xi, \eta)$	=	function defined in momentum Eq. (3.16), dimensionless
$Pe(\xi, \eta)$	=	function defined in energy Eq. (3.25), dimensionless
Pr	=	$\frac{\mu c_p}{K}$ = Prandtl number, dimensionless
p	=	pressure, lbf/ft^2 (Newton/m^2)
p_1	=	pressure at the edge of the boundary layer, lbf/ft^2 (Newton/m^2)
Q_w	=	heat transfer at the wall, BTU/ft^2 sec (cal/m^2 sec)
R	=	gas constant, ft. lbf/lbm $^{\circ}R$ (cal/Kg $^{\circ}K$)
$\bar{R}$	=	numerical constant for the sum of a series, dimensionless
R_n	=	coefficients in a series, defined in Eq. (C.1), dimensionless
Re_x	=	$\frac{u_\infty x}{\nu_\infty}$ = Reynolds number, dimensionless
$r(x)$	=	body radius from the axis of summetry, ft (m)
S	=	enthalpy function, dimensionless
$S(X)$	=	sum of a series, dimensionless
T	=	absolute temperature, $^{\circ}R$ ($^{\circ}K$)
T_1	=	temperature at the edge of the boundary layer, $^{\circ}R$ ($^{\circ}K$)
u, v	=	velocity component in a boundary layer along x and y axis, respectively ft/sec (m/sec)
u_1	=	velocity component at the edge of the boundary layer along x-axis ft/sec (m/sec)

$\bar{v}_\infty$ = $\dfrac{M_\infty\sqrt{A}}{\sqrt{Re_x}}$ = rarefaction parameter, dimensionless

W_n = coefficients in a transformed series, defined in Eq. (C.7), dimensionless

X = variable used in a series representation, dimensionless

x, y = intrinsic coordinates in a physical plane, ft (m)

x_k = upper boundary for the root of a function f(x), dimensionless

x_m = centre point between x_k and x_r, dimensionless

x_r = lower boundary for the root of a function f(x), dimensionless

Y, Z = transformations used to sum divergent series, dimensionless

z = dimensionless x-coordinate

β = shock angle, radians

δ^* = boundary layer displacement thickness, ft (m)

Δ^* = dimensionless displacement thickness

Δx = stepsize in an iteration process, dimensionless

γ = specific heat ratio, dimensionless

ς = density, lbm /ft^3 (Kg/ m^3)

ς_1 = density at the edge of the boundary layer, lbm/ft^3 (Kg/m^3)

η = transformed y-coordinate, dimensionless

θ_1 = effective body angle, radians

θ_b = body angle, radians

$\Lambda(\xi)$ = pressure gradient parameter, dimensionless

μ = dynamic viscosity, lbf sec/ft^2 (Newton sec/m^2)

ν — ematic viscosity, ft^2/sec (m^2/sec)

ξ — formed x-coordinate, dimensionless

Π = variable coefficient defined in Eq. (2.49), dimensionless

τ = $\int_0^\eta f(\xi, \eta)\, d\eta$ = series to be inverted for ordinary point analysis, dimensionless

τ_S = series to be inverted for separation point analysis, dimensionless

τ_w = shear stress at the wall, lbf/ft^2 ($Newton/m^2$)

$\varphi(\xi, \eta)$ = function defined in Eq. (3.18), dimensionless

$\varphi_e(\xi, \eta)$ = function defined in Eq. (3.27), dimensionless

$\varphi S_e(\xi, \eta)$ = function defined in Eq. (3.55), dimensionless

χ = stream function, $(ft/sec)^{\frac{1}{2}}$ or $(m/sec)^{\frac{1}{2}}$

$\bar{\chi}$ = hypersonic interaction parameter, dimensionless

χ_m = coefficients defined in Eq. (3.27), dimensionless

ω = exponent in temperature-viscosity law, dimensionless

$\sum_m$ = summation over m

(n) = $\int_0^\infty \exp(-\tau)\, \tau^{n-1}\, d\tau$ = gamma function

Subscripts:

m = 0, 1, 2, 3 . . . . .

n = 0, 1, 2, 3 . . . . .

w = conditions at the wall

o = stagnation conditions

∞	=	free stream conditions

Superscripts:

i	=	body type indicator, $i = 0$ is two dimensional, $i = 1$ is axisymmetric

SECTION I

INTRODUCTION

According to the Prandtl's [1] boundary layer concept, one can divide the flow field around a body into two regions. The region in which viscous forces are important is confined to a thin layer (called the boundary layer) adjacent to the body and to a thin wake behind it. The other regime is external to this boundary layer where inertia forces play a dominant role in describing the flow field.

Extensive discussion of the boundary layer theory exists in the literature [2 through 10]. Even though the boundary layer equations are a simplified version of Navier-Stokes equations, they are still a set of non-linear partial differential equations. The complexity increases with the inclusion of compressibility, pressure gradient, and heat transfer effects. Due to these difficulties, only a very limited number of studies, numerical and analytical, have been carried out for specific cases at the present time. In the following, various techniques for solving the ordinary boundary layer problems will be briefly described.

For flows over a flat plate and stagnation point regions, similarity solutions require the system to possess a Prandtl number of unity, linear viscosity-temperature relation across the boundary layer, an isothermal surface and a certain particular distribution of the free stream velocity. Von Karman-Pohlhausen's integral method relaxes some of these restrictions. However, the method fails rather dismally to predict the separation point for Schubauer's [11] experimentally observed pressure distribution. Extensive studies of these integral methods were

made in References 12 through 16.

The concept of the combination of the integral method and similar solutions was introduced in References 17 through 20. This approach requires the knowledge of similar solutions. Another method is based on the assumption of local similarity [3, 20, and 21] where the derivatives with respect to the x-coordinate are small compared to the derivatives with respect to the y-coordinate. Also the terms which are functions of x are assumed to take on their local values.

A very limited number of solutions have been obtained for the nonsimilar boundary layers. One approach is to replace the x derivatives with a finite difference formula and then integrate the resulting total differential equations by standard methods [23 through 26]. Since integration of coupled ordinary differential equations with variable fluid properties is involved in an iteration scheme, it requires considerable amount of computation time even on high speed computers. The other approach is due to Meksyn [27 through 35] who used the method of steepest descent in integrating the nonsimilar boundary layer equation for incompressible flow. The method is quite simple to apply and appears powerful. However, complete understanding of the convergence of the series is lacking.

Obtaining the solutions of boundary layer equations by finite difference methods has been the subject of much study in the recent literature [36 through 43]. Since the governing partial differential equations are of parabolic type, they can be solved stepwise downstream starting with the initial velocity, the temperature profiles and specific boundary conditions. The derivatives in the partial differential equations are replaced by difference formulas. In doing so, it is quite common in the literature to replace the products of derivatives or

non-linear terms with linear difference formulas in order to obtain simple linear difference equations. In addition to this drawback, one has to depend on correct initial profiles which may not be obtainable in many applications.

The bodies traveling at hypersonic velocities experience not only first order effects (i.e., simple boundary layers) but also second order effects such as those due to longitudinal curvature, transverse curvature, enthalpy gradient, entropy gradient and displacement thickness. The essential difference between the hypersonic viscous flow and the ordinary boundary layer flow is that the flow immediately outside of the hypersonic boundary layer is greatly influenced by the solution of the boundary layer equations. For instance, in the case of a uniform stream flowing over a flat plate placed along the direction of the main stream, the pressure gradient along the plate can be neglected in an ordinary boundary layer problem; but it must not be neglected in hypersonic viscous flows problems because a significant flow deflection in the boundary layer produces a curved shock in the external flow.

At hypersonic speeds, interactions of the boundary layer with the external stream become more important than in subsonic and low supersonic flows; they lead to more difficulties than in the usual compressible boundary layer theory. The most important interaction on slender bodies is boundary layer-inviscid interaction. This will be discussed more in detail in Sections II and IV. The problem of predicting the characteristics of a hypersonic laminar boundary layer that interacts with the external flow field is solved by using the tangent wedge formulation for the inviscid flow field and the method of steepest descent for the viscous flow.

The problem of the boundary layer inviscid interaction on a flat plate has been solved by Blottner [39], Dewey [21], Mann and Bradley [22], and Chan [20] among many others. Blottner, Dewey, and Chan used the tangent wedge formula for the external pressure distribution. Bradley [22] adopted the method of characteristics for the external pressure distribution and a numerical procedure for the integration of the exact boundary layer equations. Solutions of this type are time consuming and too costly for engineering applications. Blottner [39] used a finite difference technique to obtain the solution of the boundary layer equations. Since an initial profile, which may not be available for all problems, is needed for each dependent variable, he could not compute the solution for a heated flat plate. Dewey [21] used the local similarity concept whereas Chan [20] adopted a combination of similar solutions and an integral method

In this investigation, a method of analysis which was proposed by Jeng et al [112] is employed for predicting the shear stress, pressure distribution, and heat transfer coefficient for the hypersonic flow. The integration of nonsimilar boundary layer equations is carried out by the method of steepest descent. The present boundary layer solution is then applied to calculate the interaction problem in hypersonic flows with the inviscid flow solutions.

The results of the flow field calculations, shown graphically on Figs. 3 through 18, are described in Sections IV and V. A sufficient number of results based on different wall temperatures and gas properties are presented to illustrate the physical aspects of the problem. Typical results which are plotted versus a hypersonic interaction parameter $\bar{\chi}$ are pressure distribution, skin friction,

displacement thickness, and heat transfer.

In the case of an adiabatic plate, the results are in good agreement with the available experimental observations and analytical solutions. In the case of a cold plate, the agreement is reasonably good.

SECTION II

MATHEMATICAL MODELING OF PHYSICAL SYSTEMS IN COMPRESSIBLE LAMINAR BOUNDARY LAYERS

The ultimate objective of the present study is to integrate analytically the equations of continuity, motion and energy for a hypersonic flow past two-dimensional and slender axisymmetrical bodies. It is impossible to obtain a closed form solution to the general equations of motion and energy equation. However, some simplifications can be realized for certain special cases and thus yielding analytical solutions.

In this section compressible laminar boundary layer equations are considered for flows over two-dimensional or axisymmetrical slender bodies. In addition, continuity, perfect gas law and viscosity model are introduced to render a solution to the problem. Sufficient number of boundary conditions are provided to complete the formulation. This boundary layer equations are non-dimensionalized in such a way that one can seek asymptotic solutions by a well-known method. The specially introduced dependent and independent variables are due to Dorodnitsyn - Howarth - Stewartson - Meksyn's transformations, which also contain the transformation used by Mangler [44] for axisymmetrical boundary layers.

Various boundary layer parameters of interest are discussed. The most important feature of the boundary layer - inviscid interaction for hypersonic flows over slender bodies is introduced. The self-induced pressure interaction between the viscous and the inviscid flows on a slender body moving at hypersonic speed stems from the relatively large outward stream line deflection induced

by the thick boundary layer. At hypersonic speed, the deceleration of gas due to viscosity in the boundary layer generates high temperature in this region. As a result, the boundary layer in this region is rather thick, and its rate of growth is proportional to the square of the Mach number for a given Reynolds number of the external flow. This thickening of the viscous layer thus deflects the external flow significantly. At very high speeds, even small changes in the flow inclination produce large changes in pressure; and the pressure induced by the thickening of the boundary layer, in turn, feeds back into the viscous layer, thus affecting its rate of growth. This effect is introduced through a tangent wedge formula and an iteration scheme. Further details are given in Section III.

2.1 Dimensional Form of Compressible Laminar Boundary Layer Equations

(a) Partial Differential Equations:

Consider the steady flow of a perfect gas over an axisymmetrical or two dimensional body, using the intrinsic coordinate system (x,y) where x is measured along the body surface from the stagnation point and y is measured along the outward normal from the body surface. The flow of a compressible, viscous, heat conducting fluid is mathematically described by the continuity, Navier-Stokes and energy equations in addition to the equation of state, a heat conductivity law and a viscosity law. For flows at large Reynolds numbers or small viscosity, invoking the usual assumption that the boundary layer thickness is small compared to the longitudinal body radius of curvature and that the centrifugal forces are negligible, Prandtl has shown that the continuity, Navier-Stokes and energy equations can be simplified to the following compressible laminar

boundary layer equations:

continuity:

$$\frac{\partial}{\partial x}\ (\zeta u r^i)\ +\ \frac{\partial}{\partial y}\ (\zeta v r^i)\ =\ 0 \qquad (2.1)$$

x - momentum:

$$\zeta u \frac{\partial u}{\partial x} + \zeta v \frac{\partial u}{\partial y} = - \frac{\partial p}{\partial x} + \frac{\partial}{\partial y}\ \left(\mu \frac{\partial u}{\partial y}\right) \qquad (2.2)$$

y - momentum:

$$\frac{\partial p}{\partial y} = 0 \qquad (2.3)$$

Energy:

$$\zeta u \frac{\partial}{\partial x}\ (c_p T) + \zeta v \frac{\partial}{\partial y}\ (c_p T) = u \frac{\partial p}{\partial x} + \mu\left(\frac{\partial u}{\partial y}\right)^2 + \frac{\partial}{\partial y}\ \left(K \frac{\partial T}{\partial y}\right) \qquad (2.4)$$

Equation of State:

$$p = \zeta R T \qquad (2.5)$$

where $i = 0$ for a two-dimensional flow and $i = 1$ for an axisymmetrical flow, and r is the body radius from the axis of symmetry.

The above equations do not contain transverse curvature terms for axisymmetric flows (i.e., the body radius is independent of y). Since the present analysis is intended for very slender bodies and flat plates, the transverse curvature effect has not taken into accou .

It should be noted also that the body forces are neglected in formulating these equations.

(b) Viscosity Model

The most well known formula for the viscosity of a gas from kinetic theory of gases is Southerland's law. However, it is not uncommon in literature to use another linear viscosity law which is of the following form because of its simplicity and being capable of providing reasonable results.

$$\frac{\mu}{\mu_\infty} = A\left(\frac{T}{T_\infty}\right)^{\omega} \tag{2.6}$$

where A and ω are constants

The linear viscosity model (i.e., with ω taken as unity in Eq. (2.6)) is used in the following analysis.

2.2 Nondimensional Form of Boundary Layer Equations

The present study is concerned with laminar boundary layers in gases flowing over a slender body at high velocities. This subsection is mainly devoted to summarizing the procedure used for transforming the equations of the boundary layer so that they be more amenable to asymptotic series expansion.

(a) Dependent and Independent Variables:

The two independent variables are:

$$\xi = \int_0^x \left(\frac{u_1}{u_\infty}\right)\left(\frac{c_1}{c_\infty}\right)^{\frac{2\gamma}{\gamma-1}} \left(\frac{r}{L}\right)^{2i} dx \tag{2.7}$$

$$\eta = \left(\frac{r}{L}\right)^{i} \frac{u_1}{\sqrt{2\, u_\infty\, \xi\, \sqrt{A\nu_\infty}}} \int_0^y \frac{\zeta}{\zeta_\infty}\, dy \tag{2.8}$$

The two dependent variables are:

$$\chi = \sqrt{2 u_\infty \xi}\ f(\xi, \eta) \tag{2.9}$$

$$S(\xi, \eta) = \frac{h_s}{h_o} - 1 \tag{2.10}$$

where h_s is the local stagnation enthalpy, i.e.

$$h_s = h + \frac{u^2}{2} \tag{2.11}$$

The definition of the stream function (χ) is given in the following subsection.

(b) Partial Differential Equations:

Since the requirement for the existence of a stream function is the continuity condition, its relation in terms of the velocity components u and v from the continuity equation is

$$u = \left(\frac{L}{r}\right)^i \sqrt{A \nu_\infty}\ \frac{\zeta_\infty}{\zeta}\ \frac{\partial \chi}{\partial y} \tag{2.12}$$

$$v = -\left(\frac{L}{r}\right)^i \sqrt{A \nu_\infty}\ \frac{\zeta_\infty}{\zeta}\ \frac{\partial \chi}{\partial x} \tag{2.13}$$

These velocity components can be rewritten in terms of a modified stream function f as

$$u = u_1\ \frac{\partial f}{\partial \eta} \tag{2.14}$$

$$v = \left(\frac{r}{L}\right)^i \frac{T}{T_\infty} \sqrt{\frac{A \nu_\infty}{2 u_\infty \xi}}\ u_1 \left\{ f + 2\xi \frac{\partial f}{\partial \xi} + \left[2\xi \left(\frac{L}{r}\right)^{3i} \left(\frac{c_\infty}{c_1}\right)^{\frac{2\gamma}{\gamma - 1}}\ \frac{u_\infty^2}{u_1^2}\right.\right.$$

$$\frac{\partial}{\partial x}\left(\frac{r}{L}\right)^{i} u_1 - 1\Big] \eta \frac{\partial f}{\partial \eta}\Bigg\} \tag{2.15}$$

In addition to the perfect gas law, an isentropic relation is assumed for the fluid outside the boundary layer. These assumptions lead to the following relations

$$p_1 / p_\infty = \left(\frac{c_1}{c_\infty}\right)^{\frac{2\gamma}{\gamma - 1}} \tag{2.16}$$

and

$$T_o / T_1 = 1 + \frac{\gamma - 1}{2} M_1^2 \tag{2.17}$$

Since the temperature appears explicitly in a velocity relation v and later in a density ratio, it is desirable to rearrange the dimensionless temperature ratio in terms of f and S as shown below

$$\frac{T}{T_1} = \frac{T_o}{T_1}\left(\frac{c_p T}{c_p T_o} + \frac{u^2}{2 c_p T_o}\right) - \frac{u^2}{2 c_p T_1} \tag{2.18}$$

Using the definitions of the speed of sound ($c_1^2 = \gamma R T_1$), and the enthalpy function S as well as the Eqs. (2.5), (2.14), and (2.17), Eq. (2.18) becomes

$$\frac{T}{T_1} = \left(1 + \frac{\gamma - 1}{2} M_1^2\right)(S + 1) - \frac{\gamma - 1}{2} M_1^2 \left(\frac{\partial f}{\partial \eta}\right)^2 \tag{2.19}$$

Substitution of Eq. (2.19) into Eq. (2.15) yields the equation for the transverse velocity

$$v = -\left(\frac{r}{L}\right)^{i}\left(\frac{c_1}{c_\infty}\right)\sqrt{\frac{A\nu_\infty}{2u_\infty \xi}}\, u_1 \Bigg[\left(1 + \frac{\gamma - 1}{2} M_1^2\right)(S+1) - \frac{\gamma - 1}{2} M_1^2 \left(\frac{\partial f}{\partial \eta}\right)^2\Bigg]$$

$$\left\{ f + 2\xi \frac{\partial f}{\partial \xi} + \left[2\xi \left(\frac{L}{r} \right)^{3i} \left(\frac{c_\infty}{c_1} \right) \frac{2\gamma}{\gamma - 1} \frac{u_\infty}{u_1^2} \frac{\partial}{\partial x} \left(\frac{r}{L} \right)^{i} u_1 - 1 \right] \eta \frac{\partial f}{\partial \eta} \right\} \tag{2.20}$$

Making use of the above relations, the momentum and energy equations after some simplification reduce to the following form:

Momentum:

$$\frac{\partial^3 f}{\partial \eta^3} + f \frac{\partial^2 f}{\partial \eta^2} + \wedge \left[S + 1 - \left(\frac{\partial f}{\partial \eta} \right)^2 \right] = 2\xi \left(\frac{\partial f}{\partial \eta} \frac{\partial^2 f}{\partial \xi \partial \eta} - \frac{\partial f}{\partial \xi} \frac{\partial^2 f}{\partial \eta^2} \right) \tag{2.21}$$

Energy:

$$\frac{1}{Pr} \frac{\partial^2 S}{\partial \eta^2} + f \frac{\partial S}{\partial \eta} = 2\xi \left(\frac{\partial S}{\partial \xi} \frac{\partial f}{\partial \eta} - \frac{\partial S}{\partial \eta} \frac{\partial f}{\partial \xi} \right) - \frac{Pr - 1}{Pr} \frac{(\gamma - 1) M_1^2}{1 + \frac{\gamma - 1}{2} M_1^2}$$

$$\left[\left(\frac{\partial^2 f}{\partial \eta^2} \right)^2 + \frac{\partial f}{\partial \eta} \frac{\partial^3 f}{\partial \eta^3} \right] \tag{2.22}$$

where

$$\wedge = \frac{2\xi}{\left(\frac{c_\infty}{c_1} \right) u_1} \frac{d}{d\xi} \left(\frac{c_\infty}{c_1} u_1 \right) \tag{2.23}$$

Several authors derived similar to the Eqs. (2.21) and (2.22). For example, one can find in Chapter 8 of Hayes and Probstein [3] and Cohen and Reshotoko [9]. One can also find momentum equation similar to the Eq. (2.21) in Reference [35] besides familiar momentum equation in incompressible flow field. However, one should note that they are not exactly the same. They differ slightly either in the definition of independent variables, dependent variables or nondimensionlization.

2.3 Boundary Conditions

Since slip and temperature jump at the surface are important near the leading edge, the boundary layer flow is considered only after a small distance

from the leading edge. This will be discussed further in Section IV.

The boundary condition on the velocity at the wall follows from the requirement of no slip, and the surface temperature must satisfy the condition that there is no heat transfer at the wall or it exhibits a specified distribution at the wall:

$$u = v = 0 \text{ at } y = 0 \ , \tag{2.24}$$

and either $\left(\frac{\partial T}{\partial y}\right)_{y=o} = 0$ or the surface temperature, T_w is a function of x only or independent of x. At the outer edge of the boundary layer, the values of u and T are specified by the inviscid flow solution. Hence at $y = \infty$

$$u = u_1$$

$$T = T_1 \quad \text{or} \quad h = h_1 \tag{2.25}$$

To avoid rarefied gas effects or low Reynolds number effects such as velocity slip or temperature jump at the leading edge, an upper estimate of the validity of the present analysis will be specified from the existing literature. This will be discussed in detail in Section IV.

Introducing the definitions of dependent and independent variables and relations (2.14), (2.19), (2.20) into Eqs. (2.24) and (2.25), the physical boundary conditions reduce to the following nondimensional form:

<u>At $\eta = 0$:</u>

$$f = 0 \ , \ \frac{\partial f}{\partial \eta} = 0 \tag{2.26}$$

and either $\frac{\partial S}{\partial \eta} = 0$ for insulated wall

or $S = S_w$ (given) for nonadiabatic plate.

At $\eta \to \infty$, $\frac{\partial f}{\partial \eta} = 1$ and $S = 0$. (2.27)

2.4 Boundary Layer Parameters

In the study of interactions between the stream and the immersed body, one is likely to encounter the most important quantities such as viscous stress and enthalpy. The objective of the present analysis is to determine the modified stream function and the enthalpy function. Once these functions are determined, it will be a simple matter to obtain any other parameter of the boundary layer.

(a) Displacement Thickness:

The boundary layer displacement thickness is defined as

$$\delta^* = \int_0^\infty \left(1 - \frac{\zeta u}{\zeta_1 u_1} \right) dy \qquad (2.28)$$

The displacement thickness indicates the distance by which the external streamlines are shifted outwards owing to the formation of boundary layer. The effective body is the sum of geometrical body and the displacement thickness. Therefore, the displacement thickness is necessary to determine the effective body in a hypersonic flow where the interaction between the boundary layer and inviscid flow has strong influence on the external pressure distribution.

The physical definition of displacement thickness is further transformed in terms of new dependent and independent variables as shown below

$$\delta^* = \frac{\zeta_\infty}{\zeta_1} \sqrt{A \nu_\infty} \; \frac{\sqrt{2 u_\infty \xi}}{u_1} \left\{ \int_0^\infty \left[(1 - f') + \frac{\gamma - 1}{2} M_1^2 (1 - f'^2) - S \left(1 + \frac{\gamma - 1}{2} M_1^2 \right) \right] d\eta \right\} \qquad (2.29)$$

where the prime (') denotes differentiation with respect to η. (Perfect gas law

and Eq. (2.19) are used in achieving the above form). This can he further simplified by integration by parts and applying the boundary conditions. The result is

$$\delta^* = \frac{\zeta_\infty}{\zeta_1} \sqrt{A \nu_\infty} \sqrt{\frac{2 u_\infty \xi}{u_1}} \left\{ I_1 + (\gamma - 1) M_1^2 I_2 - \left(1 + \frac{\gamma - 1}{2} M_1^2\right) I_3 \right\} \qquad (2.30)$$

where

$$I_1 = \int_0^\infty f'' \eta \, d\eta$$

$$I_2 = \int_0^\infty f'' f' \eta \, d\eta \qquad (2.30a)$$

and

$$I_3 = \int_0^\infty S' \eta \, d\eta$$

(b) Shear Stress

Assuming a Newtonian Fluid, the shear stress at the wall in cartesian coordinates is

$$\tau_w = \left(\mu \frac{\partial u}{\partial y} \right)_{y=0} \qquad (2.31)$$

From the definition of η, Eq. (3.8), the partial differentiation of η with respect to y yields

$$\frac{\partial \eta}{\partial y} = \left(\frac{r}{L}\right)^i \frac{u_1}{\sqrt{2 u_\infty \xi} \sqrt{A \nu_\infty}} \frac{\zeta}{\zeta_\infty} \qquad (2.32)$$

Using Eq. (2.32), the viscosity model and the definition of the dependent variable f, one obtains the shear stress at the wall as

$$\tau_w = \zeta_\infty \frac{\sqrt{A \nu_\infty}}{\sqrt{2 u_\infty \xi}} \left(\frac{r}{L}\right)^i \frac{p_1}{p_\infty} u_1^2 \left(\frac{\partial^2 f}{\partial \eta^2}\right)_{\eta = 0} \qquad (2.33)$$

Eq. (2.33) is important in aerodynamic drag calculations and in establishing separation point in regions of adverse pressure gradient.

(c) Heat Transfer

The heat transfer at the wall by conduction is given by

$$Q_w = - \left(K \frac{\partial T}{\partial y} \right)_{y=0} \tag{2.34}$$

Instead of introducing a model for thermal conductivity K which is a function of temperature, another form of Eq. (2.34) may prove to be useful.

$$Q_w = - \left[\frac{\mu}{Pr} \frac{\partial}{\partial y} (c_p T) \right] y = 0 \tag{2.35}$$

when $Pr = \frac{\mu c_p}{K}$ = Prandtl Number.

Using the viscosity-temperature relationship, the dependent and independent variables as well as boundary conditions, Eq. (3.35) may be transformed into the following form:

$$Q_w = - \zeta_\infty \frac{\sqrt{A \nu_\infty}}{\sqrt{2 u_\infty \xi}} \frac{p_1}{p_\infty} \left(\frac{r}{L} \right)^i \frac{u_1 h_o}{Pr} \left(\frac{\partial S}{\partial \eta} \right) \eta = 0 \tag{2.36}$$

Eq. (2.36) is useful in designing heat shields on various hypersonic vehicles as well as ascertaining the effect of heat transfer on separation point.

2.5 Pressure Distribution

It is intended to carry out the analysis on slender bodies with a sharp leading edge. The interaction of the leading edge shock wave and the boundary layer is important in hypersonic boundary layer flow. The presence of leading edge shock wave is more significant because of the large outward stream line deflection caused by a thick boundary layer at hypersonic speeds. This is explained

in detail in Reference 3.

It is customary to divide the flow field into several regions as shown in Fig. 1. The rarefied gas effects (such as slip flow and the shock structure) play a major role in the leading edge region. This will be discussed in detail in Section IV.

It is difficult to establish the boundaries of these various regions. Oguchi [45] gives an estimate of the upper boundary of strong interaction region based on wedge-like flow. Since the thin shock wave assumption is involved, the validity is questionable. However, the experiments and the theory [46, 47] which describe the merged layer regime provided as estimate of upstream limit for the strong interaction regime. Therefore, the analysis presented herein is applicable only for the flow downstream of this upstream limit.

(a) Tangent-Wedge Formula

A simple, approximate, inviscid method for obtaining surface pressure distribution on two dimensional slender bodies at hypersonic speeds is the tangent wedge approximation. The surface pressure at any point on a body at an arbitrary angle of attack is taken to be equal to the pressure on a wedge whose half angle equals the local inclination angle of the streamline with respect to the free stream. Similarly, tangent cone approximations are provided for axisymmetric bodies.

The tangent wedge formula from Reference 3 (Eq. 7.3.1) is

$$\frac{p_1}{p_\infty} = 1 + \gamma M_\infty^2 \theta_1^2 \left[\frac{\gamma+1}{4} + \sqrt{\left(\frac{\gamma+1}{4}\right)^2 + \frac{1}{M_\infty^2 \theta_1^2}} \right] \qquad (2.37)$$

where θ_1 is the angle of effective body shape.

For a normal shock, the pressure ratio is

$$\frac{p_1}{p_\infty} = \frac{2\gamma}{\gamma+1} M_\infty^2 - \frac{\gamma-1}{\gamma+1} \tag{2.38}$$

For an oblique shock, the pressure ratic becomes

$$\frac{p_1}{p_\infty} = \frac{2\gamma}{\gamma+1} M_\infty^2 \sin^2 \beta - \frac{\gamma-1}{\gamma+1} \tag{2.39}$$

where β represents the oblique shock angle.

For a hypersonic flow and very slender bodies (when β and θ_1 are small), Eq. (2.39) can be approximated as

$$\frac{p_1}{p_\infty} \approx \frac{2\gamma}{\gamma+1} M_\infty^2 \theta_1^2 \frac{\beta^2}{\theta_1^2} - \frac{\gamma-1}{\gamma+1} \tag{2.40}$$

A simple relation between β and θ_1 [48] is

$$M_\infty^2 \sin^2 \beta - 1 = \frac{\gamma+1}{2} M_\infty^2 \frac{\text{Sin } \beta \text{ Sin } \theta_1}{\cos(\beta - \theta_1)} \tag{2.41}$$

For small values of θ_1 and large values of M_∞, such that $M_\infty \theta_1 > 1$, β must also be small and hence Eq. (2.41) may be approximated as

$$\frac{\beta}{\theta_1} = \frac{\gamma+1}{4} + \sqrt{\left(\frac{\gamma+1}{4}\right)^2 \frac{1}{M_\infty^2 \theta_1^2}} \tag{2.42}$$

Elimination of β between Eqs. (2.40) and (2.42) leads to the following pressure distribution formula:

$$\sqrt{\frac{p_1}{p_\infty} + \frac{\gamma-1}{\gamma+1}} = \sqrt{\frac{2\gamma}{\gamma+1}} M_\infty \theta_1 \left[\frac{\gamma+1}{4} + \sqrt{\left(\frac{\gamma+1}{4}\right)^2 + \frac{1}{M_\infty^2 \theta_1^2}}\right] \tag{2.43}$$

Combination of Eqs. (2.37) and (2.43) yields the following simplified form for the effective body shape

$$M_\infty \theta_1 = \sqrt{\frac{2}{\gamma(\gamma+1)}} \quad \frac{\frac{p_1}{p_\infty} - 1}{\sqrt{\frac{p_1}{p_\infty} + \frac{\gamma-1}{\gamma+1}}} \tag{2.44}$$

(b) Boundary Layer - Inviscid Interaction

High temperatures and low density exists in hypersonic boundary layers. These circumstances lead to large displacement thicknesses which in turn deflects significantly the external inviscid flow. (This is negligible in subsonic and low supersonic speeds). If one includes the slope of displacement thickness in addition to the geometrical body slope, the pressure distribution obtained in this manner will be appreciably different at hypersonic speeds from the pressure distribution obtained on the actual geometrical body alone. Since the displacement thickness is a function of the pressure distribution along the body and the pressure distribution is a function of the effective body shape (i.e., geometrical body plus displacement thickness), there is an interaction between the boundary layer and the external flow. Even if one avoids the leading edge bluntness by giving a sharp nose, the large displacement thickness may induce vorticity in the external inviscid field. However, such a contribution is negligible in comparison with the boundary layer-inviscid interaction at hypersonic speeds on flat plates and very slender bodies[3].

Two main approaches to the strong interaction problem are available. One is Shen's assumption [49], later extended by Li and Nagamatsu [50], that

the edge of the boundary layer is also the shock induced by the thick boundary layer. The second approach is by Lees [51 and 52] in which the edge of the boundary layer (or the displacement thickness) is taken as the boundary layer of a new body. The effect of these differences in concept are further discussed by Lees [51]. The second approach is used in the present analysis.

The effective body shape is derived in the last section as a function of the pressure distribution. This effective body shape and the displacement thickness can be related as

$$\theta_1 = \theta_b + \frac{d\delta^*}{dx} \tag{2.45}$$

To non-dimensionilize the displacement thickness and longitudinal coordinate, let

$$\Delta^* = \frac{u_\infty \delta^*}{A \nu_\infty M_\infty^5} \tag{2.46}$$

and

$$\bar{\chi} = \sqrt{\frac{A \nu_\infty}{u_\infty x}}\, M_\infty^3 \tag{2.47}$$

With these definitions, Eq. (2.45) reduces to

$$\theta_1 = \theta_b - \frac{\bar{\chi}^3}{2 M_\infty} \frac{d\Delta^*}{d\bar{\chi}} \tag{2.48}$$

Using Eq. (2.30), Eq. (2.46) can be rewritten as

$$\Delta^{*2} = 4 \frac{II^2}{M_1^4} \left(\frac{p_\infty}{p_1}\right)^2 \left(\frac{u_\infty}{u_1}\right)^2 \int_\infty^{\bar{\chi}} \left[- \frac{p_1}{p_\infty} \frac{u_1}{u_\infty} \left(\frac{r}{L}\right)^{2i} \right] \frac{d\bar{\chi}}{\bar{\chi}^3} \tag{2.49}$$

where

$$II = I_1 + (\gamma - 1) M_1^2 I_2 - (1 + \frac{\gamma - 1}{2} M_1^2) I_3$$

The integrals I_1, I_2, and I_3 have been defined in Eq. (2.30(a)).

Substitution of Eq. (2.48) into Eq. (2.44) yields

$$M_\infty \theta_b - \frac{\bar{\chi}^3}{2} \frac{d\Delta^*}{d\bar{\chi}} = \sqrt{\frac{2}{\gamma(\gamma+1)}} \frac{p_1/p_\infty - 1}{\sqrt{\frac{p_1}{p_\infty} + \frac{\gamma - 1}{\gamma + 1}}} \tag{2.50}$$

If Eq. (2.50) is integrated with respect to $\bar{\chi}$ and the resulting Δ^* is then eliminated by the use of Eq. (2.49), one obtains a single integral equation in the form

$$\frac{p_\infty}{p_1} = \frac{u_1}{u_\infty} \left[\frac{2 M_1^4}{\gamma(\gamma+1) II^2}\right]^{\frac{1}{2}} \frac{\int_\infty^{\bar{\chi}} \left[-\left(\frac{p_1}{p_\infty} - 1\right)\sqrt{p_1/p_\infty + \frac{\gamma-1}{\gamma+1}}\right] \frac{d\bar{\chi}}{\bar{\chi}^3}}{\left[-\int_\infty^{\bar{\chi}} \frac{p_1}{p_\infty} \left(\frac{r}{L}\right)^{2i} \frac{u_1}{u_\infty} \frac{d\bar{\chi}}{\bar{\chi}^3}\right]^{\frac{1}{2}}}$$

$$- \frac{u_1}{u_\infty} \frac{M_\infty M_1^2}{II} \frac{\int_\infty^{\bar{\chi}} -\theta_b \frac{d\bar{\chi}}{\bar{\chi}^3}}{\left[-\int_\infty^{\bar{\chi}} p_1/p_\infty \left(\frac{r}{L}\right)^{2i} \frac{u_1}{u_\infty} \frac{d\bar{\chi}}{\bar{\chi}^3}\right]^{\frac{1}{2}}}$$

SECTION III

SOLUTION OF BOUNDARY LAYER EQUATIONS

The solution of the boundary layer equations with appropriate boundary conditions and boundary layer-inviscid interaction is the main concern of recent interest. The complexity of the problem is increased with the inclusion of the effects of compressibility, adverse pressure gradient and heat transfer. Momentum and energy equations (Eqs. 2.21 and 2.22) are, furthermore, coupled. The solution of these equations is as hard to come by as any other problem of significance in fluid mechanics.

According to Prandtl, the velocity gradient is a rapidly decreasing function across the boundary layer. It may be possible to represent the velocity gradient with an exponential function. In the method of solution, the velocity in the boundary layer is thus expressed as a definite integral of a rapidly decreasing function. Following Meksyn, the definite integral is evaluated by the method of steepest descent which greatly simplifies the integration.

The main idea of the method is as follows: if the integrand is a rapidly decreasing function, the main contribution to the integral comes from the region close to the stationary point of the integrand. In doing so, the partial differential equations (i.e., momentum and energy equations) are reduced to nonlinear total differential equations which contain $a(\xi)$ (i.e., $\partial^2 f/\partial\eta^2$ at $\eta = 0$) and $b(\xi)$ (i.e., $\frac{\partial S}{\partial \eta}$ at $\eta = 0$) as dependent variables. The dependent variables "a" and "b" can be determined by using the boundary conditions at the edge of the boundary layer. In the end, to balance the number of equations and the number

of unknowns (i.e., to use the tangent wedge or tangent cone formula effectively), the integrals I_1, I_2, and I_3 which appear in the displacement thickness are evaluated. This type of analysis is done separately for both ordinary point and separation point regions.

Considerable amount of work in the analysis can be reduced if it is restricted to a Prandtl number of unity. In this case, dropping the last term, the energy Eq. (2.22) becomes

$$\frac{\partial^2 S}{\partial \eta^2} + f \frac{\partial S}{\partial \eta} = 2\xi \left(\frac{\partial S}{\partial \xi} \frac{\partial f}{\partial \eta} - \frac{\partial S}{\partial \eta} \frac{\partial f}{\partial \xi} \right) \tag{3.1}$$

The momentum equation remains the same as before i.e.,

$$\frac{\partial^3 f}{\partial \eta^3} + f \frac{\partial^2 f}{\partial \eta^2} = -\Lambda \left[S + 1 - \left(\frac{\partial f}{\partial \eta} \right)^2 \right] + 2\xi \left(\frac{\partial f}{\partial \eta} \frac{\partial^2 f}{\partial \xi \partial \eta} - \frac{\partial f}{\partial \xi} \frac{\partial^2 f}{\partial \eta^2} \right) \tag{3.2}$$

Besides the boundary conditions mentioned earlier (Eqs. 2.26 and 2.27), additional boundary condition at the separation point is

$$\left(\frac{\partial^2 f}{\partial \eta^2} \right)_{\eta_1 = 0} = 0 \tag{3.3}$$

and that $a(\xi)$ is small near and downstream of the separation point. Hence, it is necessary to carry the analysis separately for the flow ahead of separation and for the flow near and downstream of separation.

To obtain the solution of Eqs. (3.1) and (3.2), one expands the modified stream function $f(\xi, \eta)$ and the dimensionless enthalpy function $S(\xi, \eta)$ in a power series of η as

$$f = \sum_{m=2}^{\infty} \frac{a_m(\xi)\,\eta^m}{m!} \tag{3.4}$$

and

$$S = \sum_{m=0}^{\infty} \frac{b_m(\xi)\,\eta^m}{m!} \tag{3.5}$$

where a_m and b_m are functions of ξ only. The modified stream function f (Eq. 3.4) satisfies the boundary conditions (Eq. 2.26) at the wall. Since the momentum and energy equations are coupled, the coefficients a_m and b_m will be coupled too.

Substitution of $f(\xi,\eta)$, $S(\xi,\eta)$ as well as their derivatives into Eqs. (3.1) and (3.2) and equating equal powers of η on both sides of these equations yields for these coefficients as

$$\begin{aligned}
a_2 &= a(\xi) \\
a_3 &= -\Lambda(1+S_w) \\
a_4 &= -\Lambda b \\
a_5 &= a^2(2\Lambda-1) + 2\xi a\,a' \\
a_6 &= a(1+S_w)(4\Lambda - b\Lambda^2 - 4\xi\Lambda') \\
a_7 &= 8a\Lambda b - 4\Lambda^2(1+S_w)^2 + 6\Lambda^3(1+S_w)^2 - 8a\Lambda^2 b \\
&\quad + 2\xi\left[3\Lambda b\,a' - 5\Lambda a\,b' - 3ab\Lambda' + 2\Lambda\Lambda'(1+S_w)^2\right] \\
&\text{etc.,}
\end{aligned} \tag{3.6}$$

and

$$b_o = S_w \text{ (boundary condition)}$$

$$b_1 = b(\xi)$$

$$b_2 = 0$$

$$b_3 = 0 \qquad (3.7)$$

$$b_4 = -ab + 2\xi(2ab' - ba')$$

$$b_5 = b\wedge(1+S_w) + 2\xi\left[b\wedge'(1+S_w) - 3\wedge b'(1+S_w)\right]$$

etc.,

where primes denote differentiation with respect to ξ. These coefficients are valid for the case of constant temperature, nonadiabatic walls. The assumption of isothermal wall and Prandtl number of unity reduces considerable amounts of algebra involved in the analysis. One can relax these assumptions by assigning arbitrary Prandtl number and arbitrary surface temperature distribution without introducing any undue difficulty. Moreover, these coefficients are applicable for both ordinary point and separation point analyses.

3.1 Ordinary Point

The major problem in the solution of boundary layer equations consists in satisfying the boundary condition at infinity. The coefficients derived in the previous section contain two unknown parameters i.e., $a(\xi)$ and $b(\xi)$. They can be determined from the boundary condition at infinity. Further analysis is concerned with the development of equations which describe the boundary

conditions at infinity. To do this, it will be necessary to integrate the modified stream function f and to invert the resulting series.

Let
$$\tau = \int_0^\eta f \, d\eta \tag{3.8}$$

i.e., $$\tau = \eta^3 \sum_{m=0}^{\infty} \frac{a_{m+2}\,\eta^m}{(m+3)\,!}$$

Since τ begins with η^3, the expression of η in τ begins with $\tau^{1/3}$. Hence,

$$\eta = \sum_{m=0}^{\infty} \frac{A_m}{m+1} \tau^{\left(\frac{m+1}{3}\right)} \tag{3.9}$$

or

$$d\eta = \frac{1}{3} \sum_{m=0}^{\infty} A_m \tau^{\left(\frac{m-2}{3}\right)} d\tau \tag{3.10}$$

Dividing Eq. (3.10) by $\tau^{\frac{m+1}{3}}$ and integrating the resulting expression using Cauchy's residue theorem, the following result is obtained

$$A_m = \frac{1}{2\pi i} \int \tau^{-\left(\frac{m+1}{3}\right)} d\eta \tag{3.11}$$

where $i = \sqrt{-1}$. The integrations are carried out three times in the τ plane to dispose of the fractional powers of τ once in the η plane.

The complex variable analysis enables one to show that A_m is the coefficient of η^{-1} in the expansion of $\tau^{-\left(\frac{m+1}{3}\right)}$. Since

$$\tau^{-\left(\frac{m+1}{3}\right)} = \eta^{-(m+1)} \left(\sum_{m=0}^{\infty} -\frac{a_{m+2}\,\eta^m}{(m+3)\,!} \right)^{-\left(\frac{m+1}{3}\right)} \tag{3.12}$$

therefore, A_m is the coefficient of η^m in the expression

$$\left(\sum_{m=0}^{\infty} c_m \eta^m\right)^{-\frac{m+1}{3}} = \left(\sum_{m=0}^{\infty} \frac{a_{m+2}\eta^m}{(m+3)!}\right)^{-\left(\frac{m+1}{3}\right)} \qquad (3.13)$$

after expanding Eq. (3.13) in series form. The following equations are obtained for A_m

$$A_o = (6/a)^{1/3}$$

$$A_1 = -\frac{a_3}{36}\left(\frac{6}{a}\right)^{5/3}$$

$$A_2 = -\frac{3}{10}\frac{a_4}{a^2} + \frac{3}{8}\frac{a_3}{a^3} \qquad (3.14)$$

$$A_3 = -\frac{4}{3}\frac{a_5}{6!}\left(\frac{6}{a}\right)^{7/3} + \frac{28}{9}\frac{a_3}{4!}\frac{a_4}{5!}\left(\frac{6}{a}\right)^{10/3} - \frac{140}{81}\left(\frac{a_3}{24}\right)^3\left(\frac{6}{a}\right)^{13/3}$$

$$A_4 = \frac{5}{3}\frac{a_6}{7!}\left(\frac{6}{a}\right)^{8/3} + \frac{20}{9}\left(\frac{a_4}{5!}\right)^2\left(\frac{6}{a}\right)^{11/3} + \frac{40}{9}\left(\frac{a_3}{4!}\right)\frac{a_5}{6!}\left(\frac{6}{a}\right)^{1/3} - \frac{220}{27}\left(\frac{a_3}{4!}\right)^2\frac{a_4}{5!}\left(\frac{6}{a}\right)^{14/3} + \frac{770}{243}\left(\frac{a_3}{4!}\right)^4\left(\frac{6}{a}\right)^{17/3}$$

$$A_5 = -2\left(\frac{a_7}{81}\right)\left(\frac{6}{a}\right)^3 + 6\left(\frac{a_3}{41}\right)\frac{a_6}{71}\left(\frac{6}{a}\right)^4 + 6\left(\frac{a_4}{51}\right)$$

$$\left(\frac{a_5}{61}\right)\left(\frac{6}{a}\right)^4 - 12\left(\frac{a_3}{41}\right)^2\frac{a_5}{61}\left(\frac{6}{a}\right)^5 - 12\left(\frac{a_4}{51}\right)^2\frac{a_3}{41}$$

$$\left(\frac{6}{a}\right)^5 + 20\left(\frac{a_3}{41}\right)^3\left(\frac{a_4}{51}\right)\left(\frac{6}{a}\right)^6 - 6\left(\frac{a_3}{41}\right)^5\left(\frac{6}{a}\right)^7$$

. . . . . .

(a) Momentum Equation

Equation (3.2) is a nonlinear and nonhomogeneous partial differential equation. Replacing the dependent variables f and S in the right-hand-side of Eq. (3.2) by the use of Eqs. (3.4) and (3.5) yields

$$\frac{\partial^3 f}{\partial \eta^3} + f\frac{\partial^2 f}{\partial \eta^2} = P(\xi, \eta) \tag{3.15}$$

where

$$P(\xi,\eta) = -\Lambda\left[\sum_{m=0}^{\infty}\frac{b_m \eta^m}{m!} + 1 - \sum_{m=2}^{\infty}\sum_{n=2}^{\infty}\frac{a_n}{(n-1)!}\frac{a_m}{(m-1)!}\eta^{n+m-2}\right]$$

$$+ 2\xi\left[\sum_{n=2}^{\infty}\sum_{m=2}^{\infty}\frac{a_n}{(n-1)!}\frac{a'_m}{(m-1)!}\eta^{n+m-2} - \sum_{n=2}^{\infty}\sum_{m=2}^{\infty}\frac{a'_n}{n!}\frac{a_m}{(m-2)!}\eta^{n+m-2}\right] \tag{3.16}$$

Multiplying Eq. (3.15) by an integration factor, e^{τ}, where τ is defined in Eq. (3.8) and integrating with respect to η results in

$$\frac{\partial^2 f}{\partial \eta^2} = \exp(-\tau) \left[a(\xi) + \int_0^{\eta} P(\xi, \eta) \exp(\tau)\, d\eta \right] \quad (3.17)$$

The appropriate conditions at the solid boundary are used to obtain the above form.

To integrate Eq. (3.17), let

$$\varphi = a(\xi) + \int_0^{\eta} P(\xi,\eta) \exp(\tau)\, d\eta = \sum_{m=0}^{\infty} \frac{B_m \eta^m}{m!} \quad (3.18)$$

The coefficients B_m in Eq. (3.18) may be obtained by substituting Eqs. (3.4) and (3.8) into Eq. (3.17) and equating equal powers of η on either side of Eq. (3.17). The first six coefficients are listed below

$$\begin{aligned}
B_o &= a \\
B_1 &= -\wedge(1 + S_w) \\
B_2 &= -b\wedge \\
B_3 &= 2(a^2\wedge + \xi a a') \\
B_4 &= 6 a a_3 \wedge + 4\xi a a_3' - a\wedge(1 + S_w) \\
B_5 &= -b_4\wedge + 6 a_3^2 \wedge + 8 a a_4 \wedge + 6\xi a a_4' + 4\xi a_3 a_3'
\end{aligned} \quad (3.19)$$

$$-45a^{'} a_4 - 4ab\wedge - a_{\square}\wedge(1+S_w)$$

Integration of Eq. (3.17) with respect to η yields the following result:

$$\frac{\partial f}{\partial \eta} = \int_0^{\eta} \exp(-\tau)\,\varphi \frac{d\eta}{d\tau}\, d\tau \qquad (3.20)$$

To further simplify the above integral, let

$$\varphi \frac{d\eta}{d\tau} = \tau^{-2/3} \sum_{m=0}^{\infty} d_m \tau^{m/3} \qquad (3.21)$$

or

$$\frac{\varphi \frac{d\eta}{d\tau}}{\tau^{\frac{1}{3}(m+1)}}\, d\tau = d_m \iiint \frac{d\tau}{\tau} = 3(2\pi i)\, d_m \qquad (3.22)$$

Here, the integration is carried out in a manner as described in Subsection 3.1. Therefore, d_m is one-third of the coefficient of η^{-1} in the expression $\varphi\,\tau^{-1/3(m+1)}$ expanded in ascending powers of η, i.e., d_m is one-third of the coefficient of η^m in the expression

$$\left(c_o + c_1\eta + c_2\eta^2 + \ldots\right)^{-1/3(m+1)} \left(B_o + B_1\eta + \frac{B_2\eta^2}{2!} + \frac{B_3\eta^3}{3!} + \ldots\right)$$

The first six coefficients of Eq. (3.21) are summarized below.

$$d_0 = \frac{B_o}{3} c_o^{-1/3}$$

$$d_1 = \frac{1}{3}\, c_o^{-2/3} \left(B_1 - \frac{2}{3} B_o \frac{c_1}{c_o} \right)$$

$$d_2 = \frac{1}{3} \left\{ - B_o c_2 c_o^{-2} + B_o c_1^2 c_o^{-3} - B_1 c_1 c_o^{-2} + \frac{B_2}{2} c_o^{-1} \right\}$$

$$d_3 = \frac{1}{3} \left\{ - \frac{4}{3} B_o c_3 c_o^{-7/3} + \frac{28}{9} B_o c_1 c_2 c_o^{-10/3} - \frac{140}{81} c_1^3 B_o c_o^{-13/3} \right.$$

$$- \frac{4}{3} B_1 c_2 c_o^{-7/3} + \frac{14}{9} B_1 c_1^2 c_o^{-10/3} - \frac{2}{3} B_2 c_1 c_o^{-7/3}$$

$$\left. + \frac{B_3}{6} c_o^{-4/3} \right\} \qquad (3.23)$$

$$d_4 = \frac{1}{3} \left\{ - \frac{5}{3} c_4 B_o c_o^{-8/3} + \frac{20}{9} c_2^2 B_o c_o^{-11/3} + \frac{40}{9} c_1 c_3 B_o c_o^{-11/3} - \frac{220}{27} c_1^2 c_2 B_o c_o^{-14/3} + \frac{770}{243} c_1^4 B_o c_o^{-17/3} \right.$$

$$- \frac{5}{3} c_3 B_1 c_o^{-8/3} + \frac{40}{9} c_1 c_2 B_1 c_o^{-11/3} - \frac{220}{81} c_1^3 B_1 c_o^{-14/3}$$

$$- \frac{5}{6} c_2 B_2 c_o^{-8/3} + \frac{10}{9} c_1^2 B_2 c_o^{-11/3} - \frac{5}{18} c_1 B_3 c_o^{-8/3}$$

$$\left. + \frac{B_4}{24} c_o^{-5/3} \right\}$$

$$d_5 = \frac{1}{3}\left\{(-2c_5c_o^{-3} + 6c_1c_4c_o^{-4} + 6c_2c_3c_o^{-4} - 12c_1^2c_3c_o^{-5}\right.$$

$$- 12c_2^2c_1c_o^{-5} + 20c_1^3c_2c_o^{-6} + 6c_1^5c_o^{-7})B_o + (-2c_4c_o^{-3} + 3c_2^2$$

$$c_o^{-4} + 6c_1c_3c_o^{-4} - 12c_1^2c_2c_o^{-5} + 5c_1^4c_o^{-6})B_1 + (-2c_3c_o^{-3} +$$

$$6c_1c_2c_o^{-4} - 4c_1^3c_o^{-5})\frac{B_2}{2} + (-2c_2c_o^{-3} + 3c_1^2c_o^{-4})\frac{B_3}{6}$$

$$\left. - \frac{B_4}{12}c_1c_o^{-3} + \frac{B_5}{120}c_o^{-2}\right\}$$

Substituting Eq. (3.21) into Eq. (3.20) and extending the upper limit of integration to infinity, one obtains boundary condition at the edge of the boundary layer as

$$\frac{\partial f}{\partial \eta}(\xi, \infty) = \sum_{m=0}^{\infty} d_m \Gamma\left(\frac{m+1}{3}\right) = 1 \qquad (3.24)$$

where the symbol Γ stands for gamma function.

(b) Energy Equation

Equation (3.1) is a linear, nonhomogeneous partial differential equation. The procedure for the integration of Eq. (3.1) is the same as described in Subsection 3.1(a).

Substituting Eqs. (3.4) and (3.5) into the right-hand-side of Eq. (3.1) yields

$$\frac{\partial^2 S}{\partial \eta^2} + f \frac{\partial S}{\partial \eta} = P_e (\xi, \eta)$$

where

$$P_e (\xi, \eta) = 2\xi \left[\sum_{n=2}^{\infty} \sum_{m=0}^{\infty} \frac{a_n}{(n-1)!} \frac{b'_m}{m!} \eta^{m+n-1} \right. \qquad (3.25)$$

$$\left. - \sum_{m=1}^{\infty} \sum_{n=2}^{\infty} \frac{m}{(m-1)!} \frac{a'_n}{n!} \eta^{n+m-1} \right]$$

Using the same integrating factor and integrating Eq. (3.25), one obtains

$$\frac{\partial S}{\partial \eta} = \exp(-\tau) \cdot \left[b(\xi) + \int_0^{\eta} \exp(\tau) P_e (\xi, \eta) \, d\eta \right] \qquad (3.26)$$

To facilitate further integration, let, as before,

$$\varphi_e (\xi, \eta) = \int_0^{\eta} \exp(\tau) P_e (\xi, \eta) d\eta = \sum_{m=0}^{\infty} \frac{\chi_m (\xi)}{m!} \eta^m \qquad (3.27)$$

Substituting Eqs. (3.5), (3.8), and (3.27) into Eq. (3.26) and equating equal powers of η on both sides results in the following definitions for χ_m

$$\begin{aligned} \chi_0 &= 0 \\ \chi_1 &= 0 \\ \chi_2 &= 0 \\ \chi_3 &= 2\xi (2ab' - ba') \\ \chi_4 &= 2\xi (3a_3 b' - b a'_3) \end{aligned} \qquad (3.28)$$

$$\chi_5 = a_4 b + b_6$$

. . . . .

etc.,

After integrating once, Eq. (3.26) becomes

$$S(\xi,\eta) = \int_0^\eta \exp(-\tau)\,\varphi_e \frac{d\eta}{d\tau}\,d\tau + S_w + b\int_0^\eta \exp(-\tau)\frac{d\eta}{d\tau}\,d\tau \qquad (3.29)$$

Again, let

$$\varphi_e \frac{d\eta}{d\tau} = \tau^{-2/3} \sum_{m=0}^{\infty} D_m \tau^{m/3} \qquad (3.30)$$

where the coefficients D_m are

$$D_0 = 0$$

$$D_1 = 0$$

$$D_2 = 0$$

$$D_3 = \frac{\chi_3}{18} c_o^{-4/3} \qquad (3.31)$$

$$D_4 = \frac{1}{3}\left[-\frac{5}{18}\chi_3 c_1 c_o^{-8/3} + \frac{\chi_4}{24} c_o^{-5/3}\right]$$

$$D_5 = \frac{1}{3}\left[\frac{\chi_3}{6}(-2c_2 c_o^{-3} + 3c_1^2 c_o^{-4}) - \frac{\chi_4}{12} c_1 c_o^{-3} + \frac{\chi_5}{120} c_o^{-2}\right]$$

. . . . . .

etc.,

The information needed for the evaluation of the second integral in Eq. (3.29) has been made available in Subsection 3.1. After integration the result obtained is given below.

$$\int_0^{\eta} \exp(-\tau)\ \frac{d\eta}{d\tau}\ d\tau = \frac{1}{3} \sum_{m=0}^{\infty} A_m\ \Gamma\left(\frac{m+1}{3}\right) \qquad (3.31(a))$$

where A_m's are defined in Eq. (3.14).

Therefore, using the boundary conditions for the enthalpy function S, Eq. (3.29) becomes

$$b(\xi) = \left[-S_w - \sum_{m=0}^{\infty} D_m\ \Gamma\left(\frac{m+1}{3}\right)\right]\left[\frac{1}{3}\sum_{m=0}^{\infty} A_m\ \Gamma\left(\frac{m+1}{3}\right)\right]^{-1} \qquad (3.32)$$

Eqs. (3.24) and (3.32) are coupled together. They contain two unknown parameters $a(\xi)$ and $b(\xi)$ and their derivatives. The solutions obtained and the transformations given above are only valid within a finite radius of convergence of η. The range of η in the solution has been extended to infinity because of the lack of exact knowledge of the edge of the boundary layer. For this reason, the series expansions become divergent and they have to be summed by Euler's transformation as shown in Section IV.

(c) Displacement Thickness

It is apparent from the above discussion that the Eqs. (3.24) and (3.32) contain not only the unknown parameters $a(\xi)$ and $b(\xi)$ but also the pressure gradient term $\Lambda(\xi)$. If the pressure distribution is known for low speed flows either by experiment or by inviscid flow theory, it is a simple matter to determine

the unknowns "a" and "b" from the two Eqs. (3.24) and (3.32). However, this is not the case in hypersonic flow. Here, the presence of various interactions (such as pressure interaction, vorticity interaction, etc.,) adds another unknown pressure gradient parameter $\Lambda(\xi)$, hence another equation is necessary to balance the number of unknowns and the number of equations. This additional equation could be either the tangent wedge formula for the two-dimensional case (or the tangent cone formula for the axisymmetric case) or the use of the method of characteristics. Since the tangent wedge formula is relatively simple and at the same time provides enough accuracy for very slender bodies [3,39], this formula has been used in this investigation.

The tangent wedge formula is derived in Section II (Eq. (2.51)). However, Eqs. (2.51) and (2.49) contain three unknown integrals, defined in Eq. (2.30(a)). These integrals will now be evaluated.

Substituting Eq. (3.17) and (3.18) into the definition of the integral I_1, one obtains

$$I_1 = \int_0^\infty \exp(-\tau)\, \varphi \frac{d\eta}{d\tau}\, \eta\, d\tau \tag{3.33}$$

To simplify this integral, let

$$\varphi \frac{d\eta}{d\tau}\, \eta = \tau^{-2/3} \sum_{m=1}^{\infty} D1_m\, \tau^{m/3}$$

With a procedure similar to that used in Subsection 3.1(a), one obtains the following for $D1_m$:

$$D1_1 = \frac{1}{3} B_o c_o^{-2/3}$$

$$D1_2 = \frac{1}{3}(-B_o c_1 c_o^{-2} + B_1 c_o^{-1})$$

$$D1_3 = \frac{1}{3}\left\{ B_o \left(-\frac{4}{3} c_2 c_o^{-7/3} + \frac{14}{9} c_1^2 c_o^{-10/3}\right) - \frac{4}{3} B_1 c_1 c_o^{-7/3} + \frac{B_2}{2} c_o^{-4/3} \right\}$$

$$D1_4 = \frac{1}{3}\left\{ B_o \left(-\left(5/3\ c_3 c_o^{-8/3} + \frac{40}{9} c_1 c_2 c_o^{-11/3} - \frac{220}{81} c_1^3 c_o^{-14/3}\right) + B_1 \left(-\frac{5}{3} c_2 c_o^{-8/3} + \frac{20}{9} c_1^2 c_o^{-11/3}\right) - \frac{5}{6} B_2 c_1 c_o^{-8/3} + \frac{B_3}{6} c_o^{-5/3} \right\} \right. \quad (3.34)$$

$$D1_5 = \frac{1}{3}\left\{ B_o \left(-2 c_4 c_o^{-3} + 3 c_2^2 c_o^{-4} + 6 c_1 c_3 c_o^{-4} - 12 c_1^2 c_2 c_o^{-5} + 5 c_1^4 c_o^{-6}\right) + B_1 \left(-2 c_3 c_o^{-3} + 6 c_1 c_2 c_o^{-4} - 4 c_1^3 c_o^{-5}\right) + \frac{B_2}{2} \left(-2 c_2 c_o^{-3} + 3 c_1^2 c_o^{-4}\right) - \frac{B_3}{3} c_1 c_o^{-3} + \frac{B_4}{24} c_o^{-2} \right\}$$

. . . . . .

It is now straightforward matter to write down the final form of Eq. (3.33) as

$$I_1 = \sum_{m=1}^{\infty} D1_m \Gamma\left(\frac{m+1}{3}\right) \tag{3.35}$$

To evaluate the integral I_2, one may write

$$I_2 = \int_0^{\infty} \exp(-\tau) \varphi \frac{\partial f}{\partial \eta} \eta \frac{d\eta}{d\tau} d\tau \tag{3.36}$$

For further simplification, let

$$\varphi \frac{\partial f}{\partial \eta} \eta \frac{d\eta}{d\tau} = \tau^{-2/3} \sum_{m=2}^{\infty} D2_m \tau^{m/3} \tag{3.37}$$

The following definitions for $D2_m$ are obtained by following the same procedure as described in Subsection 3.1(a).

$$D2_2 = \frac{B_o}{3} a c_o^{-1}$$

$$D2_3 = \left(\frac{B_o a_3}{6} - \frac{B_1 a}{3}\right) c_o^{-4/3} - \frac{4}{9} B_c a c_1 c_o^{-7/3}$$

$$D2_4 = \frac{1}{3} \left\{ \left(\frac{B_o a_4}{6} + \frac{B_1 a_3}{2} + \frac{B_2 a}{2}\right) c_o^{-5/3} - \frac{5}{3} \left[c_1 \left(\frac{B_o a_3}{2} + B_1 a\right) + B_o a c_2 \right] c_o^{-8/3} + \frac{20}{9} c_1^2 B_o a c_o^{-11/3} \right\} \tag{3.38}$$

$$D2_5 = \frac{1}{3}\left\{ B_o a \left(-2 c_3 c_o^{-3} + 6 c_1 c_2 c_o^{-4} - 4 c_1^3 c_o^{-5}\right)\right.$$

$$+ \left(\frac{B_o a_3}{2} + B_1 a\right)\left(-2 c_2 c_o^{-3} + 3 c_1^2 c_o^{-4}\right) - 2 c_1 c_o^{-3}$$

$$\left(\frac{B_o a_4}{6} + \frac{B_1 a_3}{2} + \frac{B_2 a}{2}\right) + \left(\frac{B_o a_5}{24} + \frac{B_1 a_4}{6} + \frac{B_2 a_3}{4}\right.$$

$$\left.\left. + \frac{B_3 a}{6}\right) c_o^{-2} \right\}$$

$$D2_6 = \frac{1}{3}\left\{ B_o a \left[-\frac{7}{3} c_4 c_o^{-10/3} + \frac{35}{9}\left(c_2^2 + 2 c_1 c_3\right) c_o^{-13/3}\right.\right.$$

$$\left. - \frac{455}{27} c_1^2 c_2 c_o^{-16/3} + \frac{1820}{243} c_1^4 c_o^{-19/3}\right] + \left(\frac{B_o a_3}{2} + B_1 a\right)$$

$$\left(-\frac{7}{3} c_3 c_o^{-10/3} + \frac{70}{9} c_1 c_2 c_o^{-13/3} - \frac{455}{81} c_1^3 c_o^{-16/3}\right) +$$

$$\left(\frac{B_o a_4}{6} + \frac{B_1 a_3}{2} + \frac{B_2 a}{2}\right)\left(-\frac{7}{3} c_2 c_o^{-10/3} + \frac{35}{9} c_1^2 c_o^{-13/3}\right)$$

$$- \frac{7}{3} c_1 c_o^{-10/3}\left(\frac{B_o a_5}{24} + \frac{B_1 a_4}{6} + \frac{B_2 a_3}{4} + \frac{B_3 a}{6}\right) + \left(\frac{B_o a_6}{120}\right.$$

$$\left. + \frac{B_1 a_5}{24} + \frac{B_2 a_4}{12} + \frac{B_3 a_3}{12} + \frac{B_4 a}{24}\right) c_o^{-7/3}$$

. . . . . .

Therefore, Eq. (3.36) reduces to

$$I_2 = \sum_{m=2}^{\infty} D2_m \left(\frac{m+1}{3}\right) \tag{3.39}$$

Substitution of Eqs. (3.26) and (3.27) into the definition of the integral I_3 leads to

$$I_3 = \int_0^{\infty} \exp(-\tau)\ \varphi_e\ \eta\ \frac{d\eta}{d\tau}\ d\tau \tag{3.40}$$

To simplify further, let

$$\varphi_e\ \eta\ \frac{d\eta}{d\tau} = \tau^{-2/3} \sum_{m=1}^{\infty} D3_m\ \tau^{m/3} \tag{3.41}$$

The coefficients $D3_m$ are obtained in a similar way,

$$D3_1 = \frac{1}{3}\ \chi_o\ c_o^{-2/3}$$

$$D3_2 = -\frac{\chi_o}{3}\ c_1\ c_o^{-2}$$

$$D3_3 = \frac{\chi_o}{3}\left(-\frac{4}{3} c_2\ c_o^{-7/3} + \frac{14}{9}\ c_1^2\ c_o^{-10/3}\right)$$

$$D3_4 = \frac{1}{3}\left[\chi_o\left(-\frac{5}{3} c_3\ c_o^{-8/3} + \frac{40}{9} c_1\ c_2\ c_o^{-11/3} - \frac{220}{81}\ c_1^3\ c_o^{-14/3}\right) + \frac{\chi_3}{6}\ c_o^{-5/3}\right] \tag{3.42}$$

$$D3_5 = \frac{1}{3}\left[\chi_o \left(-2 c_4 c_o^{-3} + 3 c_2^2 c_o^{-4} + 6 c_1 c_3 c_o^{-4} - 12 c_1^2 \right.\right.$$

$$\left.\left. c_2 c_o^{-5} + 5 c_1^4 c_o^{-6} \right) - \frac{\chi_3}{3} c_1 c_o^{-3} + \frac{\chi_4}{24} c_o^{-2} \right]$$

. . . . . .

Equation (3.40) now becomes

$$I_3 = \sum_{m=1}^{\infty} D3_m \Gamma\left(\frac{m+1}{3}\right) \qquad (3.43)$$

With the integrals I_1, I_2, I_3 evaluated, one can now make use of the pressure distribution formula. The three unknowns $a(\xi)$, $b(\xi)$ and $\wedge(\xi)$ can be determined by simultaneously solving Eqs. (3.24) and (3.32) and the pressure distribution formula.

3.2 Separation Point

The difference between the separation point and ordinary point is the fact that the value of $a(\xi)$ (i.e., $\frac{\partial^2 f}{\partial \eta^2}$ at $\eta = 0$) is small near and downstream of the separation point. Because of this separate analyses are required for each region. The major difference between the ordinary point analysis and the separation point analysis lies in the inversion of the series in order to integrate the energy and momentum equations (i.e., Eqs. (3.1) and (3.2) respectively), the additional condition at the separation point is

$$a = \frac{\partial^2 f}{\partial \eta^2} = 0 \text{ at } \eta = 0 \qquad (3.44)$$

whence $f(\xi, \eta)$ starts with the term η^3.

Since the expressions will be applied to the flow downstream of separation, let

$$F = \int_0^\eta f \, d\eta \tag{3.45}$$

or

$$\exp(-F) = \exp\left(-\frac{a\eta^3}{6}\right) \exp(-\tau_S)$$

where

$$\tau_S = \frac{a_3 \eta^4}{4!} + \frac{a_4 \eta^5}{5!} + \frac{a_5 \eta^6}{6!} + \ldots$$

$$= \eta^4 \sum_{n=0}^{\infty} \frac{a_{n+3}}{(n+4)!} \eta^n \tag{3.46}$$

One can expand the exponential term in series as

$$\exp\left(-\frac{a\eta^3}{6}\right) = 1 - \frac{a\eta^3}{6} + \frac{a^2\eta^6}{72} - \frac{a^3\eta^9}{1296} + \ldots \tag{3.47}$$

Inverting the series of Eq. (3.46) as described in Subsection 3.1, one arrives at the following results:

$$\eta = \sum_{m=0}^{\infty} \frac{AS_m}{m+1} \tau_S^{\left(\frac{m+1}{4}\right)} \tag{3.48}$$

where

$$AS_o = \left(\frac{a_3}{24}\right)^{-1/4}$$

$$AS_1 = -\frac{a_4}{240} \left(\frac{a_3}{24}\right)^{-3/2}$$

$$AS_2 = -\frac{a_5}{960}\left(\frac{a_3}{24}\right)^{-7/4} + \frac{21}{32}\left(\frac{a_4}{120}\right)^2\left(\frac{a_3}{24}\right)^{-11/4} \tag{3.49}$$

$$AS_3 = -\frac{a_6}{5040}\left(\frac{a_3}{24}\right)^{-2} + 2\left(\frac{a_4}{120}\right)\left(\frac{a_5}{720}\right)\left(\frac{a_3}{24}\right)^{-3} - \left(\frac{a_4}{120}\right)^3\left(\frac{a_3}{24}\right)^{-4}$$

$$AS_4 = -\frac{5}{4}\left(\frac{a_7}{40320}\right)\left(\frac{a_3}{24}\right)^{-9/4} + \frac{45}{32}\left[\left(\frac{a_5}{720}\right)^2 + 2\left(\frac{a_4}{120}\right)\left(\frac{a_6}{5040}\right)\right]\left(\frac{a_3}{24}\right)^{-13/4} - \frac{585}{128}\left(\frac{a_4}{120}\right)^2\frac{a_5}{720}\left(\frac{a_3}{24}\right)^{-17/4} + \frac{9945}{6144}\left(\frac{a_4}{120}\right)^4\left(\frac{a_3}{24}\right)^{-21/4}$$

. . . . .

It is to be noted that the coefficients "a_m" are already obtained in Section III (see Eq. (3.6)). The coefficients AS_m do not contain the unknown parameter $a(\xi)$ in the denominator. Thus, the singularity is avoided.

(a) Momentum Equation

The integration of the momentum Eq. (3.2) will remain the same up to the development of Eq. (3.19) as in Subsection 3.1(a). Since there is difference between τ and τ_s, the counterpart of Eq. (3.17) for the separation problem is

$$\frac{\partial^2 f}{\partial \eta^2} = \varphi\left(1 - \frac{a\eta^3}{6} + \frac{a^2\eta^6}{72} - \ldots\right) \exp\left(-\tau_s\right) \tag{3.50}$$

After integrated once, Eq. (3.50) becomes

$$\frac{\partial f}{\partial \eta} = \int_0^{\eta} \exp(-\tau_S)\, \varphi \left(1 - \frac{a\eta^3}{6} + \frac{a^2\eta^6}{72} - \ldots\right) \frac{d\eta}{d\tau_S}\, d\tau_S \tag{3.51}$$

For simplification, let

$$\varphi \left(1 - \frac{a\eta^3}{6} + \frac{a^2\eta^6}{72} - \ldots\right) \frac{d\eta}{d\tau_S} = \tau^{-3} \sum_{m=0}^{\infty} dS_m \tau^{m/4} \tag{3.52}$$

Similar to the procedure used in the ordinary point anulyses, one can identify the coefficients dS_m as

$$dS_o = \frac{B_o}{4} \left(\frac{a_3}{24}\right)^{-1/4}$$

$$dS_1 = \frac{1}{4}\left[-\frac{1}{2}\left(\frac{a_4}{120}\right) B_o \left(\frac{a_3}{24}\right)^{-3/2} + B_1 \left(\frac{a_3}{24}\right)^{-1/2}\right]$$

$$dS_2 = \frac{1}{4}\left\{B_o\left[-\frac{3}{4}\left(\frac{a_5}{720}\right)\left(\frac{a_3}{24}\right)^{-7/4} + \frac{21}{32}\left(\frac{a_4}{120}\right)^2 \left(\frac{a_3}{24}\right)^{-11/4}\right.\right.$$

$$\left.\left. - \frac{3}{4} B_1 \left(\frac{a_4}{120}\right)\left(\frac{a_3}{24}\right)^{-7/4} + \frac{B_2}{2}\left(\frac{a_3}{24}\right)^{-3/4}\right\}\right.$$

$$dS_3 = \frac{B_o}{4}\left[-\frac{a_6}{5040}\left(\frac{a_3}{24}\right)^{-2} + 2\left(\frac{a_4}{120}\right)\left(\frac{a_5}{720}\right)\left(\frac{a_3}{24}\right)^{-3}\right.$$

$$\left. -\left(\frac{a_4}{120}\right)^3 \left(\frac{a_3}{24}\right)^{-4}\right] + \frac{B_1}{4}\left[-\frac{a_5}{720}\left(\frac{a_3}{24}\right)^{-2} + \left(\frac{a_4}{120}\right)^2 \left(\frac{a_3}{24}\right)^{-3}\right]$$

$$- \frac{B_2}{8} \left(\frac{a_4}{120}\right)\left(\frac{a_3}{24}\right)^{-2} + \left(\frac{B_3 - aB_o}{24}\right)\left(\frac{a_3}{24}\right)^{-1}$$

$$dS_4 = \frac{1}{4}\Bigg\{ B_o \Bigg[- \frac{5}{4}\left(\frac{a_7}{40320}\right)\left(\frac{a_3}{24}\right)^{-9/4} + \frac{45}{32}\left(\left(\frac{a_5}{720}\right)^2 + 2 \left(\frac{a_4}{120}\right)\left(\frac{a_6}{5040}\right)\right)\left(\frac{a_3}{24}\right)^{-13/4} - \frac{585}{128}\left(\frac{a_4}{120}\right)^2 \frac{a_5}{720}\left(\frac{a_3}{24}\right)^{-17/4} +$$

$$\frac{3315}{2048}\left(\frac{a_4}{120}\right)^4\left(\frac{a_3}{24}\right)^{-21/4}\Bigg] + B_1\Bigg[- \frac{5}{4}\left(\frac{a_6}{5040}\right)\left(\frac{a_3}{24}\right)^{-9/4}$$

$$+ \frac{45}{16}\left(\frac{a_4}{120}\right)\frac{a_5}{720}\left(\frac{a_3}{24}\right)^{-13/4} - \frac{195}{128}\left(\frac{a_4}{120}\right)^3\left(\frac{a_3}{24}\right)^{-17/4}\Bigg]$$

$$+ \frac{B_2}{2}\Bigg[- \frac{5}{4}\left(\frac{a_5}{720}\right)\left(\frac{a_3}{24}\right)^{-9/4} + \frac{45}{32}\left(\frac{a_4}{120}\right)^2\left(\frac{a_3}{24}\right)^{-13/4}\Bigg]$$

$$- \frac{5}{4}\left(\frac{B_3 - aB_o}{6}\right)\left(\frac{a_4}{120}\right)\left(\frac{a_3}{24}\right)^{-9/4} + \left(\frac{B_4}{24} - \frac{aB_1}{6}\right)\left(\frac{a_3}{24}\right)^{-5/4}\Bigg\}$$

. . . . . (3.53)

If the upper limit of integration is extended to infinity, Eq. (3.51) becomes

$$\frac{\partial f}{\partial \eta}(\xi, \infty) = \sum_{m=0}^{\infty} dS_m \, \Gamma\left(\frac{m+1}{4}\right) = 1 \qquad (3.54)$$

therefore, this is the boundary condition at the edge of the boundary layer near and downstream of the separation point.

(b) Energy Equation

Following the same procedure as used in Subsection 3.1 (b) up to the development of Eq. (3.28), Eq. (3.1) becomes

$$\frac{\partial s}{\partial \eta} = e^{-\tau_S} \left(1 - \frac{a\eta^3}{6} + \frac{a^2\eta^6}{72} - \ldots\right) \varphi S_e \qquad (3.55)$$

where $\varphi S_e = b + \sum_{m=0}^{\infty} \frac{\chi_m}{m!} \eta^m$

and χ_m are defined in Eq. (3.28).

It is to be noted that the above equation is obtained after replacing the expression for τ in Eq. (3.26) with an equivalent definition from Eqs. (3.45) and (3.47).

Integrating once, Eq. (3.55) becomes

$$S(\xi, \eta) = \int_0^{\eta} \exp(-\tau_S) \left[\left(1 - \frac{a\eta^3}{6} + \frac{a^2\eta^6}{72} - \ldots \varphi S_e\right)\right] \frac{d\eta}{d\tau_S} d\tau_S \qquad (3.56)$$

To simplify the integral in Eq. (3.56), let

$$\varphi S_e \left(1 - \frac{a\eta^3}{6} + \frac{a^2\eta^6}{72} - \ldots\right) \frac{d\eta}{d\tau_S} = \tau^{-3/4} \sum_{m=0}^{\infty} DS_m \tau^{m/4} \qquad (3.57)$$

With a procedure similar to that used in Subsection 3.1 (a), one obtains the coefficients DS_m as

$$DS_o = b_{/4} \left(\frac{a_3}{24}\right)^{-1/4}$$

$$DS_1 = -b/8 \left(\frac{a_4}{120}\right) \left(\frac{a_3}{24}\right)^{-3/2}$$

$$DS_2 = \left[\frac{b}{4} - \frac{3}{4}\left(\frac{a_5}{720}\right)\left(\frac{a_3}{24}\right)^{-7/4} + \frac{21}{32}\left(\frac{a_4}{120}\right)^2\left(\frac{a_3}{24}\right)^{-11/4}\right]$$

$$DS_3 = \left[\frac{b}{4} - \frac{a_6}{5040}\left(\frac{a_3}{24}\right)^{-2} + 2\left(\frac{a_4}{120}\right)\left(\frac{a_5}{720}\right)\left(\frac{a_3}{24}\right)^{-3} - \left(\frac{a_4}{120}\right)^3\left(\frac{a_3}{24}\right)^{-4}\right] + \left(\frac{\chi_3 - ab}{24}\right)\left(\frac{a_3}{24}\right)^{-1}$$

$$DS_4 = -\frac{1}{4}\left\{ b\left[-\frac{5}{4}\left(\frac{a_7}{40320}\right)\left(\frac{a_3}{24}\right)^{-9/4} + \frac{45}{32}\left(\left(\frac{a_5}{720}\right)^2 + \frac{a_4}{60}\left(\frac{a_6}{5040}\right)\right)\left(\frac{a_3}{24}\right)^{-13/4}\right] - \frac{585}{128}\left(\frac{a_4}{120}\right)^2\left(\frac{a_5}{720}\right)\left(\frac{a_3}{24}\right)^{-17/4} + \frac{3315}{2048}\left(\frac{a_4}{120}\right)^4\left(\frac{a_3}{24}\right)^{-21/4} - \frac{5}{4}\left(\frac{\chi_3 - ab}{6}\right)\frac{a_4}{120}\left(\frac{a_3}{24}\right)^{-9/4} + \frac{\chi_4}{24}\left(\frac{a_3}{24}\right)^{-5/4}\right\} \qquad (3.58)$$

. . . . . .

If the upper limit of integration is extended to infinity, Eq. (3.56) reduces to

$$S(\xi, \infty) = \sum_{m=0}^{\infty} DS_m \Gamma\left(\frac{m+1}{4}\right) = 0 \qquad (3.59)$$

This is the boundary condition for the enthalpy function at the edge of the boundary layer.

(c) Displacement Thickness

The main task here is to develop the expressions for the integrals I_1, I_2, and I_3. Since the procedure is essentially the same as that described in Subsection 3.1 (c), the definition of these integrals and the end results are given below.

$$I_1 = \int_{\infty}^{\infty} \exp(-\tau_s)\, \varphi\left(1 - \frac{a\eta^3}{6} + \frac{a^2\eta^6}{72} - \cdots\right)\eta \frac{d\eta}{d\tau_s} d\tau_s \qquad (3.60)$$

or

$$I_1 = \sum_{m=1}^{\infty} DS1_m \Gamma\left(\frac{m+1}{4}\right)$$

where

$$DS1_1 = \frac{B_o}{4}\left(\frac{a_3}{24}\right)^{-1/2}$$

$$DS1_2 = \frac{1}{4}\left[-\frac{3}{4}\left(\frac{a_4}{120}\right) B_o \left(\frac{a_3}{24}\right)^{-7/4} + B_1\left(\frac{a_3}{24}\right)^{-3/4}\right]$$

$$DS1_3 = \frac{1}{4}\left\{ B_o\left[-\frac{a_5}{720}\left(\frac{a_3}{24}\right)^{-2} + \left(\frac{a_4}{120}\right)^2\left(\frac{a_3}{24}\right)^{-3}\right]\right.$$

$$\left. - B_1\left(\frac{a_4}{120}\right)\left(\frac{a_3}{24}\right)^{-2} + \frac{B_2}{2}\left(\frac{a_3}{24}\right)^{-1}\right.$$

$$DS1_4 = \frac{1}{4}\Big\{B_o\Big[-\frac{5}{4}\Big(\frac{a_6}{5040}\Big)\Big(\frac{a_3}{24}\Big)^{-9/4} + \frac{45}{16}\Big(\frac{a_4}{120}\Big)$$

$$\Big(\frac{a_5}{720}\Big)\Big(\frac{a_3}{24}\Big)^{-13/4} - \frac{195}{128}\Big(\frac{a_4}{120}\Big)^3\Big(\frac{a_3}{24}\Big)^{-17/4}\Big] + B_1$$

$$\Big[-\frac{5}{4}\Big(\frac{a_5}{720}\Big)\Big(\frac{a_3}{24}\Big)^{-9/4} + \frac{45}{32}\Big(\frac{a_4}{120}\Big)^2\Big(\frac{a_3}{24}\Big)^{-13/4}\Big]$$

$$-\frac{5}{8}B_2\Big(\frac{a_4}{120}\Big)\Big(\frac{a_3}{24}\Big)^{-9/4} + \Big(\frac{B_3 - aB_o}{6}\Big)\Big(\frac{a_3}{24}\Big)^{-5/4}$$

$$DS1_5 = \frac{1}{4}\Big\{B_o\Big[-\frac{3}{2}\Big(\frac{a_7}{40320}\Big)\Big(\frac{a_3}{24}\Big)^{-5/2} + \frac{15}{8}$$

$$\Big(\Big(\frac{a_5}{720}\Big)^2 + 2\Big(\frac{a_4}{120}\Big)\Big(\frac{a_6}{5040}\Big)\Big)\Big(\frac{a_3}{24}\Big)^{-7/2} - \frac{105}{16}\Big(\frac{a_4}{120}\Big)^2$$

$$\frac{a_5}{720}\Big(\frac{a_3}{24}\Big)^{-9/2} + \frac{315}{128}\Big(\frac{a_4}{120}\Big)^4\Big(\frac{a_3}{24}\Big)^{-11/2}\Big] + B_1$$

$$\Big[-\frac{3}{2}\Big(\frac{a_6}{5040}\Big)\Big(\frac{a_3}{24}\Big)^{-5/2} + \frac{15}{4}\Big(\frac{a_4}{120}\Big)\Big(\frac{a_5}{720}\Big)\Big(\frac{a_3}{24}\Big)^{-7/2} -$$

$$\frac{35}{16}\Big(\frac{a_4}{120}\Big)^3\Big(\frac{a_3}{24}\Big)^{-9/2}\Big] + \frac{B_2}{2}\Big[-\frac{3}{2}\Big(\frac{a_5}{720}\Big)\Big(\frac{a_3}{24}\Big)^{-5/2} +$$

$$\frac{15}{8}\left(\frac{a_4}{120}\right)^2\left(\frac{a_3}{24}\right)^{-7/2}\Bigg] - \frac{3}{2}\left(\frac{B_3 - aB_0}{6}\right)\frac{a_4}{120}$$

$$\left(\frac{a_3}{24}\right)^{-5/2} + \frac{B_4 - 4aB_1}{24}\left(\frac{a_3}{24}\right)^{-3/2}\Bigg\} \qquad (3.61)$$

. . . . .

etc.,

$$I_2 = \int_0^\infty e^{-\tau_S}\,\varphi\left(1 - \frac{a\eta^3}{6} + \frac{a^2\eta^6}{72} - \ldots\right)\frac{\partial f}{\partial \eta}\,\eta\,\frac{d\eta}{d\tau_S}\,d\tau_S \qquad (3.62)$$

or

$$I_2 = \sum_{m=2}^{\infty} dS2_m\,\Gamma\left(\frac{m+1}{4}\right)$$

where

$$DS2_2 = \frac{1}{4}B_o\,a\left(\frac{a_3}{24}\right)^{-3/4}$$

$$DS2_3 = \frac{1}{4}\left[-B_o\,a\left(\frac{a_4}{120}\right)\left(\frac{a_3}{24}\right)^{-2} + \left(\frac{B_o\,a_3}{2} + B_1 a\right)\left(\frac{a_3}{24}\right)^{-1}\right]$$

$$DS2_4 = \frac{1}{4}\Bigg\{B_o\,a\left[-\frac{5}{4}\left(\frac{a_5}{720}\right)\left(\frac{a_3}{24}\right)^{-9/4} + \frac{45}{32}\left(\frac{a_4}{120}\right)^2\left(\frac{a_3}{24}\right)^{-13/4}\right.$$

$$\left. - \frac{5}{4}\left(\frac{B_o\,a_3}{2} + B_1 a\right)\left(\frac{a_4}{120}\right)\left(\frac{a_3}{24}\right)^{-9/4} + \left(\frac{B_o\,a_4}{6} + \frac{B_1 a_3}{2}\right)\right.$$

$$+ \frac{B_2 a}{2}\left(\frac{a_3}{24}\right)^{-5/4}\Bigg]\Bigg\}$$

$$DS2_5 = \frac{1}{4}\Bigg\{ B_o a\Bigg[-\frac{3}{2}\left(\frac{a_6}{5040}\right)\left(\frac{a_3}{24}\right)^{-5/2} + \frac{15}{4}\left(\frac{a_4}{120}\right)\left(\frac{a_5}{720}\right)$$

$$\left(\frac{a_3}{24}\right)^{-7/2} - \frac{35}{16}\left(\frac{a_4}{120}\right)^3\left(\frac{a_3}{24}\right)^{-9/2}\Bigg] + \left(\frac{B_o a_3}{2} + B_1 a\right)$$

$$-\left[\frac{3}{2}\left(\frac{a_5}{720}\right)\left(\frac{a_3}{24}\right)^{-5/2} + \frac{15}{8}\left(\frac{a_4}{120}\right)^2\left(\frac{a_3}{24}\right)^{-7/2}\right] - \frac{3}{2}$$

$$\left[\frac{B_o a_4}{6} + \frac{B_1 a_3}{2} + \frac{B_2 a}{2}\right]\frac{a_4}{120}\left(\frac{a_3}{24}\right)^{-5/2} + \left[\frac{B_o a_5}{24} +$$

$$\frac{B_1 a_4}{6} + \frac{B_2 a_3}{4} + \frac{B_3 a}{6}\right]\left(\frac{a_3}{24}\right)^{-3/2}\Bigg\}$$

$$DS2_6 = \frac{1}{4}\Bigg\{ B_o a\Bigg[-\frac{7}{4}\left(\frac{a_7}{40320}\right)\left(\frac{a_3}{24}\right)^{-11/4} + \frac{77}{32}\Bigg(\left(\frac{a_5}{720}\right)^2$$

$$+ 2\left(\frac{a_4}{120}\right)\left(\frac{a_6}{5040}\right)\Bigg)\left(\frac{a_3}{24}\right)^{-15/4} - \frac{1155}{128}\left(\frac{a_4}{120}\right)^2\frac{a_5}{720}$$

$$\left(\frac{a_3}{24}\right)^{-19/4} + \frac{7315}{2048}\left(\frac{a_4}{120}\right)^4\left(\frac{a_3}{24}\right)^{-23/4}\Bigg] + \left[\frac{B_o a_3}{2} + B_1 a\right]$$

$$-\left[\frac{7}{4}\left(\frac{a_6}{5040}\right)\left(\frac{a_3}{24}\right)^{-11/4} + \frac{77}{16}\left(\frac{a_4}{120}\right)\frac{a_5}{720}\left(\frac{a_3}{24}\right)^{-15/4}\right.$$

$$\left. - \frac{385}{128}\left(\frac{a_4}{120}\right)^3\left(\frac{a_3}{24}\right)^{-19/4}\right] + \left[\frac{B_o a_4}{6} + \frac{B_1 a_3}{2} + \frac{B_2 a}{2}\right]$$

$$\left[-\frac{7}{4}\left(\frac{a_5}{720}\right)\left(\frac{a_3}{24}\right)^{-11/4} + \frac{77}{32}\left(\frac{a_4}{120}\right)^2\left(\frac{a_3}{24}\right)^{-15/4}\right] - \frac{7}{4}$$

$$\left[\frac{B_o a_5}{24} + \frac{B_1 a_4}{6} + \frac{B_2 a_3}{4} + \frac{B_3 a}{6}\right]\frac{a_4}{120}\left(\frac{a_3}{24}\right)^{-11/4} +$$

$$\left.\left[\frac{B_o a_6}{120} + \frac{B_1 a_5}{24} + \frac{B_2 a_4}{12} + \frac{B_3 a_3}{12} + \frac{B_4 a}{24}\right]\left(\frac{a_3}{24}\right)^{-7/4}\right\}$$

etc., (3.63)

and

$$I_3 = \int_0^\infty e^{-\tau_S}\, \varphi S_e \left(1 - \frac{a\eta^3}{6} + \frac{a^2\eta^6}{72} - \ldots\right)\eta\, \frac{d\eta}{d\tau_S}\, d\tau_S \qquad (3.64)$$

or

$$I_3 = \sum_{m=1}^{\infty} DS3_m\, \Gamma\left(\frac{m+1}{4}\right)$$

where

$$DS3_1 = \frac{b}{4}\left(\frac{a_3}{24}\right)^{-1/2}$$

$$DS3_2 = -\frac{3}{16}\left(\frac{a_4}{120}\right) b \left(\frac{a_3}{24}\right)^{-7/4}$$

$$DS3_3 = \frac{1}{4}\left\{ b \left[-\frac{a_5}{720}\left(\frac{a_3}{24}\right)^{-2} + \left(\frac{a_4}{120}\right)^2 \left(\frac{a_3}{24}\right)^{-3} \right] \right\}$$

$$DS3_4 = \frac{1}{4}\left\{ b \left[-\frac{5}{4}\left(\frac{a_6}{5040}\right)\left(\frac{a_3}{24}\right)^{-9/4} + \frac{45}{16}\left(\frac{a_4}{120}\right)\frac{a_5}{720} \right.\right.$$

$$\left.\left. \left(\frac{a_3}{24}\right)^{-13/4} - \frac{195}{128}\left(\frac{a_4}{120}\right)^3 \left(\frac{a_3}{24}\right)^{-17/4} \right] + \left(\frac{\chi_3 - ab}{6}\right)\left(\frac{a_3}{24}\right)^{-5/4} \right\}$$

$$DS3_5 = \frac{1}{4}\left\{ b \left[-\frac{3}{2}\left(\frac{a_7}{40320}\right)\left(\frac{a_3}{24}\right)^{-5/2} + \frac{15}{8}\left(\left(\frac{a_5}{720}\right)^2 + 2 \right.\right.\right.$$

$$\left.\left.\left. \left(\frac{a_4}{120}\right)\left(\frac{a_6}{5040}\right) \right)\left(\frac{a_3}{24}\right)^{-7/2} - \frac{105}{16}\left(\frac{a_4}{120}\right)^2 \frac{a_5}{720}\left(\frac{a_3}{24}\right)^{-9/2} \right.\right.$$

$$\left.\left. + \frac{315}{128}\left(\frac{a_4}{120}\right)^4 \left(\frac{a_3}{24}\right)^{-11/2} \right] - \frac{3}{2}\left(\frac{\chi_3 - ab}{6}\right)\frac{a_4}{120}\left(\frac{a_3}{24}\right)^{-5/2} \right.$$

$$\left. + \frac{\chi_4}{24}\left(\frac{a_3}{24}\right)^{-3/2} \right\} \qquad (3.65)$$

etc.,

The integrals I_1, I_2, and I_3 are expressed in terms of the same unknowns $a(\xi)$, $b(\xi)$ and $\Lambda(\xi)$. These unknowns can be determined by simultaneously solving Eqs. (3.54) and (3.59) and the pressure distribution formula.

SECTION IV

NUMERICAL SOLUTIONS FOR A FLAT PLATE

It has been recognized for a long time that boundary layer theory is inadequate in the immediate neighborhood of the sharp leading edge of a flat plate. Almost two decades ago, Becker [53] drew interest to this problem when he published data showing the surface pressure much above the predictions of compressible boundary layer theory.

Very few reviews of the problem exist. Hayes and Probstein [3] gave a comprehensive review of the inviscid-viscous interaction phenomena. Later, Jain and Li [54] reviewed the departures that occur from strong interaction theory, both in experimental and theoretical terms. Recently, Pan and Probstein [55] briefly reviewed the entire problem of the viscous interaction for all the flow regimes shown in Fig. 1. Additionally, Charwat [56] has given a brief summary of near free molecule flow problems.

The shock angles indicate that, for Rankine-Hugoniot conditions, the pressure should continue to rise as the leading edge is approached, provided the pressure does not vary with the coordinate normal to the body surface. This is contradicted by pressure measurements which show a slight drop near the leading edge. Therefore, the flow near the leading edge does not have the Rankine-Hugoniot shock-layer structure.

To establish the region of validity of the present analysis, the flow field classification and the available literature are discussed in Subsection 1. The iteration scheme employed in the solution of the coupled equations is explored

in Subsection 2. Numerical results for various problems of the present day interest are given in Subsections 3, 4, and 5.

4.1 Classification of Flow Field

Hypersonic flow over a slender body with a sharp leading edge provided a challenging physical example of transition from microscopic kinetic theory to macroscopic, continuum gasdynamics. The general flow models used in the presently available analytical treatments of the sharp leading edge problem are discussed below by dividing the flow field into several regions (Fig. 1). Far downstream on a flat plate immersed in a hypersonic flow, the boundary layer phenomena are adequately described by compressible boundary layer theory. Upstream of this, towards the leading edge of the plate, the weak interaction region is encountered [3, 57 through 63]. Here the viscous layer causes a perturbation of the inviscid flow field because of the effect of the boundary layer displacement. In that case, although surface pressures and skin friction are affected, coupling between shock and boundary layer has not become significant.

Upstream of this region, there is a strong interaction region [21, 22, 51, 64 through 71]. Here, the developments of both inviscid and viscous flows are coupled. The distinctions between the strong and weak interaction regions are based on the relative importance of the effects of the shock strength and of the boundary layer displacement. In both regions, the shock wave is assumed to be thin and an inviscid region separates the shock from the outer edge of the boundary layer. A tabulated comparison of the various theoretical analyses applicable to the strong interaction region are given in Moulic and Maslach [72]. The results of the strong interaction solutions apply in general for values of the

interaction parameter $\bar{\chi}$ much greater than unity. On the other hand, the results of the weak interaction solutions are applicable for $\bar{\chi}$ much less than unity. There is a transition region in between the strong and weak interaction regions. Typical analytical results are plotted in Fig. 2. From this figure, it is clear that bridging the gap between these two asymptotic solutions is not an easy task. A regime exists upstream of the strong interaction in which there is present strong interaction between boundary layer and inviscid flow in addition to slip conditions at the body surface. It is assumed that there is still a distinct inviscid layer [73 through 77] separating the thin shock wave and the boundary layer, but the significant rarefaction phenomenon accounting for departures from viscous interaction theory is assumed to be velocity slip and temperature jump at the wall. The next region upstream is the viscous layer region [45, 78 through 82], which is characterized by the merge of the thin shock wave with a fully developed viscous shock layer. In this region, the boundary layer is assumed to extend from the plate to the downstream surface of the shock layer.

The next region upstream of the viscous layer is the merged layer [55, 83 through 86]. In this merged region, the shock wave is still merged with the completely viscous shock layer, but the shock is so thick that the jump conditions across the shock must be modified. McCroskey, Bogdonoff, and McDougal [90] have observed large reductions in the density ratio in the merged regime as the leading edge is approached. This implies reduced pressure immediately behind the shock, even though the shock angle is increasing. This may indicate that the shock structure is the dominant mechanism upstream of the strong interaction regime.

Upstream of the merged layer, molecular treatments of the flow are encountered in the near-free [56, 91 through 95] and free molecule flow regions [3, 46, 63, 96 through 98]. However, recent experiments [46, 89, 99] cast doubt on the existence of a free molecular flow region.

It is generally recognized that strong interaction theory fails to predict the behavior of the flow very near the leading edge. The determination of the actual point of departure from strong interaction was considered by Becker and Boylan [46]. They indicate that the strong interaction theory appears to fail in the range $0.1 \leq \bar{V}_\infty \leq 0.3$ as suggested by Talbot [47]. They also indicate that the onset of merging of shock and boundary layer corresponds to initial departures of p_1 / p_∞ from strong interaction theory. This has been observed at $\bar{V}_\infty \approx 0.15$.

Since the viscous interaction parameter $\bar{\chi}$ is equal to the product of the square of free stream Mach number and the rarefaction parameter $\bar{V}_\infty$, the strong influence of Mach number on the initial departure from strong interaction theory can be obtained in terms of $\bar{\chi}$ as 15 and 93.75 for Mach numbers 10 and 25 respectively if $\bar{V}_\infty = 0.15$. Following this, if the criterion for strong interaction is $\bar{\chi} \geq 10$, then strong interaction will not exist until $M_\infty \geq 8$. Therefore, for lower Mach numbers, the merged layer regime may directly extend to the weak interaction regime.

4.2 Numerical Scheme

The equations which are to be solved numerically are summarized here for convenient reference. They are taken from Section III, and are specialized for a flat plate.

$$\sum_{m=0}^{\infty} dm \left[\left(\frac{m+1}{3} \right) = 1 \right. \tag{4.1}$$

$$b = \left[- S_w - \sum_{m=0}^{\infty} Dm \left[\left(\frac{m+1}{3} \right) \right. \right. \quad \frac{1}{3} \sum_{m=0}^{\infty} Am \left[\left(\frac{m+1}{3} \right) \right] \tag{4.2}$$

$$\frac{p_\infty}{p_1} = \frac{u_1}{u_\infty} \left[\frac{2 M_1^4}{\gamma (\gamma+1) \Pi^2} \right]^{\frac{1}{2}} \frac{\int_\infty^{\bar{X}} \left[- \sqrt{\frac{p_1/p_\infty - 1}{\frac{p_1}{p_\infty} + \frac{\gamma-1}{\gamma+1}}} \right] \frac{d\bar{X}}{\bar{X}^3}}{\left[- \int_\infty^{\bar{X}} \frac{p_1}{p_\infty} \frac{u_1}{u_\infty} \frac{d\bar{X}}{\bar{X}^3} \right]^{\frac{1}{2}}} \tag{4.3}$$

where dm, Dm and II are defined in Section III. Further simplifications can be foreseen from the following isentropic relationship:

$$\frac{u_1}{u_\infty} = \left[1 + \frac{1 - \left(\frac{p_1}{p_\infty} \right)^{\frac{\gamma-1}{\gamma}}}{\frac{\gamma-1}{2} M_\infty^2} \right]^{\frac{1}{2}} \tag{4.4}$$

For $M_\infty = 10$, $\gamma = 1.4$, a maximum pressure ratio (p_1/p_∞) of 11 may exist for an adiabatic plate. Therefore, the maximum error in assuming u_1 approximately equal to u_∞ is about 2.5% at the leading edge and the error approaches zero in the downstream.

For convenience, let in Eq. (4.3)

$$z = \frac{1}{\bar{X}^3} \tag{4.5}$$

Thus,

$$\frac{p_\infty}{p_1} = \frac{M_1^2}{\sqrt{\gamma(\gamma+1)}}\ \Pi\ \frac{\int_0^z \frac{p_1/p_\infty - 1}{\sqrt{p_1/p_\infty + \frac{\gamma-1}{\gamma+1}}}\, dz}{\left[\int_0^z \frac{p_1}{p_\infty}\, dz\right]^{\frac{1}{2}}} \tag{4.6}$$

The assumption of $u_1 \approx u_\infty$ is justified because of the approximate representation of inviscid pressure distribution by the tangent wedge formula.

Equations (4.1), (4.2), and (4.6) implicitly contain three unknowns, namely, a, b, and Λ as well as their derivatives. These equations, containing highly divergent series, are not only nonlinear but also are coupled. There is no direct way of solving them with any existing technique. Therefore, one has to depend on an iteration scheme.

The definition of Λ is rewritten in terms of the new coordinate z in Appendix B. Similarly, the following relations are specialized for a flat plate as functions of z.

$$\xi \frac{da}{d\xi} = \frac{p_\infty}{p_1} \frac{da}{dz} \cdot \int_0^z \frac{p_1}{p_\infty}\, dz \tag{4.7}$$

$$\xi \frac{d\Lambda}{d\xi} = \Lambda + \frac{\gamma-1}{\gamma} \frac{p_\infty}{p_1} \frac{d^2}{dz^2}\left(\frac{p_\infty}{p_1}\right)\cdot\left(\int_0^z \frac{p_1}{p_\infty}\, dz\right)^2 \tag{4.8}$$

and

$$\xi \frac{db}{d\xi} = \frac{p_\infty}{p_1} \frac{db}{dz} \cdot \int_0^z \frac{p_1}{p_\infty}\, dz \tag{4.9}$$

The usual approaches to the solution of a set of nonlinear differential equations are either to integrate them numerically by Runge-Kutta integration technique, or to linearize the equations by Taylor's series expansion and then solve the linearized set by standard methods such as subdomain method [100] or Pade approximation [101]. However, these methods are not feasible for the above set of equations.

It is important to examine the series involved before applying any method for the solution of the equations. This can be done easily by neglecting the primed quantities in the first attempt. A typical series obtained in the solution of these equations is given below.

$$1.5341 - 1.1829 + 0.0105 + 0.7974 + 0.2694 + \ldots$$

The series is divergent. One has to apply the Euler transformation to sum these series, the procedure of which is given in Appendix C. As explained there, the Euler transformation should be applied in such a way that the best convergence and the least last term is obtained. One can obtain the following form after applying the Euler transformation to the above series beginning with the second term.

$$1.5341 - 0.5914 - 0.2931 - 0.0456 + 0.0944 + \ldots$$

Since the series is still divergent, one can obtain the following form by applying the Euler transformation to the last two terms.

$$1.5341 - 0.5914 - 0.2931 - 0.0228 + 0.0122 + \ldots$$

Now the series looks reasonably convergent. The experience here confirms the

observation of Meksyn [35] that it is not advisable to apply Euler transformation more than twice. The reason is that the convergence rate decreases as more Euler transformations are applied. Therefore, it is better to use as few transformations as possible. There is no unique way of summing these series. They differ slightly from one type of transformation to another. The type of transformation to be employed should be decided by trial and error in such a way that the best convergence and the least last term requirement will be met for the same number of transformations.

Fortunately, the first three terms in the series expressions (4.1), (4.2) as well as in the integrals I_1, I_2, and I_3 do not contain any derivatives. The next three terms in all these expressions contain only first derivatives. Most of the contribution in summing these series comes from the first few terms. Therefore, this present method has the advantage over the methods of finite difference in that even if a slight error is introduced into the last few terms by a finite difference representation, it will not significantly alter the net result.

Besides Meksyn, Hayday and Bowles [102, 103] investigated the solution of equations for stagnation point flows by using different number of terms. They concluded that the results obtained by using more than five terms differed little from the results using only five terms. However, Meksyn concluded that at least seven terms should be used for flows near the separation point. Since the numerical solutions presented in this study are applicable to a flat plate, six terms are retained in Eqs. (4.1) and (4.2). Five terms are used for the integrals I_1, I_2, and I_3.

The expression for II contains three quantities. The second and third quantities are directly proportional to the square of Mach number. Since the analysis presented here is for hypersonic flow, it is possible to drop the first term (i.e., I_1) without loss of much accuracy.

Similarity solutions are the exact solutions for a physical problem at the stagnation point. Lees [104] obtained the pressure gradient parameter for similar hypersonic boundary layers as

$$\Lambda = \frac{\gamma - 1}{\gamma} \qquad (4.5)$$

This is used for starting the numerical computations near to the leading edge.

Iteration schemes for obtaining values for the three unknowns (i.e., a, b, and Λ or p_∞/p_1) will be described below. Because of the nonlinearity of the equations, and the questions of convergence of the iteration scheme employed, it should be emphasized that no hard and fast rules can be laid down for the establishment of stable results.

Equation (4.6) is an implicit integral equation for the pressure ratio. An iterative scheme for its solution follows. An approximate value for the pressure ratio on the right hand side of Eq. (4.6) will be assumed and a new value will be computed by performing the two integrations numerically. The new value will be used in the integrands and the procedure will be repeated until the assumed and the calculated results agree within the tolerance limits set up. The results show that only three iterations are required for three digit accuracy. To start the iteration process, the initial estimate for p_1 / p_∞ from strong interaction theory may be used. The pressure ratio is expanded into asymptotic series in

terms of the viscous interaction parameter for the leading edge strong interaction region as

$$\frac{p_i}{p_\infty} = a_1 \bar{X} + b_1 \tag{4.11}$$

The coefficients a_1 and b_1 can be obtained by substituting Eq. (4.11) into Eq. (4.6) and equating equal powers of $\bar{X}$ on either side, resulting

$$a_1 = \frac{3}{2\sqrt{2}} \sqrt{\gamma\ (\gamma+1)}\ (\gamma-1)\, II$$

and

$$b_1 = \frac{2\,(3\gamma+1)}{7\,(\gamma+1)} \tag{4.12}$$

To obtain an initial estimate for the iteration process, one begins with the value of II determined by Eq. (4.10). The value of II thus determined yields a value for a_1 from Eq. (4.12) which, in turn, gives an initial estimate for p_i/p_∞ from Eq. (4.11). For the calculations of the other quantities needed, one first drops all the primed quantities in their series representation (i.e., neglecting their ξ dependence in the formulation), what remains are the similarity results for the quantities concerned.

Equation (4.2) is an implicit equation for the evaluation of the parameter b. The iteration scheme operates on the same principle just described. Here also, an initial estimate of b is needed. This can be set equal to zero. The result converges to the desired accuracy in three or four iterations. The series in the denominator of the right-hand-side of Eq. (4.2) converges without the

need of the Euler transformation. However, for extremely cold wall conditions, the Euler transformation may be desirable.

Mueller's iterative technique is used to find the parameter $a(\xi)$ from Eq. (4.1). This is described in detail in Appendix D. The well known Newton-Raphson method is not feasible for the type of Eq. (4.1) since it is highly divergent. The analytical or numerical differentiation with respect to the unknown parameter $a(\xi)$ is necessary in the case of Newton-Raphson method. For Mueller's iterative technique, one has to specify the range of the unknown parameter $a(\xi)$. The boundaries of this range should be specified in such a way that they satisfy the requirement mentioned in Appendix D. The results converge in about five iterations.

The procedure used in the solution of Eqs. (4.1), (4.2), and (4.6) is summarized below:

(1) Assume that the pressure gradient parameter Λ (given by Eq. (4.10) remains constant over the entire body.

(2) Calculate II from similarity solutions (i.e., by neglecting the primed quantities a', b', etc.,)

(3) Find the pressure distribution from Eq. (4.6).

(4) Determine the pressure gradient parameter and its derivative from Eqs. (4.7) and (4.8) respectively.

(5) Mueller's iterative technique determines a certain value for the unknown parameter $a(\xi)$. Then, obtain the parameter $b(\xi)$ from Eq. (4.2) by applying information already obtained.

(6) Check whether or not the obtained parameters $a(\xi)$, $b(\xi)$, and

$\Lambda(\xi)$ satisfy Eq. (4.1).

(7) If Eq. (4.1) is not satisfied, repeat steps (5) and (6) until the results converge within the stated limits.

(8) Re-calculate II.

(9) Repeat the steps (3) through (8) for every station along the entire body.

(10) Repeat the steps (3) through (9) using local values of Λ and II for the entire body. This repetition should continue until the pressure distribution on the body converges to the value in the previous iteration. The results show that three iterations are adequate for third digit accuracy.

Once the unknown parameters a (ξ), b (ξ), and $\Lambda(\xi)$ are determined, it is a straight forward matter to obtain the boundary layer parameters. These are summarized below for a flat plate in terms of the new variables.

Modified displacement thickness:

$$M_1^2 \Delta^* = \sqrt{2} \frac{u_1}{u_\infty} \frac{p_\infty}{p_1} \text{II} \left[\int_0^z (p_1/p_\infty) \frac{u_1}{u_\infty} dz \right]^{\frac{1}{2}} \tag{4.13}$$

Because

$$\tau_w = C_f \frac{\zeta_\infty u_\infty^2}{2} \tag{4.14}$$

Eq. (2.34) can be written in terms of skin friction coefficient as

$$M_\infty^3 C_f = \sqrt{2} \frac{p_1}{p_\infty} \left(\frac{u_1}{u_\infty} \right)^2 \frac{a(\xi)}{\left[\int_0^z \frac{p_1}{p_\infty} \frac{u_1}{u_\infty} dz \right]^{\frac{1}{2}}} \tag{4.15}$$

Similarly, introducing the heat transfer coefficient

$$-Q_w = C_h \; \zeta_\infty \; u_\infty \; (h_o - h_w) \tag{4.16}$$

Eq. (2.37) becomes

$$M_\infty^3 \; C_h = \frac{p_1}{p_\infty} \; \frac{u_1}{u_\infty} \left(\sqrt{\frac{-1}{2' \; Pr \; S_w}} \right) \left[\frac{b(\xi)}{\int_0^z \left(\frac{p_1}{p_\infty} \right) \frac{u_1}{u_\infty} \, dz} \right]^{\frac{1}{2}} \tag{4.17}$$

4.3 Cold Plate

The numerical results are calculated for various boundary conditions at the wall and different specific heat ratios. Before accepting the results obtained from the above procedure, one should check for two things: The first one is the effect of the initial starting location. There are two possible approaches for this problem. One approach is to use the experimental results or analytical solutions at the initial location. The other alternative is to start arbitrarily at different locations close to the leading edge by using known similarity solutions. Fig. 3 shows the results of such a process. Even though the curves start entirely differently near the leading edge (large values of $\bar{\chi}$), they merge into a single curve very rapidly as $\bar{\chi}$ decreases. One should not consider the results valid beyond the point where the curves depart from each other significantly.

The second one is to check the validity of convergence of the iteration scheme described under step (10). The pressure distribution calculated for each effective body shape is shown in Fig. 4. The second iteration data and third iteration data merged into a single curve, thus the convergence is satisfactory.

The behavior of the parameter a (ξ) versus $\bar{X}$ is shown in Fig. 5 for $T_w / T_e = 0.15$. The parameter remains essentially constant for a wide range of $\bar{X}$ at the leading edge. This implies the validity of the similarity solutions at the leading edge. For $\bar{X}$ less than 20, the parameter drops significantly, implying the need either of a local similarity approach, or of a nonsimilar approach.

The variation of the pressure gradient parameter is shown in Fig. 6. This parameter exhibits a trend similar to that of parameter a. However, the pressure gradient parameter drops faster in the weak interaction region. The parameter b is plotted in Fig. 7. Compared to the other two parameters, this parameter varies very slowly along the body. However, the pattern remains the same as the other two parameters.

The pressure distribution is shown in Fig. 8. The experimental results from Hall and Golian [105] are also plotted on the same graph. The agreement with experimental results is better in the weak interaction and in the transition regions than in the strong interaction region. The similar solutions of Li and Nagamatsu and the exact solution of Blottner are also included here for comparison purposes. The pressure distribution obtained in the present work is somewhat higher than the above mentioned available theoretical and experimental results. The reason for this difference may be due to the fact that only five terms are considered in the calculation of displacement thickness. For very cold and very hot plates, the use of more than five terms is desirable.

The distribution of the skin friction coefficient is shown in Fig. 9. Blottner's solution and the zeroth order strong interaction solution are included for

comparison purposes. Since the pressure distribution calculated in the present work is slightly higher, the predicted skin friction coefficient, is also slightly higher as expecied from Eq. (4.15). The heat transfer distribution is shown in Fig. 10. The experimental results of Hall and Golian [105] and some other theoretical results are shown. The agreement is satisfactory.

It may be noted that the experimental data is higher than the present result even though the predicted pressure distribution is slightly higher. The reason is as follows. Equation (4.17) indicates that the heat transfer coefficient is proportional to the pressure distribution but inversely proportional to the Prandtl number. It is widely accepted that the Prandtl number for real gases is slightly less than unity. For example, the Prandtl number may be taken as 0.72 for air. The Prandtl number is assumed as unity in the present analysis. The experimental data most probably represent the case where the Prandtl number is less than unity. Therefore, the predicted heat transfer distribution is considered as slightly higher than the available data and analytical results.

The dimensionless displacement thickness is shown in Fig. 11. There is no experimental data available. The approximate equations derived by Cox and Crabtree [106] (chapters 7 and 8) are used for the purpose ot comparison for both weak and strong interaction regions as applicable. To interpret these equations in terms of dimensionless displacement thickness, the following relation is used:

$$\Delta^* = \frac{M_1 \frac{\delta^*}{x}}{\bar{\chi}^2} \tag{4.18}$$

Since a limited numb·· of terms (five) are used in the calculation of the integrals

I_1, I_2, and I_3 and comparison is made with only asymptotic solutions, the agreement is found to be satisfactory.

4.4 Adiabatic Plate

Since there is no heat transfer at the body surface, the energy equation is dropped from the governing set of equations. The number of unknowns is reduced to two (namely $a(\xi)$ and $\Lambda(\xi)$ or p_1) as compared to three in the previous case. The procedure in solving these equations remains the same. A considerable amount of simplification is realized, however. The simplified equations for the flat plate can be obtained by assuming $b(\xi)$ as zero.

The pressure distribution is shown in Fig. 12. Excellent agreement is obtained with Kendal and Bertram's [61,62] experimental results. Moulic and Maslach [72] also conducted experiments in the range of Mach numbers from 5 to 6. The wall-to-stagnation absolute temperature ratio was maintained within the limits of 0.93 to 0.98. These results are also shown in the same figure. The data covers the region where the hypersonic interaction parameter is greater than 3.5. Since the strong interaction region may not exist for such a low Mach number, the results may be interpreted as satisfactory. The zeroth order strong interaction solution and Blottner's numerical solution are also included in this figure. The overall agreement is good.

The skin friction distribution is shown in Fig. 13. The agreement with Li and Nagamatsu zeroth order strong interaction solution is satisfactory. Since the displacement thickness is higher than in the cold plate case, a sliding scale is introduced to represent both weak and strong interaction regions on the same graph. The present result is compared with the solution of Cox and Crabtree [106].

4.5 Heated Plate

Experimental measurements of surface pressure and heat transfer distributions are fairly numerous in the literature for adiabatic and cold flat plates. However, such measurements are not, to the author's knowledge, available for a heated flat plate. This is probably due to difficulties in simulating the phenomena. There are, however, quite a few practical situations where the body temperature is much higher than the stagnation temperature of the flow field. One such situation is obviously the final phase of a re-entry vehicle. Blottner [39] could not calculate the heated plate example because of the lack of similarity profiles for this case at the initial station. However, this case is investigated with the present approach.

The equations and the procedure essentially remain the same as for the cold flat plate. The numerical example is done for the case of wall-to-stagnation temperature ratio of 2.0. The results are shown in Figs. 15 through 18 as pressure, skin friction coefficient, heat transfer coefficient, and displacement thickness distributions. In each of these figures, the results are given for a monoatomic gas and a diatomic gas when the condition of the plate is heated ($T_w/T_o = 2.0$), cooled ($T_w/T_o = .15$) or adiabatic ($T_w/T_o = 1.0$).

The pressure, skin friction and heat transfer coefficients, and displacement thickness are more sensitive to heating than cooling. The effect of cooling the surface reduces these boundary layer parameters whereas the opposite effect is true of heating. Similarly, cooling of the surface reduces the strong interaction region as well as the strong interaction effects between the shock wave and the boundary layer and has the greatest effect near the leading edge. The results indicate that a monoatomic gas increases the boundary layer parameters significantly in comparison to a diatomic gas.

SECTION V

CONCLUSIONS AND RECOMMENDATIONS

The compressible laminar boundary layer equations are solved by the method of steepest descent. The external pressure distribution is calculated by tangent-wedge formula for two dimensional bodies. Since the hypersonic boundary layer-inviscid interaction is coupled to the solution of boundary layer equations, three resulting coupled equations are solved by an iterative process.

The analysis presented in this study concerns the case of an isothermal body and a Prandtl number of unity. To check the validity of the analysis, numerical results are computed for a flat plate. The results are in good agreement with the available theoreis and experimental results. It is found that the convergence rate of the series for displacement thickness is slower than the series for the velocity and enthalpy at the edge of the boundary layer. Since only five terms are used in the calculation of displacement thickness integrals, the results are found to be satisfactory. However, use of more than five terms may yield much better results.

Occasionally, there exists a situation where there is no unique way of summing these series. With the exception of this restriction, the method is a powerful analytical tool, that is easy to apply. Additional study is needed to understand deeper into the convergence of the series.

The method of solution is not restricted to a particular fluid property or a particular body. The assumption of a Prandtl number of unity and of an isothermal body serve only to reduce considerable amount of algebra involved in the analysis.

One can relax these assumptions easily without any change in the present method of approach. The simplicity of the method permits the solution to be obtained on small computers such as IBM 1130.

The numerical example given in Section IV represents the flat plate in hypersonic flow. The present method of approach is applicable even to wedges, compression surfaces or axisymmetrical slender bodies. Analogous to the use of tangent-wedge formula for two dimensional bodies, one may use tangent-cone formula for symmetrical bodies. However, the use of boundary layer-inviscid interaction or neglecting the other interactions should be justified.

BIBLIOGRAPHY

1. Prandtl, L., "Uber Flussigkeitsbewegung bei sehr kleiner reibung" Verhandlgndes III. Internat. Mathn-Kongr., Heidelberg, 1904.

2. Schlichting, H., "Boundary Layer Theory", McGraw Hill Book Co. Inc., New York, June 1962.

3. Hayes, W.D. and Probstein, R.F., "Hypersonic Flow Theory", Academic Press, New York, 1959.

4. Howarth, L., "Modern Developments in Fluid Dynamics", Oxford University Press, 1953.

5. Goldstein, S., "Modern Developments in Fluid Dynamics", Dover Publications, Inc., New York, 1965.

6. Dorrance, W.H., "Viscous Hypersonic Flow", McGraw Hill Book Co., Inc., New York, 1962.

7. Rosenhead, L., "Laminar Boundary Layers", Oxford University Press, 1963.

8. Curle, N., "The Laminar Boundary Layer Equations", Oxford University Press, 1962.

9. Thwaites, B., "Incompressible Aerodynamics", Oxford University Press, 1960.

10. Moore, F.K., "Theory of Laminar Flows", Princeton University Press, New Jersey, 1964.

11. Schubauer, G.B., "Air Flow in a Separating Laminar Boundary Layer", NACA Technical Report No. 527 (1935).

12. Morduchow, M. and Clarke, J.H., "Method for Calculation of Compressible Laminar Boundary Layer Characteristics in Axial Pressure Gradient with Zero Heat Transfer", NACA TN 2784, Sept. 1952.

13. Libby, P.A. and Morduchow, M., "Method for Calculation of Compressible Laminar Boundary Layer with Axial Pressure Gradient and Heat Transfer", NACA TN 3157, Jan. 1954.

14. Morduchow, M., "Analysis and Calculation by Integral Methods of Laminar Compressible Boundary Layer with Heat Transfer and Without Pressure Gradient", NACA Report 1245, 1955.

15. Yang, K.T., "An Improved Integral Procedure for Compressible Laminar Boundary Layer Analysis", J. of Applied Mechanics, Mar. 1961, pp. 9-20.

16. Launder, B.E., "An Improved Pohlhausen-Type Method of Calculating the Two Dimensional Laminar Boundary Layer in a Pressure Gradient", Trans. ASME, J. of Heat Transfer, Aug. 1964.

17. Thwaites, B., "Approximate Calculation of the Laminar Boundary Layer", The Aeronautical Quarterly, Vol. 1, Nov. 1949.

18. Rott, N. and Crabtree, L.E., "Simplified Laminar Boundary Layer Calculations for Bodies of Revolution and for Yawed Wings", J. of Aero. Scienc.s, Vol. 19, No. 8, 1952.

19. Cohen, C.B. and Reshotko, E., "The Compressible Laminar Boundary Layer with Heat Transfer and Arbitrary Pressure Gradient", NACA Report, 1294 (1956).

20. Chan, Y.Y., "Integral Method in Compressible Laminar Boundary Layers and its Application", The Physics of Fluid, Vol. 9, No. 2 (Feb. 1966).

21. Dewey, C.F., "Use of Local Similarity Concepts in Hypersonic Viscous Interaction Problems", AIAA Journal, Vol. 1, No. 1 (Jan. 1963).

22. Mann, M.W. and Bradley, R.G., "Hypersonic Viscid-Inviscid interaction Solutions for Perfect Gas and Equilibrium Real Air Boundary Layer Flow", J. of the Astronautical Science, Spring 1963.

23. Manohar, R., "A Characteristic Difference Method for the Calculation of Steady Boundary Layer Flow", Proc. of 4th Congress Theoret. App. Mech. (1958), Indian Soc. Theoret. App. Mech. Kharagpur.

24. Smith, A.M.O. and Clutter, D.W., "Solutions of the Incompressible Laminar Boundary Layer Equations", AIAA Journal, Vol. 1 (1963).

25. Clutter, D.W. and Smith, A.M.O., "Solution of the General Boundary Layer Equations for Compressible Laminar Flow, Including Transverse Curvature", Douglas Aircraft Co., Report LB 31088 (Feb. 1963).

26. Smith, A.M.O. and Clutter, D.W., "Machine Calculation of Compressible Laminar Boundary Layers", AIAA Journal, Vol. 3, No. 4 (Apr. 1965).

27. Meksyn, D., "The Laminar Boundary Layer Equations, II. Integration of non-Linear Ordinary Differential Equations", Proc. Roy. Soc. London, Series A (192), pp. 567 (1948).

28. Meksyn, D., "Integration of the Boundary Layer Equations for a Plane in a Compressible Fluid", Proc. Roy. Soc. London, Series A (195), pp. 180 (1948).

29. Meksyn, D., "Integration of the Boundary Layer Equations for a Plane in Compressible Flow with Heat Transfer", Proc. Roy. Soc. London, Series A (231) pp. 274 (1955).

30. Meksyn, D., "Integration of the Boundary Layer Equations", Proc. Roy. Soc. London, Series A (237), pp 543 (1956).

31. Meksyn, D., "The Boundary-Layer Equation for Axially Symmetric Flow Past a Body of Revolution--Motion of a Sphere", J. of the Aerospace Sciences, Oct. 1958.

32. Meksyn, D., "The Boundary Layer Equations of Compressible Flow-Separation", J. of Applied Mathematics and Mechanics (ZAMM), Vol. 38, No. 9/10, Sept./Oct. 1958.

33. Meksyn, D., "Supersonic Flow Past a Semi-Infinite Plane", Journal of Applied Mathematics and Physics (ZAMP), Vol. 16, pp. 344, (1965).

34. Meksyn, D., "Magneto-Hydrodynamic Flow Past a Semi-Infinite Plate", ZAMP, Vol. 17, pp. 397, (1966).

35. Meksyn, D., "New Methods in Laminar Boundary Layer Theory", Pergamon Press (1961).

36. Baxter, D.C. and Flugge-Lotz, I., "The Solution of Compressible Laminar Boundary Layer Problems by a Finite Difference Method, Part II. Further Discussion of the Method and Computation of Example". Tech. Report No. 110, Div. of Eng. Mech., Stanford Univ. (Oct. 1957).

37. Flugge-Lotz, I. and Baxter, D. C., "The Solution of Compressible Laminar Boundary Layer Problems by a Finite Method", Tech. Report No. 103, Div. of Eng. Mech., Stanford Univ. (Sept. 1956).

38. Flugge-Lotz, I. and Yu, Er-Yung, "Development of a Finite-Difference Method for Computing a Compressible Laminar Boundary Layer with Interaction", Tech. Report No. 127, Div. of Eng. Mech., Stanford Univ. (May 1960).

39. Blottner, F.G., "Computation of the Compressible Laminar Boundary Layer Flow Including Displacement Thickness Interaction Using Finite-Difference Methods", Doctoral Dissertation, Stanford Univ., (Jan. 1962).

40. Krause, E., "Numerical Solution of the Boundary Layer Equations", AIAA Journal, Vol. 5, pp. 1231 (1967).

41. Kramer, R.F. and Liberstein, H.M., "Numerical Solution of the Boundary Layer Equations Without Similarity Assumptions", J. of the Aerospace Sciences, Vol. 26, (Aug. 1959).

42. Forsythe and Wasow, "Finite Difference Methods for Partial Differential Equations", John Wiley & Sons, Inc., New York (1960).

43. McCracken, D.D. and Dorn, W.S., "Numerical Methods and Fortran Programming", John Wiley & Sons, Inc., New York (1964).

44. Mangler, W., "Zusammenhang Zwischen ebenen und rotationssymmetrischen Grenzschichten in Kompressiblen Flussigkeiten", ZAMM, Vol. 28, (1948).

45. Oguchi, H., "The Sharp Leading Edge Problem in Hypersonic Flow", Div. of Engineering, ARL TN 60-133, Brown University, Providence, R. I. (1960).

46. Becker, M. and Boylan, D.E., "Experimental Flow Field Investigations Near the Sharp Leading Edge of a Cooled Flat Plate in a Hypervelocity, Low Density Flow", Rarefied Gas Dynamics, Vol. 4, Academic Press, New York (1967).

47. Talbot, L., "Criterion for Slip Near the Leading Edge of a Flat Plate in Hypersonic Flow", AIAA Journal, Vol. 1, No. 5, pp. 1169 (1963).

48. Liepmann, H.W. and Roshko, A., "Elements of Gasdynamics", John Wiley & Sons, Inc., New York (1957).

49. Shen, Shan-Fu, "An Estimate of Viscosity Effect on the Hypersonic Flow Over an Insulated Wedge", J. of Math and Physics, Vol. 31, No. 3, (1952).

50. Li, T. Y. and Nagamatsu, H.T., "Shock Wave Effects on the Laminar Skir Friction of an Insulated Flat Plate at Hypersonic Speeds", J. of Aero. Science, Vol. 20, No. 5, (1953).

51. Lees, L., "Hypersonic Flow", Fifth International Aeronautical Conference (June 1955), Inst. Aero. Science, Inc., (1955) pp. 241-276.

52. Lees, L., "Influence of the Leading Edge Shock Wave on the Laminar Boundary Layer at Hypersonic Speeds", J. of Aeronautical Sciences, Vol. 23, No. 6, (1956).

53. Becker, J.V., "Results of Recent Hypersonic and Unsteady Flow Research at the Langley Aeronautical Laboratory", J. of Applied Physics, Vol. 21, pp. 619, (1950).

54. Jain, A.C. and Li, T.Y., "A Critical Assessment of the Problem of Sharp Leading Edge of a Flat Plate in Hypersonic Flow", Univ. of Cinn., Dept. of Aero. Eng., Tech. Report AE6401, (1964).

55. Pan, Y. S. and Probstein, R. F., "Rarefied Flow Transition at a Leading Edge", M.I.T. Fluid Mech. Lab. Pub. No. 64-8 (1964).

56. Charwat, A. F., "Molecular Flow Study of the Hypersonic Sharp Leading Edge Interaction", Rarefied Gas Dynamics (Editor-L. Talbot), Academic Press, New York (1961).

57. Lees, L. and Probstein, R. F., "Hypersonic Viscous Flow Over a Flat Plate", Princeton Univ., Dept. of Aero. Eng., Rept. 195 (1952).

58. Casaccio, A., "First-Order Solution to the Compressible Laminar Boundary Layer in Slip Flow", J. of Aero. Sciences, Vol. 27 (1960).

59. Maslen, S. H., "Second Order Effects in Laminar Boundary Layers", AIAA Journal, Vol. 1, pp. 33 (1963).

60. Bertran, M. H., "An Approximate Method for Determining the Displacement Effects and Viscous Drag of Laminar Boundary Layers in Two-Dimensional Hypersonic Flow", NACA Technical Note 2773 (1953).

61. Kendall, J. M., Jr., "An Experimental Investigation of Leading Edge Shock Wave-Boundary Layer Interaction at Mach 5.8", J. of Aeronautical Sciences, Vol. 24, pp. 47, 1957.

62. Bertram, M. H., "Boundary Layer Displacement Effects in Air at Mach Numbers of 6.8 and 9.6", NACA Technical Note 4133 (1958).

63. Wallace, J. E. and Burke, A. F., "An Experimental Study of Surface and Flow Field Effects in Hypersonic Low Density Flow Over a Flat Plate", Rarefied Gas Dynamics (Editor-J.H. de Leeuw), Vol. 2, Academic Press, New York (1966).

64. Stewartson, K., "On the Motion of a Flat Plate at High Speed in a Viscous Compressible Fluid-II. Steady Motion", J. of Aero. Sciences, Vol. 22, pp. 303 (1955).

65. Oguchi, H., "First Order Approach to a Strong Interaction Problem in Hypersonic Flow Over an Insulated Flat Plate", Univ. of Tokyo, Japan--Aerospace Res. Inst. Rept. 330 (1958).

66. Li, T. Y. and Nagamatsu, H. T., "Hypersonic Viscous Flow on Non-insulated Flat Plate", Proc. 4th Midwestern Conference on Fluid Mechanics, pp. 273, Purdue Univ. (1955).

67. Cheng, H.K.; Hall, J.G.; Golian, T.C.; and Hertzberg, A., "Boundary Layer Displacement and Leading Edge Bluntness Effects in High Temperature Hypersonic Flow", J. of Aero. Sciences, Vol. 28, pp. 353 (1961).

68. Tien, C.L., "On Hypersonic Viscous Flow Over an Insulated Flat Plate With Surface Mass Transfer", J. of Aero. Sciences, Vol. 29, pp. 1024 (1962).

69. Li, T.Y. and Gross, J.F., "Hypersonic Strong Viscous Interaction on a Flat Plate with Surface Mass Transfer", Proc. of the 1961 Heat Transfer and Fluid Mechanics Institute, Stanford Univ. Press, Stanford, Calif. (1961).

70. White, F.M., Jr., "Hypersonic Laminar Viscous Interactions on Inclined Flat Plates", ARS Journal, Vci. 32, pp. 780 (1962).

71. Inger, G. R., "Nonequilibrium Hypersonic Flat Plate Boundary Layer Flow with a Strong Induced Pressure Field", AIAA Journal, Vol. 2, pp. 452 (1964).

72. Moulic, Eugene S. and Maslach, George J., "Induced Pressure Measurements on a Sharp-Edged Insulated Flat Plate in Low Density Hypersonic Flow", Rarefied Gas Dynamics, Supp. 4, Vol. II, Academic Press, New York (1967).

73. Schaaf, S. A. and Chambre, P. L., "Flow of Rarefied Gases", Princeton Aeronautical Paperbacks, Princeton University Press, New Jersey (1961).

74. Aroesty, J., "Strong Interaction with Slip Boundary Conditions", Air Force Aeronautical Research Labs. Rept. 64 (1961).

75. Aroesty, J., "Slip Flow and Hypersonic Boundary Layers", AIAA Journal, Vol. 2, pp. 189 (1964).

76. Vidall, R. J. and Wittliff, C.E., "Hypersonic Low Density Studies of Blunt and Slender Bodies", Rarefied Gas Dynamics (Editor-J.A. Laurmann), Vol. 2, Academic Press, New York (1963).

77. Galkin, V. S., "Investigation of a Hypersonic Flow of Slightly Rarefied Viscous Gas Around a Flat Plate", Translated by Foreign Tech. Div., AFSC Wright Patterson Air Force Base (AD-607970)-Russian Article (1961).

78. Oguchi, H., "The Sharp Leading Edge Problem in Hypersonic Flow", Rarefied Gas Dynamics (Editor-L. Talbot), Academic Press, New York (1961).

79. Oguchi, H., "Leading Edge Slip Effects in Rarefied Hypersonic Flow", Rarefied Gas Dynamics (Editor-J.A. Laurmann), Vol. 2, Academic Press, New York (1963).

80. Bendor, E., "Rarefied Viscous Flow Near a Sharp Leading Edge", AIAA Journal, Vol. 1, pp. 956 (1963).

81. Jain, A.C. and Li, T.Y., "The Problem of Sharp Leading Edge in Hypersonic Flow", Aeronautical Research Laboratory Report, pp. 63-161 (1963).

82. Ii, J.M. and Street, R.E., "The Incipient Continuum Flow Near the Leading Edge of a Flat Plate", Rarefied Gas Dynamics (Editor-J.H. de Leeuw), Vol. 1, Academic Press, New York (1966).

83. Probstein, R.F. and Pan, Y.S., "Shock Structure and The Leading Edge Problem", Rarefied Gas Dynamics (Editor-J.A. Laurmann), Vol. 2, Academic Press, New York (1963).

84. Garvine, R. W., "Hypersonic Viscous Flow Near a Sharp Leading Edge", AIAA Journal, Vol. 2, pp. 1660 (1964).

85. Laurmann, J., "Hypersonic Interaction at High Altitudes", Lockheed Missiles and Space Co. Rept. No. 6-90-63-83 (1963).

86. Laurmann, J., "Structure of the Boundary Layer at the Leading Edge of a Flat Plate in Hypersonic Slip Flow", AIAA Journal, Vol. 2, pp. 1655 (1964).

87. Rudman, S. and Rubin, S.G., "Hypersonic Viscous Flow Over Slender Bodies with Sharp Leading Edges", AIAA preprint 68-3 (1968).

88. Shorenstein, M.L. and Probstein, R.F., "The Hypersonic Leading Edge Problem", AIAA preprint 68-4 (1968).

89. Joss, W.W.; Vas, I.E.; and Bogdonoff, S.M., "Studies of the Leading Edge Effect on the Rarefied Hypersonic Flow Over a Flat Plate", AIAA preprint 68-5 (1968).

90. McCroskey, W.J.; Bogdonoff, S.M.; and McDougall, J.G., "An Experimental Model for the Sharp Flat Plate in Rarefied Hypersonic Flow", AIAA Journal, Vol. 4, pp. 1580 (1966).

91. Charwat, A.F., "Theoretical Analysis of Near-Free Molecule Hypersonic Flow at the Sharp Leading Edge of a Flat Plate", Rand Corp. Memo. RM-2553-PR (1963).

92. Elrod, H.G., Jr., "A First-Collision Theory Analysis for Hypersonic Flow in the Vicinity of the Sharp Leading Edge of a Flat Plate", AVCO Res. and Adv. Dev. Div. Tech. Memo. (RAD-TM-62-72), 1962.

93. Kogan, M.N. and Degtiarev, L.M., "On the Computation of Flow at Large Knudsen Numbers", Astronautica Acta, Vol. 11, pp. 36 (1965).

94. Ziering, S.; Chi, L.; and Fante, R., "Kinetic Theory of the Leading Edge", Rarefied Gas Dynamics (Editor-J.H. de Leeuw) Vol. 1, Academic Press, New York (1966).

95. Bird, G.A., "Aerodynamic Properties of Some Simple Bodies in the Hypersonic Transition Regime", AIAA Journal, Vol. 4, pp. 55 (1966).

96. Burke, A.F.; Smith, W.C.; Dowling, E.D.; and Carlson, D.R., "Lifting Surfaces in Rarefied Hypersonic Air Flow-Part I, Bluntness and Angle of Attack Effects on Flow Over Flat Plates", CAL Rept. AA-1596-Y-1 (1962).

97. Videl, R.J.; Golian, T.C.; and Bartz, J.A., "An Experimental Study of Hypersonic Low Density Viscous Effects on a Sharp Flat Plate", AIAA preprint 63-435 (1963).

98. Chuan, R.L. and Waiter, S.A., "Experimental Study of Hypersonic Rarefied Flow Near the Leading Edge of a Thin Flat Plate", Rarefied Gas Dynamics (Editor-J.A. Laurmann), Vol. 2, Academic Press, New York (1963).

99. Vas, I.E. and Allegre, J., "The N-4 Hypersonic Low Density Facility and Some Preliminary Results on a Sharp Flat Plate", Rarefied Gas Dynamics, Vol. 4, Academic Press, New York (1967).

100. Crandall, S., "Engineering Analysis", McGraw Hill Book Co., New York, pp. 147 (1956).

101. Magnus, D. and Schecter, H., "Analysis and Application of the Pade Approximation for the Integration of Chemical Kinetic Equations", General Applied Science Inc., Westbury, L.I., New York, Technical Rept. No. 642, (1967).

102. Hayday, A.A. and Bowles, D.A., "On the Flow of Air at Chemical Equilibrium Near a Stagnation Point", ZAMP, Vol. 17 (1966).

103. Hayday, A.A. and Bowles, D.A., "Integration of Coupled Nonlinear Equations in Boundary Layer Theory with Specific Reference to Heat Transfer Near the Stagnation Point in Three Dimensional Flow", International Journal of Heat and Mass Transfer, Vol. 10, pp. 415-426 (1967).

104. Lees, L., "On the Boundary-Layer Equations in Hypersonic Flow and Their Approximate Solutions", Journal of the Aeronautical Sciences, Feb. 1953.

105. Hall, J.G. and Golian, T.C., "Shock Tunnel Studies of Hypersonic, Flat Plate Airflows", Cornell Aeronautical Laboratory, Inc., Report No. AD-1052-A-10, (1960).

106. Cox, R.N. and Crabtree, L.F., "Elements of Hypersonic Aerodynamics", The English University Press Ltd., London (1965).

107. Debye, P., "Naherungsformeln fur die Zylinderfunktionen fur grosse Werte des Arguments und unbeschrankt veranderliche Werte des Index", Mathematische Annalen, Vol. 67, pp. 535 (1909).

108. Watson, G.N., "A Treatise on the Theory of Bessel Functions", Second Edition, Cambridge University Press (1944).

109. Merk, H.J., "Rapid Calculations for Boundary Layer Transfer Using Wedge Solutions and Asymptotic Expansions", J. of Fluid Mechanics, Vol. 5, pp. 460, 1959.

110. Euler, L., "Institutiones Calculi Differentialis (Pars Posterior), Edited by G. Kowalevski, Leipzig and Berlin (1913).

111. Kristiansen, G.K., "Zeros of Arbitrary Function", Data Processing for Science and Engineering, Vol. 3, pp. 205-206, 1963.

112. D. R. Jeng, R. W. Blanton, R. D. Wood, and Rao V. S. Yalamanchili, "Laminar Boundary Layer-Inviscid Flow Interaction at Hypersonic Speed", Final Report for North American Aviation Inc., Contract No. M6NDDX-954065 University of Alabama Research Institute (1967)

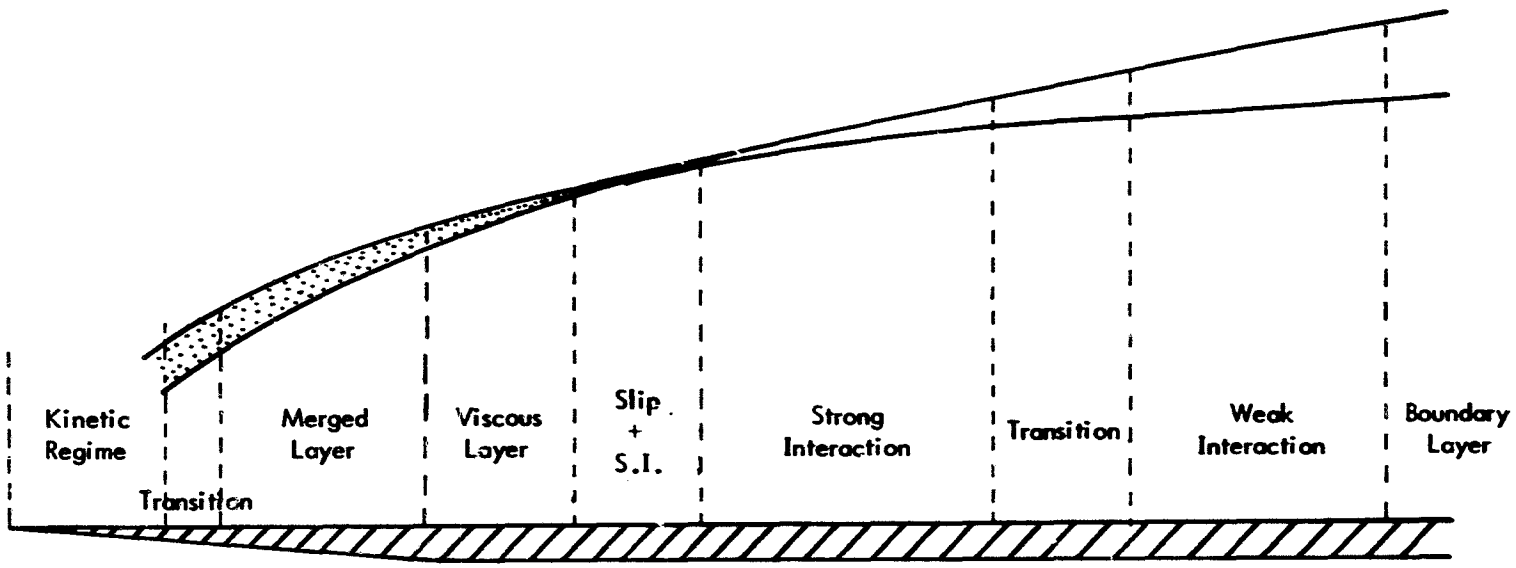

FIG. 1 FLOW REGIMES

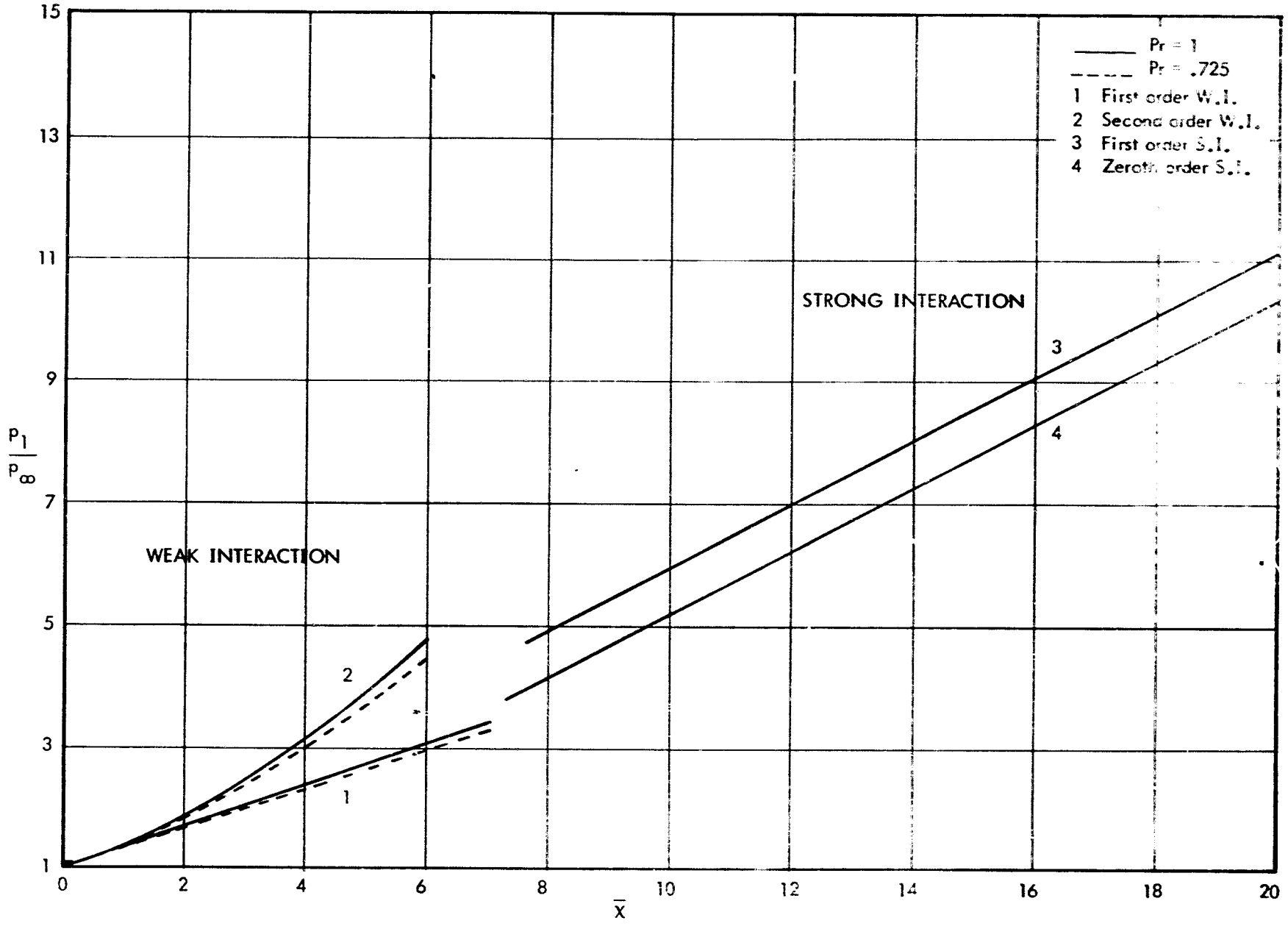

FIG. 2 STRONG AND WEAK INTERACTION THEORIES

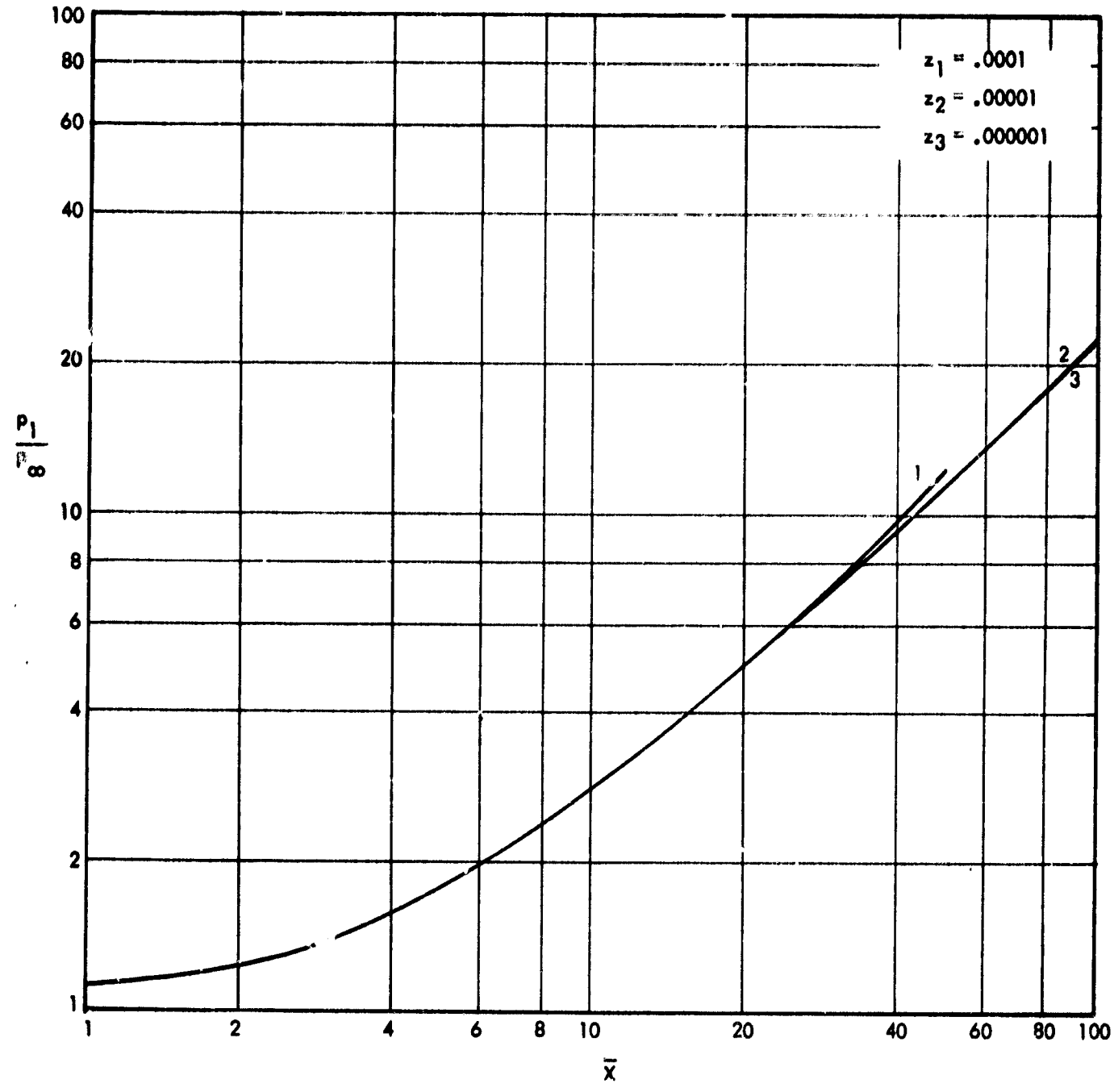

FIG. 3 EFFECT OF INITIAL LOCATION

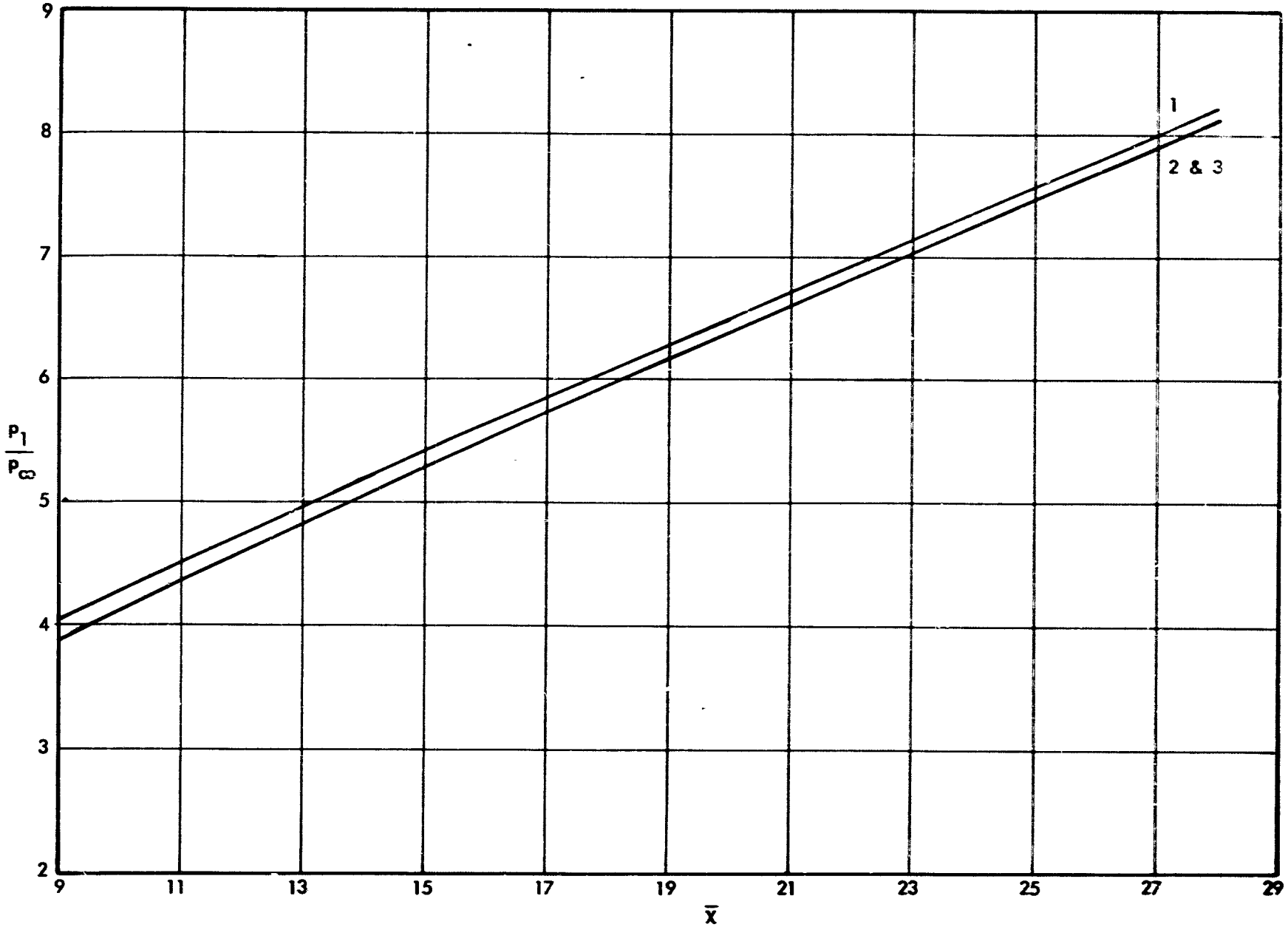

FIG. 4 CONVERGENCE OF PRESSURE RATIO IN AN ITERATION PROCEDURE

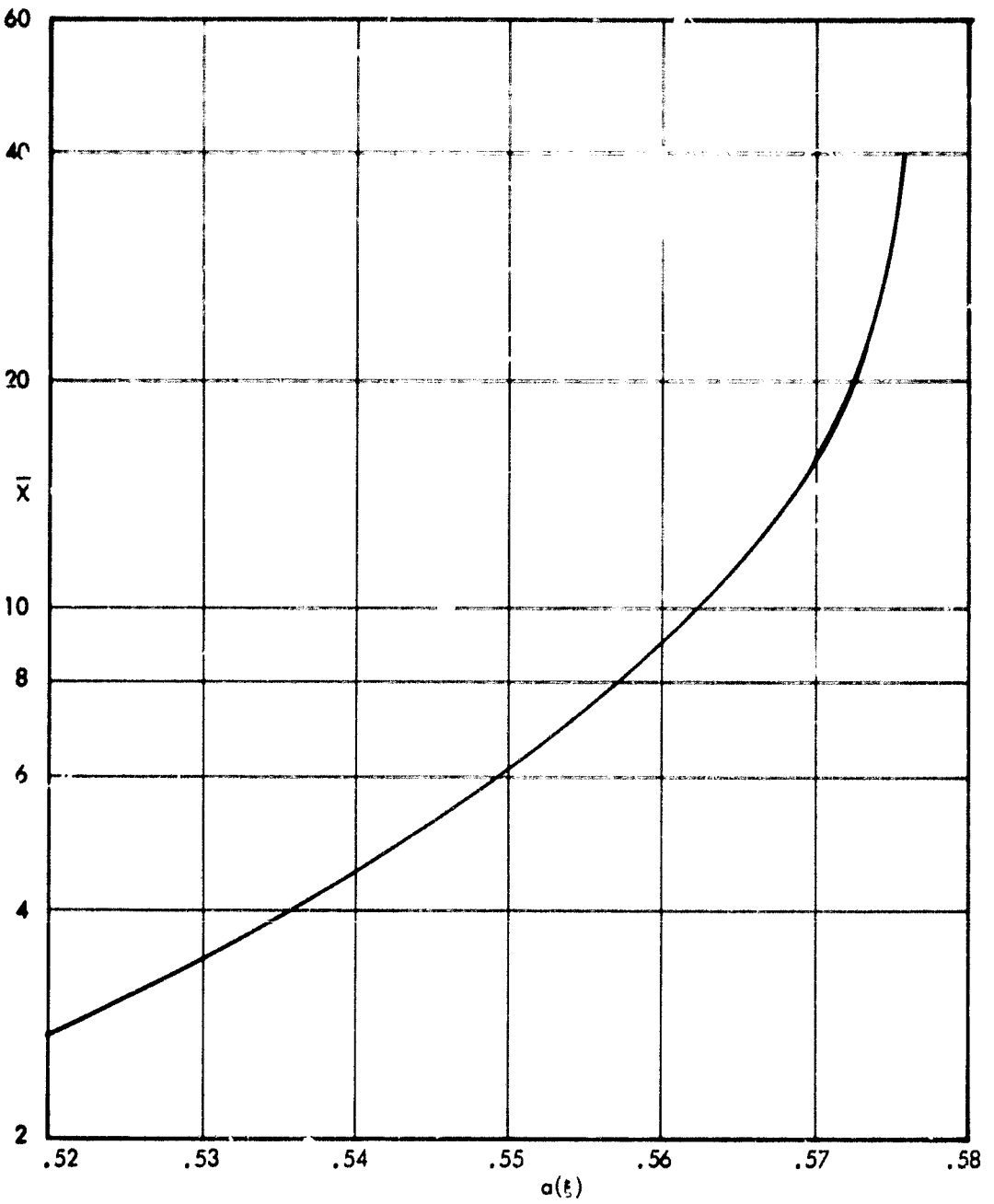

FIG. 5 BEHAVIOR OF $a(\xi)$

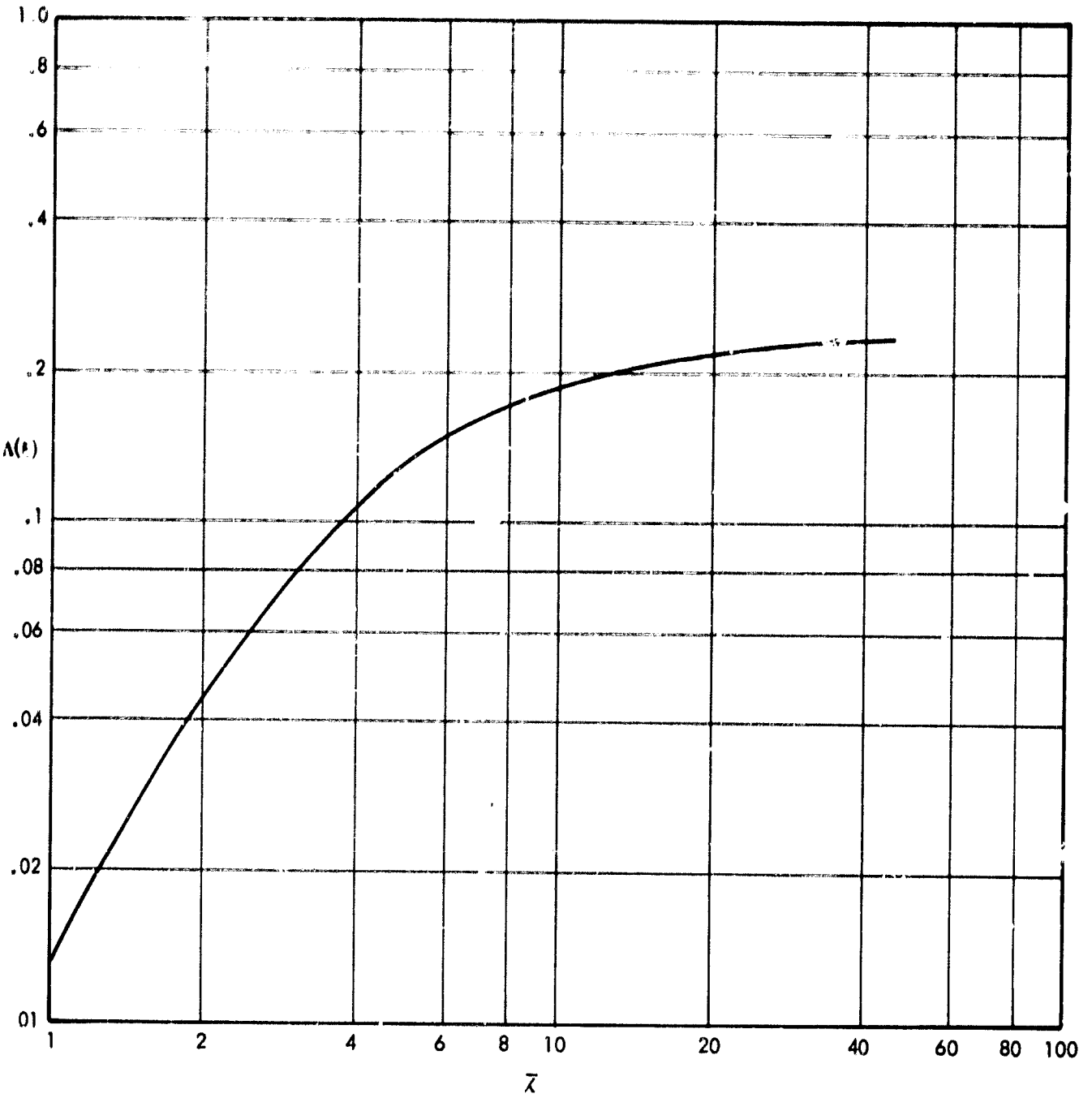

FIG. 6 BEHAVIOR OF PRESSURE GRADIENT PARAMETER Λ(β)

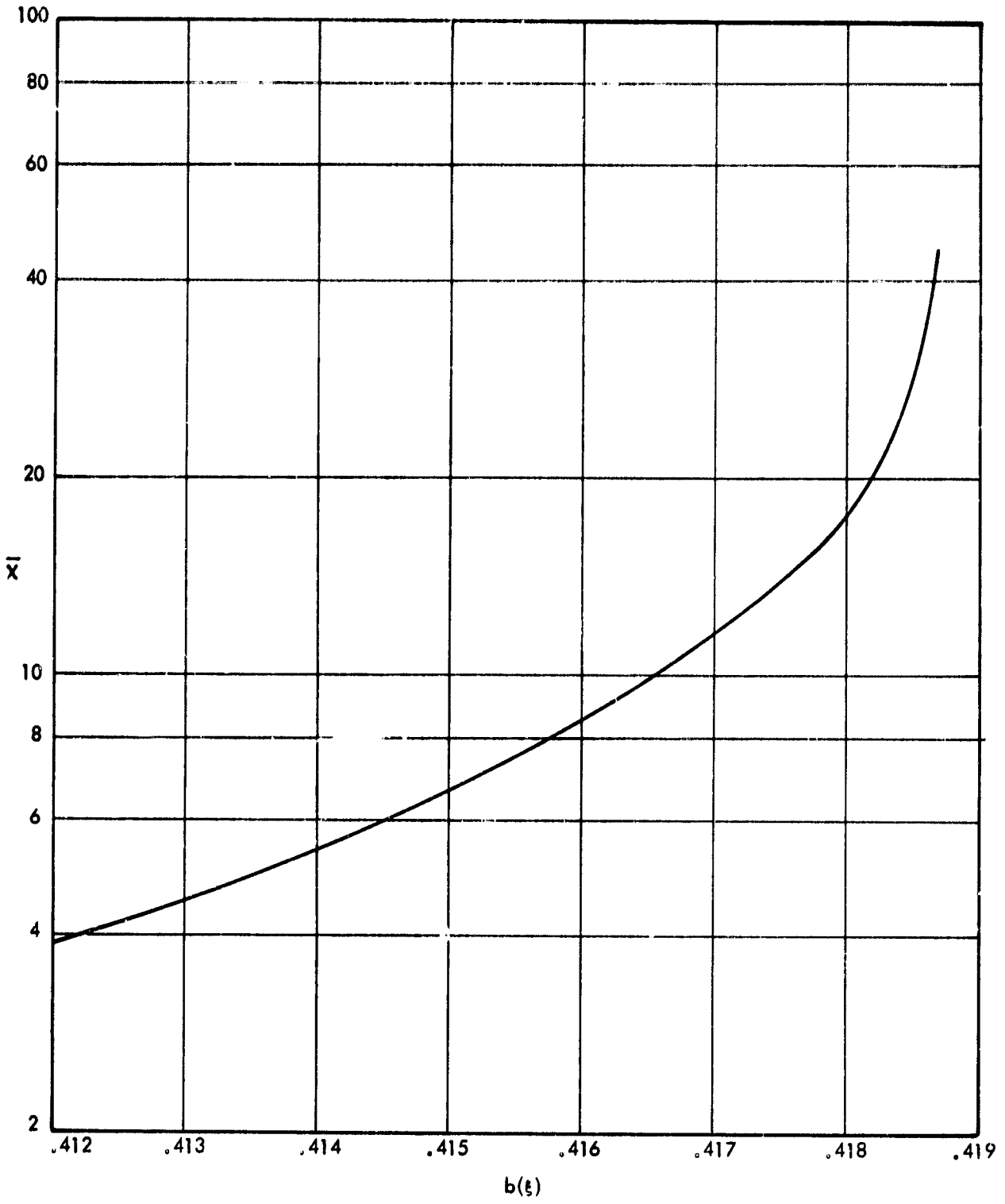

FIG. 7 BEHAVIOR OF b(ξ)

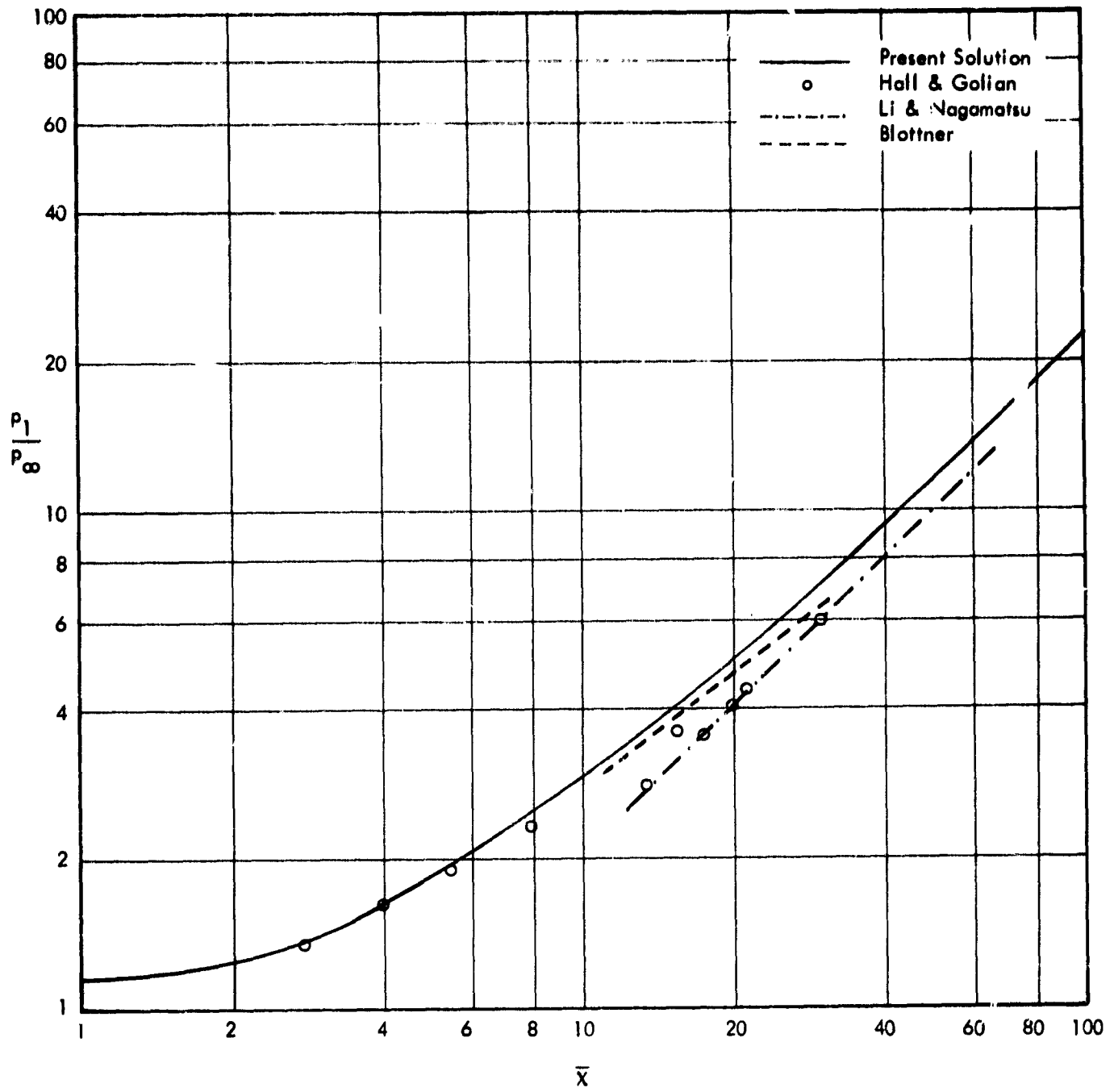

FIG. 8 PRESSURE DISTRIBUTION ON A COLD FLAT PLATE

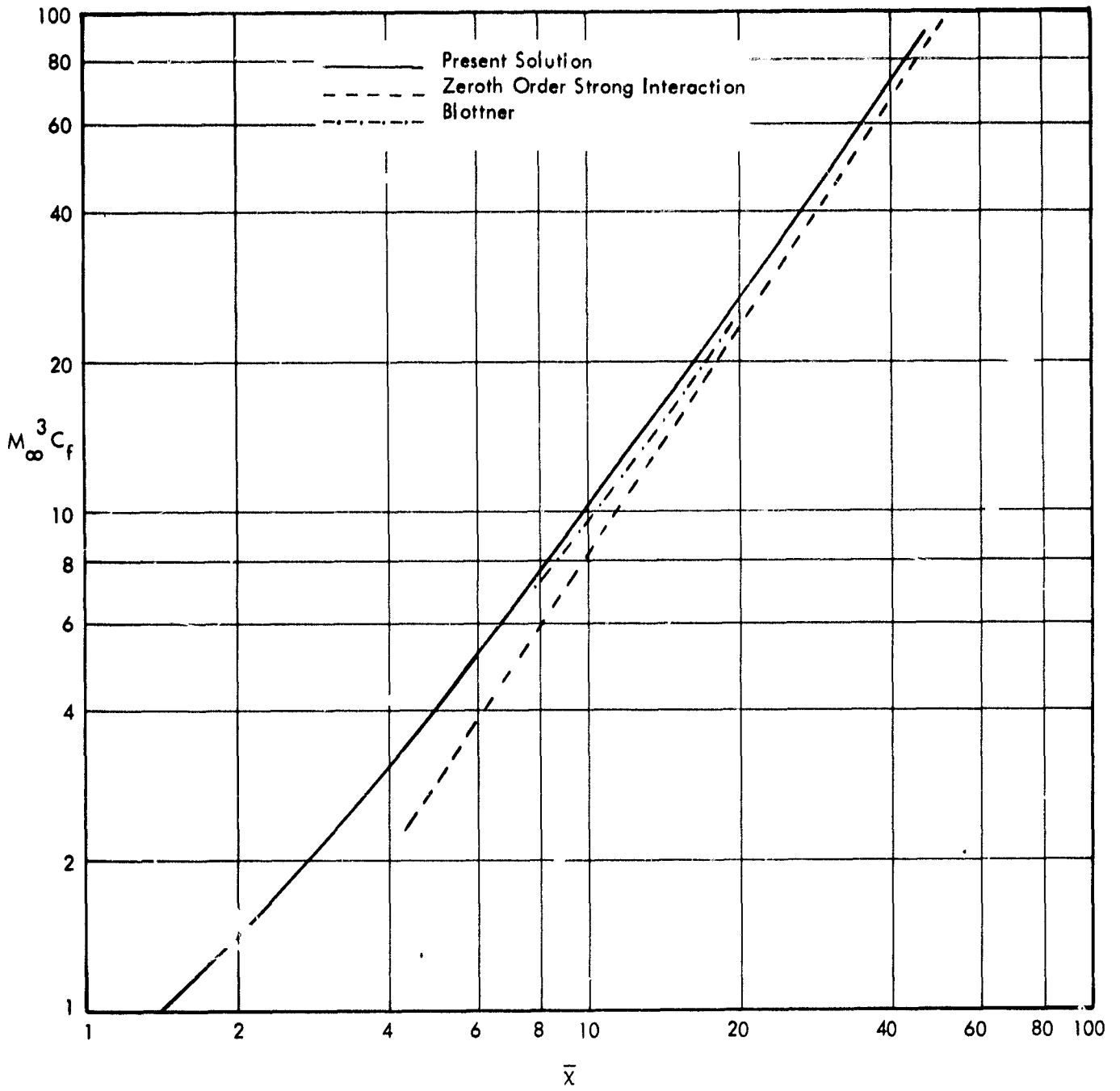

FIG. 9 SKIN FRICTION COEFFICIENT ON A COLD PLATE

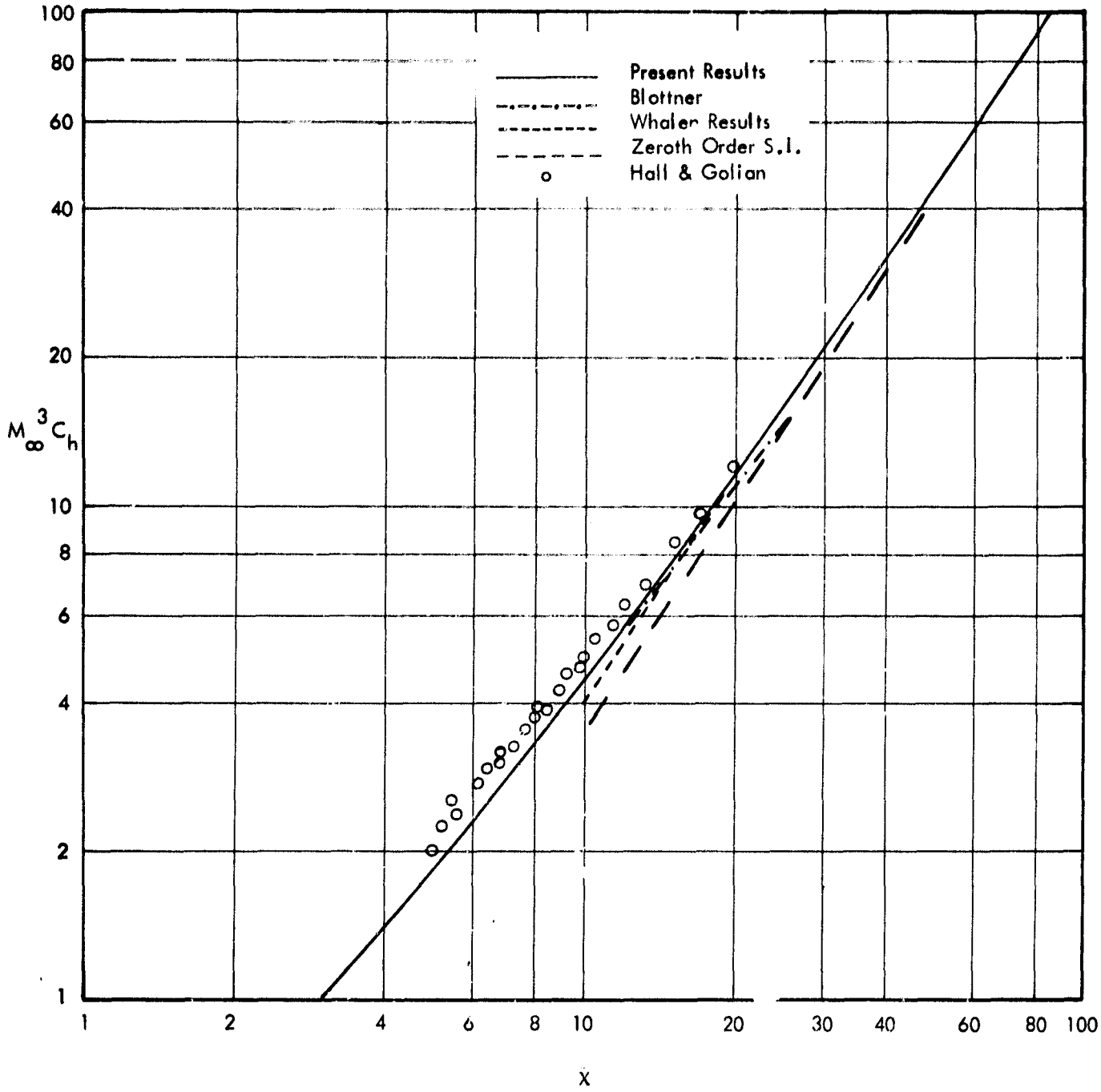

FIG. 10 HEAT TRANSFER COEFFICIENT ON A COLD PLATE

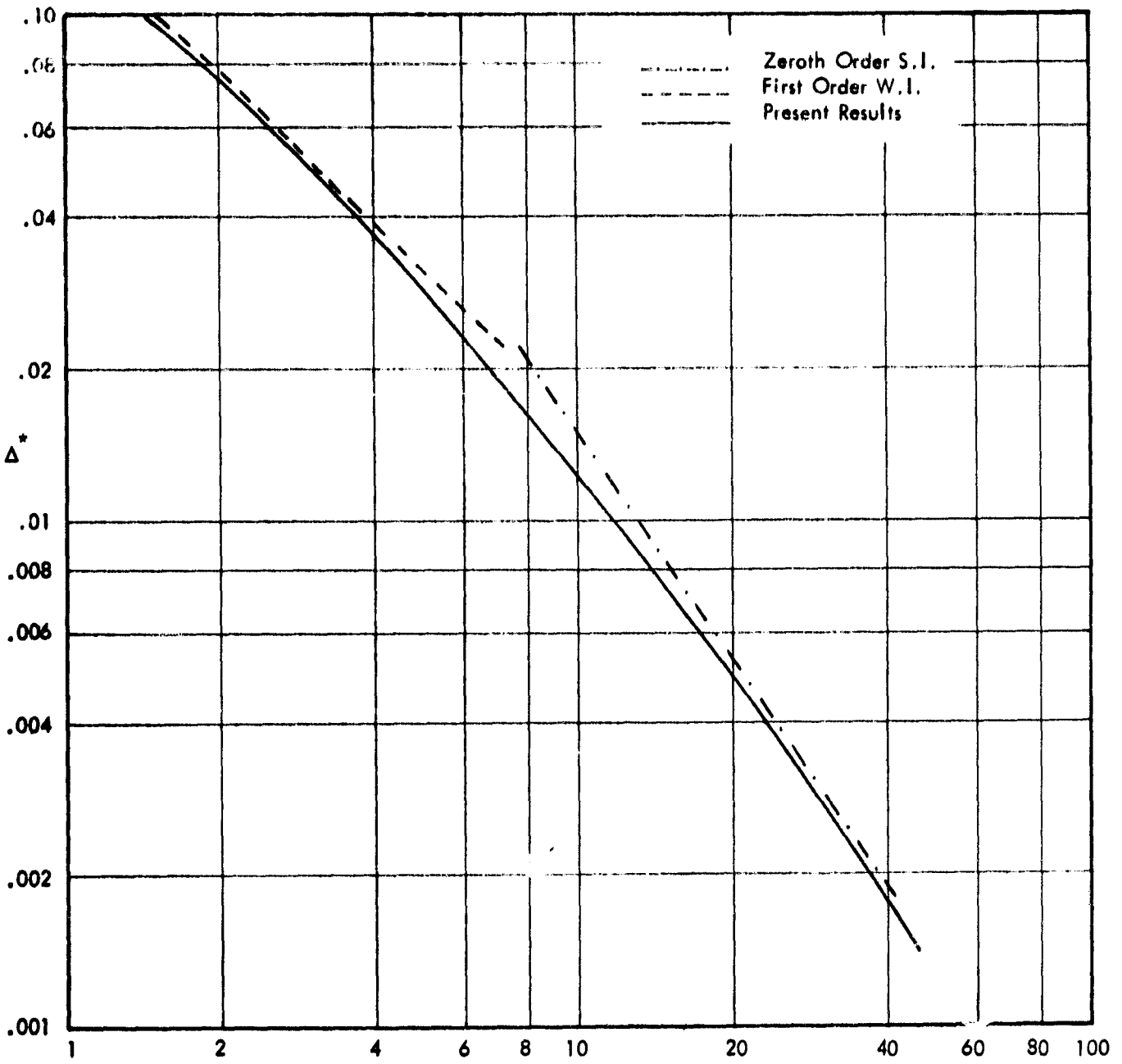

FIG. 11 DIMENSIONLESS DISPLACEMENT THICKNESS ON A COLD PLATE

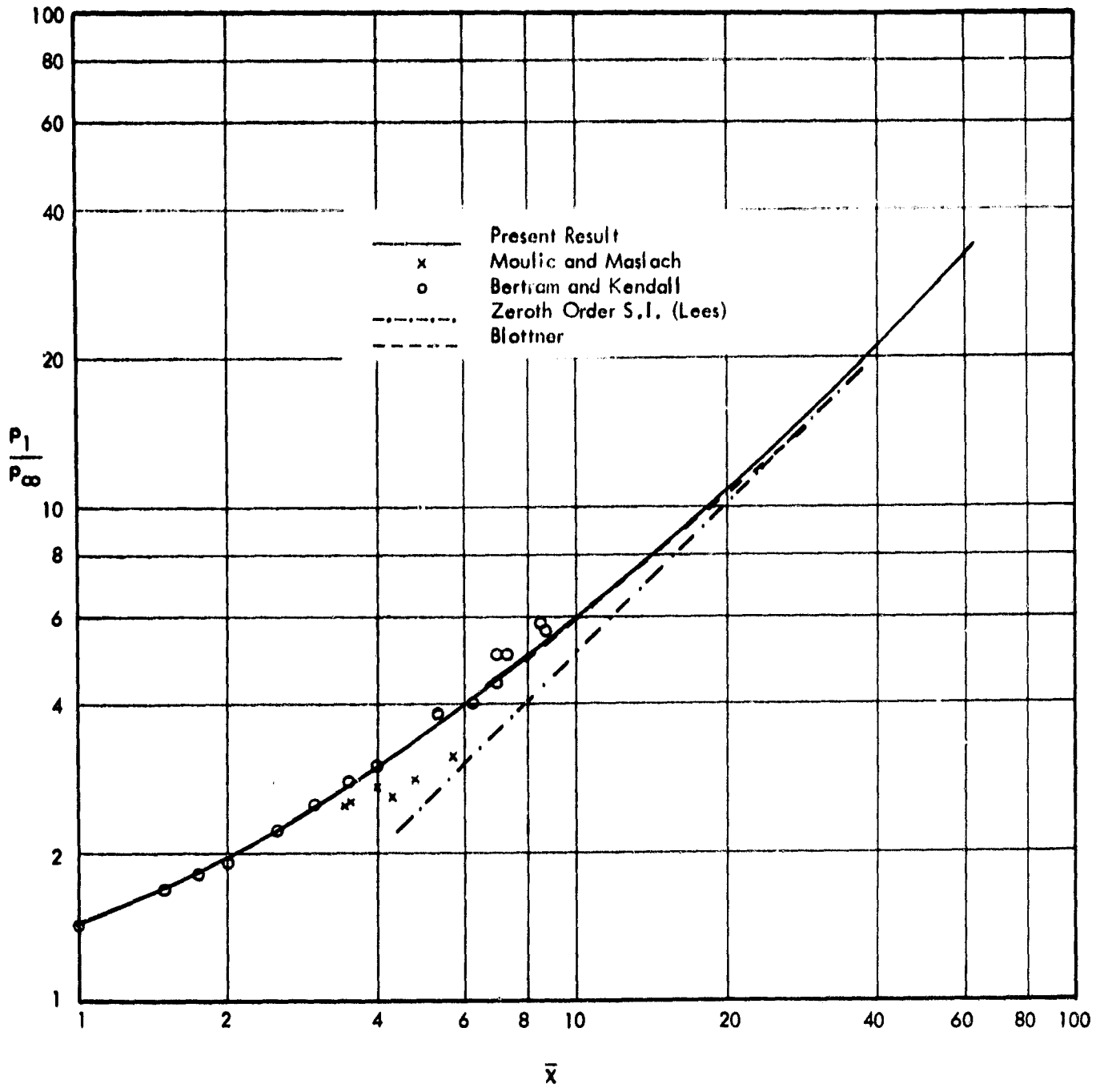

FIG. 12 PRESSURE DISTRIBUTION ON AN ADIABATIC FLAT PLATE

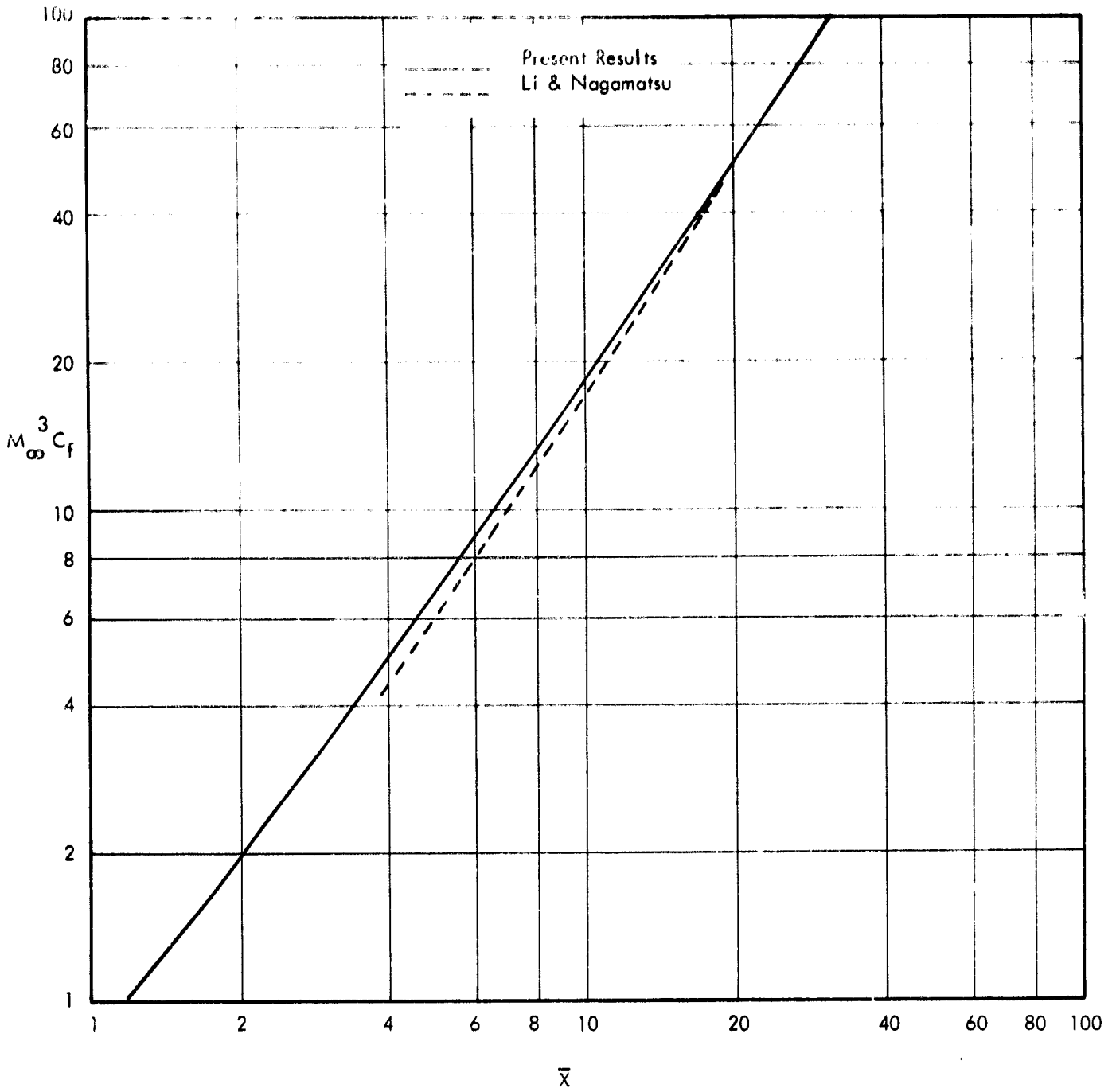

FIG. 13 SKIN FRICTION COEFFICIENT ON AN ADIABATIC PLATE

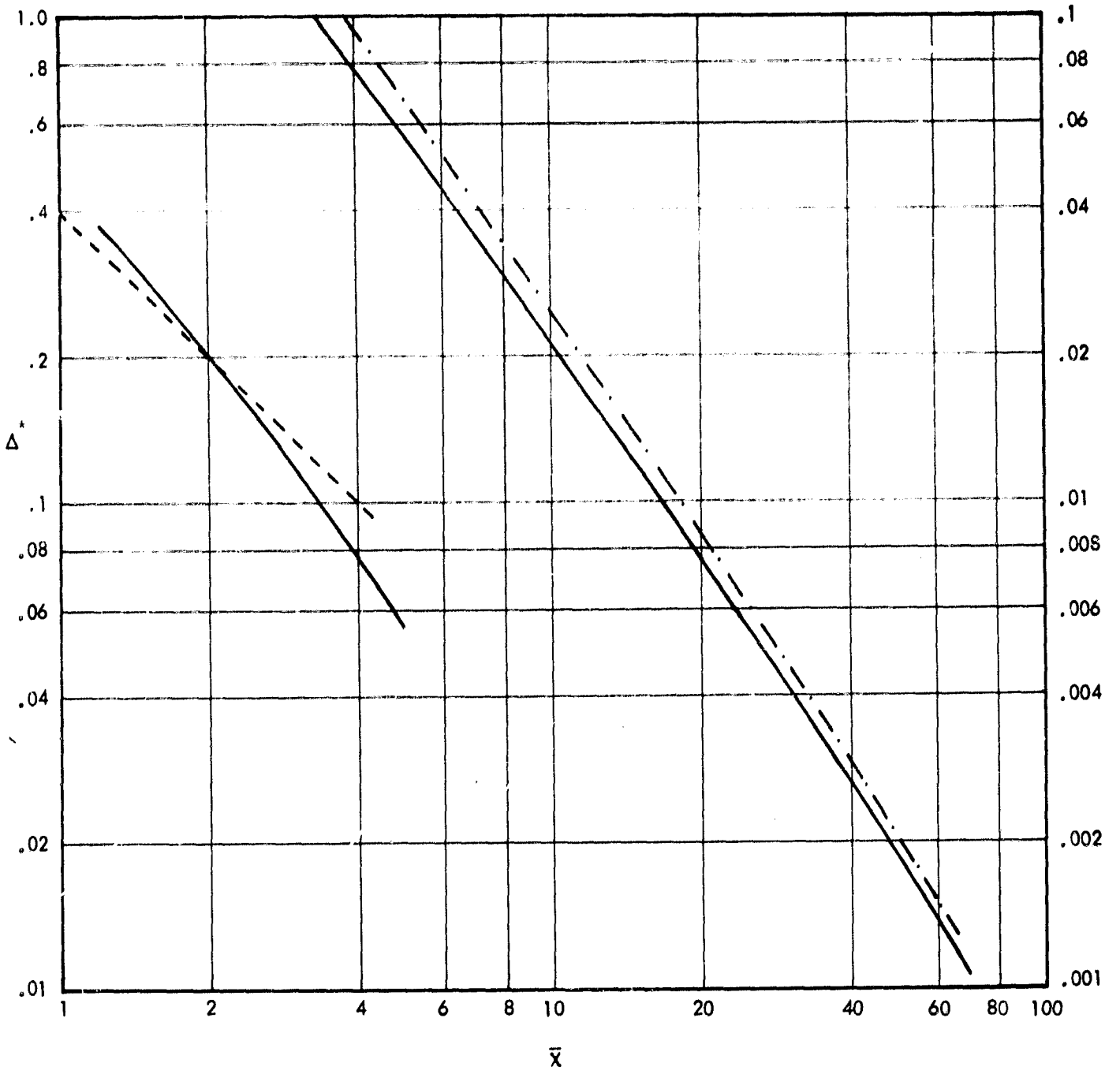

FIG. 14 DIMENSIONLESS DISPLACEMENT THICKNESS ON AN ADIABATIC PLATE

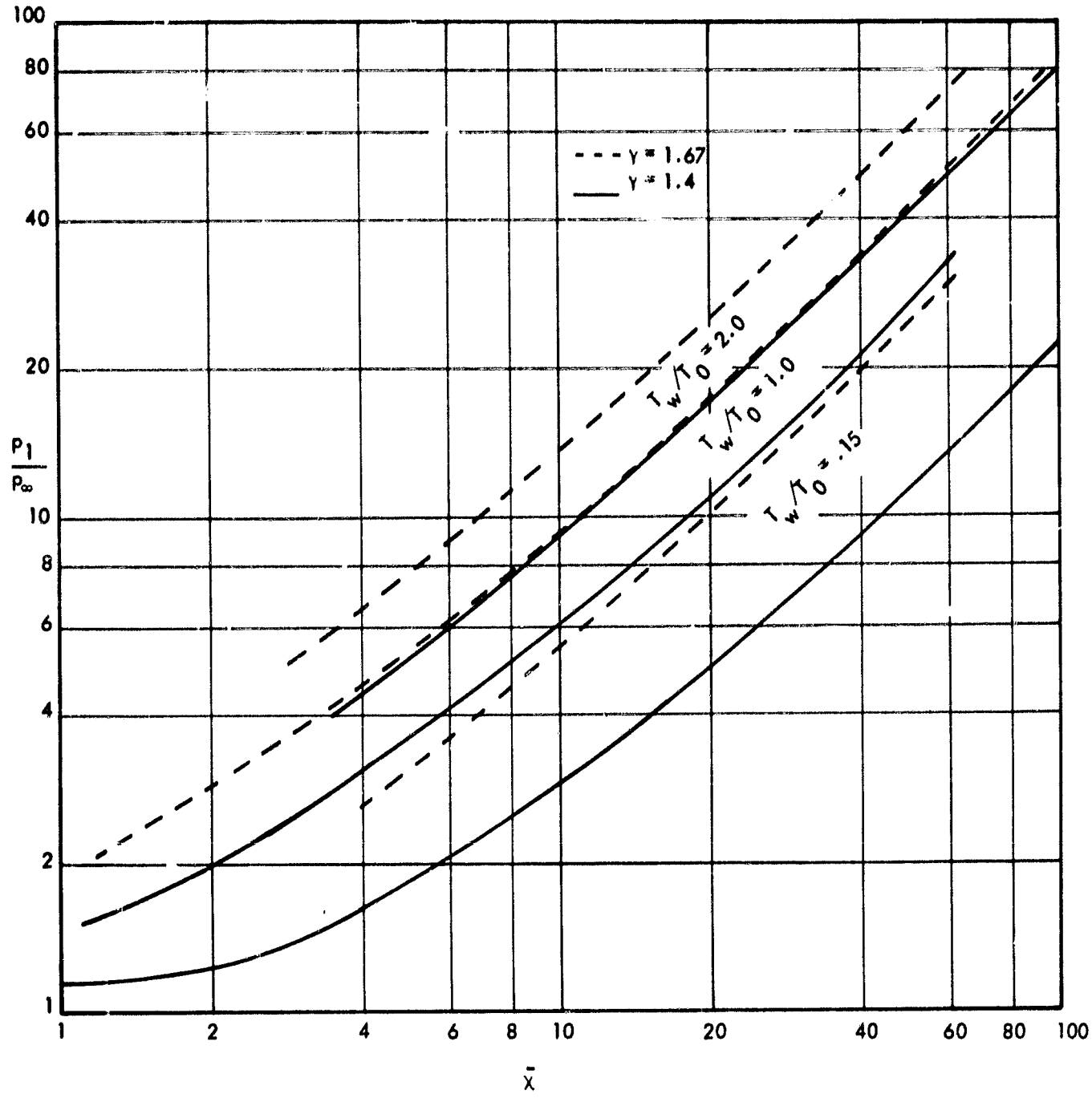

FIG. 15 PRESSURE DISTRIBUTIONS FOR VARIOUS DIMENSIONLESS WALL TEMPERATURES AND SPECIFIC HEAT RATIOS

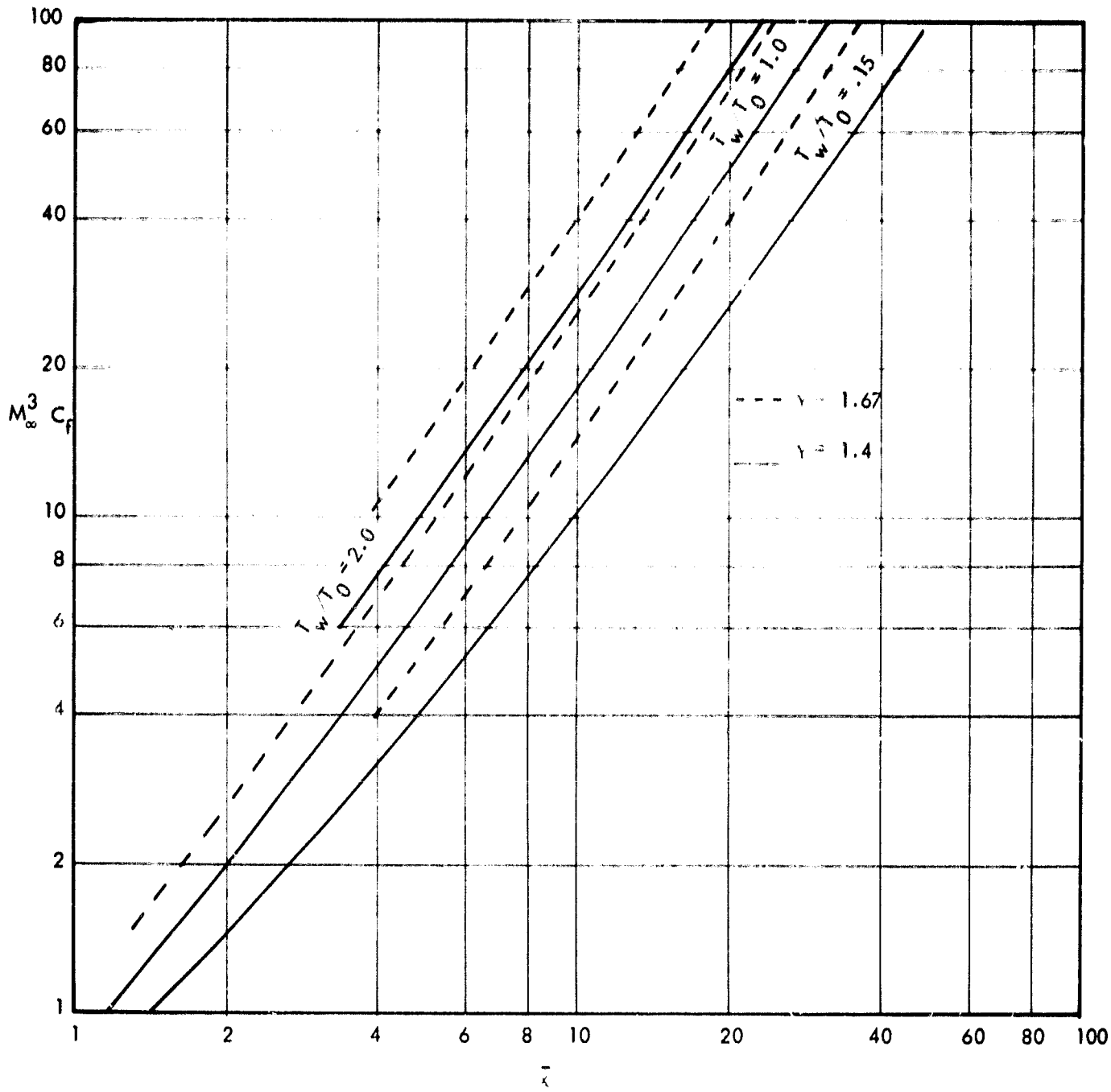

FIG. 16 SKIN FRICTION COEFFICIENTS FOR VARIOUS DIMENSIONLESS WALL TEMPERATURES AND SPECIFIC HEAT RATIOS

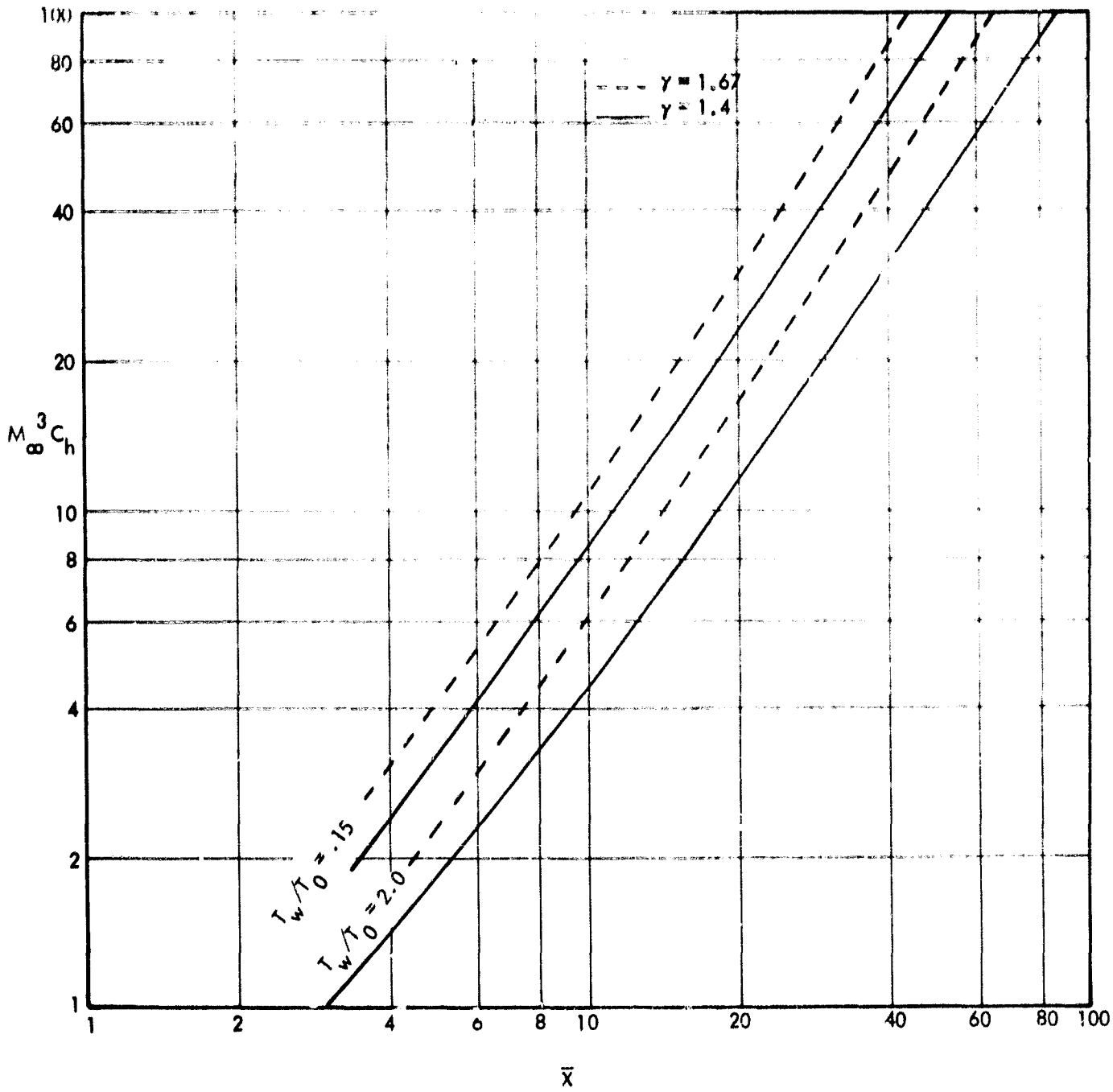

FIG. 17 HEAT TRANSFER COEFFICIENTS FOR VARIOUS DIMENSIONLESS WALL TEMPERATURES AND SPECIFIC HEAT RATIOS

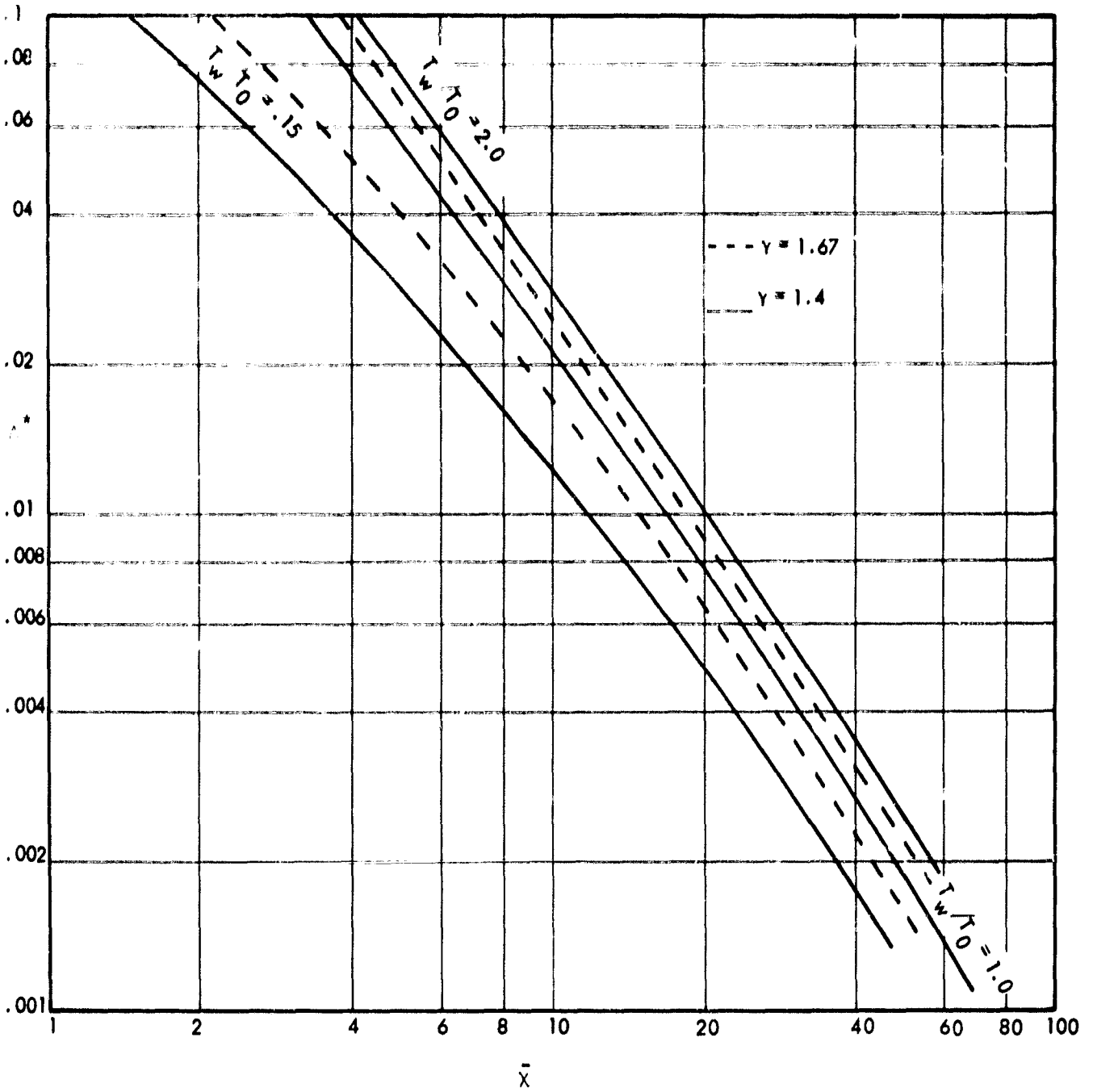

FIG. 18 DIMENSIONLESS DISPLACEMENT THICKNESSES FOR VARIOUS DIMENSIONLESS WALL TEMPERATURES AND SPECIFIC HEAT RATIOS

APPENDIX A

GENERAL PROCEDURE FOR THE EVALUATION OF THE INTEGRAL BY THE METHOD OF STEEPEST DESCENT

The integrals are of the form

$$\int_0^\infty \exp\ (-F(\eta))\ \varphi(\eta)\ d\eta$$

where $\varphi(\eta)$ is slowly varying and $F(\eta)$ is a positive function with a stationary point at $\eta = 0$, where η is positive.

The method of steepest descent, or saddle-point method, is due to Debye [107] who applied it to the evaluation of Bessel functions of large order. A detailed account of it is given in Watson [108]. This is exclusively applied for boundary layers by Meksyn [27 through 35], Merk [109], and Hayday and Bowles [102, 103].

To evaluate the integral, put

$$F(\eta) = \tau \qquad (A.1)$$

Invert the expression (A-1) (i.e., write η as a function of τ) and express the integrand in terms of τ

The function $F(\eta)$ is usually multiplied by a large positive parameter, and the series expanded in inverse powers of this parameter. In boundary layers, the large parameter is unity. Therefore, the behavior of $F(\eta)$ and $\varphi(\eta)$ is very important. In the majority of cases, the expressions obtained are very divergent; they are then summed by Euler's transformation.

APPENDIX B

DERIVATION OF Λ

The definition of Λ from Eq. (2.26) can be rewritten as

$$\Lambda = 2\xi \frac{d}{d\xi} \ln \frac{c_\infty}{c_1} u_1 \tag{B.1}$$

Using Eqs. (2.10) and (2.19), Λ becomes

$$\Lambda = \frac{\gamma-1}{\gamma} \frac{d(p_\infty/p_1)}{dx} \frac{\int_0^x \frac{u_1}{u_\infty}^{2i} \frac{r}{L} \frac{p_1}{p_\infty} dx}{\frac{u_1}{u_\infty}^{2i} \frac{r}{L}} + \frac{2\xi}{u_1} \frac{du_1}{d\xi} \tag{B.2}$$

Assuming isentropic, perfect gas low for the flow external to the boundary layer, one can obtain the following relation.

$$c_1^2 + \frac{\gamma-1}{2} u_1^2 = c_\infty^2 + \frac{\gamma-1}{2} u_\infty^2$$

or

(B.3)

$$u_1^2 = \frac{2}{\gamma-1} c_\infty^2 + \frac{\gamma-1}{2} u_\infty^2 - c_\infty^2 \frac{p_1}{p_\infty}^{\frac{\gamma-1}{\gamma}}$$

Differentiating Eq. (B.3) with respect to ξ and further simplification results in

$$\frac{1}{u_1} \frac{du_1}{d\xi} = \frac{1}{\gamma M_1^2} \frac{1}{p_\infty/p_1} \frac{d(p_\infty/p_1)}{d\xi} \tag{B.4}$$

Therefore, Eq. (B.2) becomes

$$\Lambda = \frac{\gamma - 1}{\gamma} + \frac{2}{\gamma M_1^2} \frac{d}{dx} \frac{p_\infty}{p_1} \frac{\int_0^x \left(\frac{u_1}{u_\infty}\right)^{2i} \frac{r}{L} \frac{p_1}{p_\infty} dx}{\left(\frac{u_1}{u_\infty}\right)^{2i} \frac{r}{L}} \tag{B.5}$$

Introducing further transformation

$$z = \frac{1}{\bar{\chi}^2} \quad (\bar{\chi} \text{ is defined in Eq. (2.48)} \tag{B.6}$$

Equation (B.5) reduces to

$$\Lambda = \frac{\gamma - 1}{\gamma} + \frac{2}{\gamma M_1^2} \frac{d}{dz} p_\infty/p_1 \frac{\int_0^z \left(\frac{u_1}{u_\infty}\right)^{2i} \frac{r}{L} \frac{p_1}{p_\infty} dz}{\left(\frac{u_1}{u_\infty}\right)^{2i} \frac{r}{L}} \tag{B.7}$$

It is important to note that the second term in Eq. (B.7) contributes very little in hypersonic flow and thus further simplification can be foreseen for high speed flows.

APPENDIX C

EULER'S TRANSFORMATION

The transformation is due to Euler [110] who used it to sum apparently divergent series. It has been extensively applied by Meksyn in his new method in boundary layer theory.

According to Euler, the sum of a divergent series is the finite numerical value of the convergent expression from which the divergent series is derived. First, the general form of Euler's transformation will be given. Suppose the series

$$\sum_{n=0}^{\infty} R_n X^{n+1} \tag{C.1}$$

converges to $S(X)$ for sufficiently small values of X. Let

$$Y = \frac{X}{1+X}$$

or (C.2)

$$X = \frac{Y}{1-Y}$$

Substituting (C.2) instead of X in the series (C.1) and expanding it in powers of Y, one can obtain

$$S(X) = \sum_{p=0}^{\infty} R_p Y^{p+1} (1-Y)^{-(p+1)} \tag{C.3}$$

Since

$$(1-Y)^{-(p+1)} = 1 + (1+p)Y + \frac{(p+1)(p+2)}{2!}Y^2 + \frac{(p+1)(p+2)(p+3)}{3!}Y^3 + \ldots$$

$$= \sum_{m=0}^{\infty} \binom{p+m}{m} Y^m \qquad (C.4)^*$$

Therefore,

$$S(X) = \sum_{p=0}^{\infty} R_p \sum_{m=0}^{\infty} \binom{p+m}{m} Y^{p+m+1} = \sum_{p=0}^{\infty} R_p \sum_{n=p}^{\infty} \binom{n}{n-p} Y^{n+1} \qquad (C.5)$$

Inverting the order of summation, Eq. (C.5) transforms to

$$S(X) = \sum_{n=0}^{\infty} Y^{n+1} \sum_{p=0}^{\infty} \binom{n}{n-p} R_p = \sum_{n=0}^{\infty} W_n Y^{n+1} \qquad (C.6)$$

where

$$W_n = \sum_{p=0}^{\infty} \binom{n}{p} R_p$$

i.e.,

$$\begin{aligned} W_0 &= R_0 \\ W_1 &= R_0 + R \\ W_2 &= \binom{2}{0} R_0 + \binom{2}{1} R_1 + \binom{2}{2} R_2 \\ &\cdots\cdots\cdots\cdots\cdots\cdots \\ W_n &= R_0 + \binom{n}{1} R_1 + \binom{n}{2} R_2 + \ldots + R_n \end{aligned} \qquad (C.7)$$

---

* $\binom{p+m}{m}$ is a binomial coefficient i.e., $\frac{(p+1)(p+2)\ldots(p+m)}{m!}$

Equation (C.6) is valid for sufficiently small Y. For large values of X, the series (C.1) may become divergent, while series (B.6) is convergent. It then represents the sum of S(X).

If the transformed series (C.6) is divergent, the transformation is repeated as shown below

$$\frac{Y}{1+Y} = Z \qquad \text{or} \quad Y = \frac{Z}{1-Z} \tag{C.8}$$

until a convergent expression is obtained.

The aim of Euler's transformation is to eliminate a singularity which was introduced by the method of expansion, but which does not belong to the function itself.

Euler also considered the particular case when $X = 1$ (i.e., $Y = 1/2$)

Now

$$S(1) = \sum_{n=0}^{\infty} R_n = \sum_{n=0}^{\infty} W_n \, 2^{-(n+1)} \tag{C.9}$$

The expression (C.9) often times is referred to as Euler's transformation, which has the following general form.

$$S(X) = \sum_{n=0}^{\infty} R_n \, X^{n+1} = \sum_{n=0}^{\infty} W_n \, Y^{n+1} \tag{C.10}$$

To elucidate the procedure, consider the series

$$S(X) = \frac{X}{1+4X} = X - 4X^2 + 16X^3 - 64X^4 + 256X^5 - 1024X^6 + \ldots \tag{C.11}$$

For $X = 1$.

$$S(1) = 1 - 4 + 16 - 64 + 256 - 1024 + \ldots.$$

$$W_0 = 1$$

$$W_1 = R_0 + R_1 = -3$$

$$W_2 = R_0 + 2R_1 + R_2 = 9 \qquad \text{(C.12)}$$

$$W_3 = R_0 + \binom{3}{1} R_1 + \binom{3}{2} R_2 + R_3 = R_0 + 3R_1 + 3R_2 + R_3$$

$$= 1 - 12 + 48 - 64 = -27$$

$$W_4 = R_0 + 4R_1 + 6R_2 + 4R_3 + R_4 = 81$$

It is clear that these coefficients can be conveniently obtained in the following manner by arranging the coefficient of R_n in the table

$$\begin{array}{cccccc}
1 & -4 & 16 & -64 & 256 & -1024 \\
-3 & 12 & -48 & 192 & -768 & \\
9 & -36 & 144 & -576 & & \\
-27 & 108 & -432 & & & \\
81 & -324 & & & & \\
-243 & & & & &
\end{array} \qquad \text{(C.13)}$$

where each term in the second row is obtained by taking the algebraic sum of the two adjacent terms above it, similarly for the third tow, etc.

$$W_0 = 1,\ W_1 = -3,\ W_2 = 9,\ W_3 = -27,\ W_4 = 81,\ W_5 = -243 \qquad \text{(C.14)}$$

Therefore, Eq. (C.9) becomes

$$S(1) = \sum_{n=0}^{\infty} R_n = \frac{1}{2} - \frac{3}{2^2} + \frac{9}{2^3} - \frac{27}{2^4} + \frac{81}{2^5} - \frac{243}{2^6} + \ldots \qquad \text{(C.15)}$$

which is still divergent. Repeating Euler's transformation:

$$\begin{array}{ccccccc}
\frac{1}{2} & -\frac{3}{4} & \frac{9}{8} & -\frac{27}{16} & \frac{81}{32} & -\frac{243}{64} & \\
-\frac{1}{4} & \frac{3}{8} & -\frac{9}{16} & \frac{27}{32} & -\frac{81}{64} & & \\
\frac{1}{8} & -\frac{13}{16} & \frac{9}{32} & -\frac{27}{64} & & & \\
-\frac{1}{16} & \frac{3}{32} & -\frac{9}{64} & & & & \\
\frac{1}{32} & -\frac{3}{64} & & & & & \\
-\frac{1}{64} & & & & & &
\end{array} \qquad \text{(C.16)}$$

Hence,

$$S(1) = \frac{1}{4} - \frac{1}{16} + \frac{1}{64} - \frac{1}{256} + \frac{1}{1024} - \frac{1}{4096} + \ldots$$

$$= .25 - .0625 + .01563 - .00391 + .000977 - .000244 + \ldots$$

$$= .19993 \approx 1/5 \qquad (C.17)$$

The following properties of Euler's transformation should be noted.

(1) $$\sum_{n=0}^{\infty} CR_n = C \sum_{n=0}^{\infty} R_n$$

(2) $$\sum_{n=0}^{\infty} (R_n + W_n) = \sum_{n=0}^{\infty} R_n + \sum_{n=0}^{\infty} W_n$$

(3) $$R_0 + (R_1 + R_2 + R_3 + \ldots) = R_0 + R_1 + R_2 + R_3 + \ldots$$

i.e., if $R_0 + R_1 + R_2 + \ldots$, is summable to $\bar{R}$, the series $(R_1 + R_2 + \ldots)$ is summable to $(\bar{R} - R_0)$. Euler's sum of a series does not change if a finite number of terms are separated and then added to the sum of the remaining terms; but an infinite number of zero terms cannot be disregarded without changing the value of the sum.

Euler's transformation does not always improve the convergence of convergent series. Euler also applied the transformation to semi-convergent series. In this case, the subsequent transformations need not be applied from the first term.

In the application of Euler's transformation to sum a series, the transformation is applied to a certain number of terms, and the initially convergent

terms only are retained; the procedure is then repeated for the remaining terms. The above procedure gives a better approximation than if the same number of transformations are applied to all terms starting from the first one.

The following rules may be noted in applying the transformation:

1. Since only a limited number of terms is usually available, all terms including zeros, should be retained.
2. The transformation can be started from any term; the best result is obtained if the last term in the expression is the smallest one, and the convergence is better for the same number of transformations. The final results corresponding to different reasonable combinations should, however, differ but slightly.
3. Repeated transformations not only improve the convergence but also slow it down. It is therefore advisable to use only as few transformations as possible.

APPENDIX D

MULLER'S ITERATIVE TECHNIQUE FOR SOLVING NONLINEAR EQUATIONS

This technique finds a root of the general nonlinear equation $f(x) = 0$ in the range of x from x_k to x_r. Muller's iteration scheme at successive bisection and inverse parabolic interpolation is used. The procedure assumes

$$f(x_k) \cdot f(x_r) \leq 0 \qquad \text{(D.1)}$$

An iterative step can be described as shown in the following sketch:

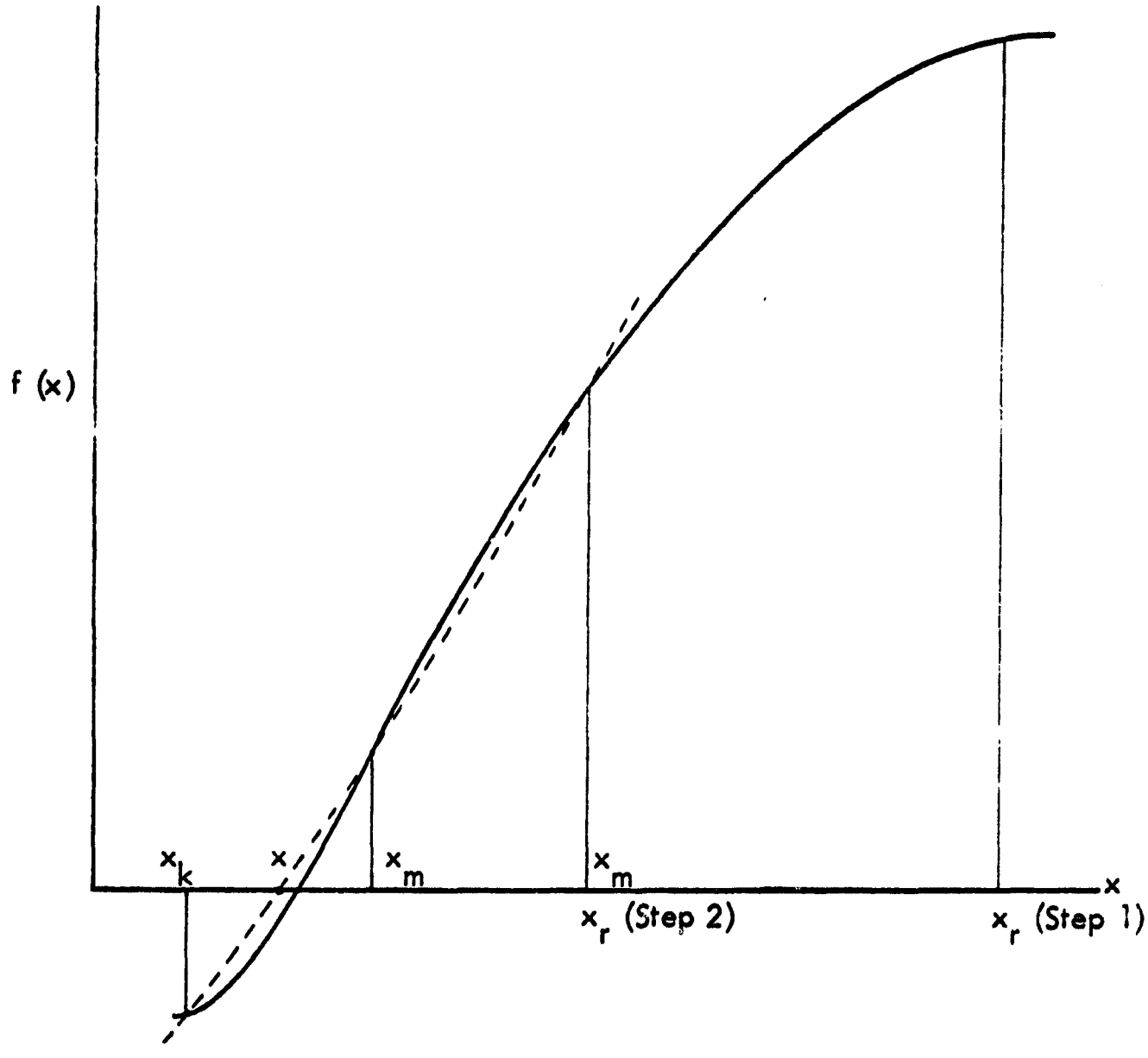

At first, the middle of the interval will be computed.

i.e.,

$$x_m = \frac{1}{2}(x_k + x_r) \tag{D.2}$$

In case $f(x_m) \cdot f(x_r) < 0$, x_k and x_r are interchanged, thus program make sure that

$$f(x_m) \cdot f(x_r) > 0 \tag{D.3}$$

In case, $f(x_m) \geq f(x_r)$, x_r is replaced by x_m and the sequence is repeated. If after a specified number of successive bisections $f(x_m) \geq f(x_r)$, the error parameter is set equal to two and the procedure returns to the calling program.

The second bisection steps lead to $f(x_m) < f(x_r)$. Thus, one can compute by inverse parabolic interpolation:

$$x = x_k - \Delta x$$

where

$$\Delta x = f(x_k) \cdot \frac{x_m - x_k}{f(x_m) - f(x_k)} \left[1 + f(x_m) \right.$$

$$\left. \frac{f(x_r) - 2f(x_m) + f(x_k)}{[f(x_r) - f(x_m)]\,[f(x_r) - f(x_k)]} \right] \tag{D.4}$$

This iterative procedure can end if the relative error $\frac{\Delta x}{x}$ is less than a specified tolerance. If it is not and if done less than a specified number of iteration steps, it sets $x_r = x$ in case $f(x) \cdot f(x_k) < 0$ or $x_r = x_m$ and $x_k = x$

in case $f(x) \cdot f(x_k) > 0$ and the procedure starts from the very beginning.

Each iteration step requires two evaluations of $f(x)$ and usually the procedure guarantees quadratic convergence. However, convergence may fail due to rounding errors. In this case also, the error parameter is set equal to two and the procedure returns to the calling program. Further details can be obtained from Reference [111].